
Byzantine-Resilient Zero-Order Optimization for Communication-Efficient Heterogeneous Federated Learning

Maximilian Egger¹ Mayank Bakshi² Rawad Bitar¹

Abstract

We introduce CYBER-0, a Byzantine-resilient federated zero-order optimization method that is robust under Byzantine attacks and provides significant savings in uplink and downlink communication costs. We introduce transformed robust aggregation to give convergence guarantees for general non-convex objectives under client data heterogeneity. Empirical evaluations for standard learning tasks and fine-tuning large language models show that CYBER-0 exhibits stable performance with only a few scalars per-round communication cost and reduced memory requirements.

1 Introduction

Federated Learning (FL) (McMahan et al., 2017) has emerged as an attractive paradigm for training a machine-learning model on the data owned by distributed clients, without exposing the clients’ raw data. Despite its appeal, FL can incur prohibitive communication costs, particularly in bandwidth-limited or wireless scenarios. In a typical FL epoch, every participating client transmits its (potentially high-dimensional) local update to a central *federator*, which then consolidates these updates and returns a global model to the clients. A large body of research has accordingly focused on reducing the communication overhead of transmitting and receiving model updates (Wen et al., 2017; Karimireddy et al., 2019; Vogels et al., 2019; M Abdelmoniem et al., 2021; Makkuva et al., 2024; Tang et al., 2024b; Qin et al., 2023).

¹This is a follow-up work on the preliminary version (Neto et al., 2024), where we first introduced a specific version of CYBER-0. This project has received funding from the German Research Foundation (DFG) under Grant Agreement Nos. BI 2492/1-1 and WA 3907/7-1. The work of Mayank Bakshi is supported by the National Science Foundation under Grant No. CCF-2107526. ²School of Computation, Information and Technology, Technical University of Munich ³School of Electrical, Computer, and Energy Engineering, Arizona State University. Correspondence to: Maximilian Egger <maximilian.egger@tum.de>.

Byzantine adversaries. The distributed nature of FL makes it vulnerable to attacks from *Byzantine clients*, *i.e.*, adversarial clients that craft harmful updates to derail the training process. Without suitable countermeasures, even one Byzantine client can prevent the global model from converging (Blanchard et al., 2017). A common countermeasure is the use of robust aggregation rules to assimilate different clients’ updates by the federator (Shen et al., 2016; Blanchard et al., 2017; Li et al., 2020; Yin et al., 2018; Rodríguez-Barroso et al., 2023). As such defenses typically entail slower convergence, the communication cost of FL becomes even more critical in adversarial settings.

Data heterogeneity. Another key challenge that hinders FL in real-world scenarios is *data heterogeneity*, *i.e.*, the clients’ data might stem from different underlying distributions. Data heterogeneity can pose challenges for model convergence (Zhao et al., 2018; Zhu et al., 2021), and indirectly lead to privacy loss by skewing the clients’ model updates (Schlegel et al., 2023; Egger et al., 2023; Jahani-Nezhad et al., 2023; Zhu & Philip, 2019; Truex et al., 2019; Bagdasaryan et al., 2019; Wei et al., 2020; Tang et al., 2024a). The effect of data heterogeneity in FL is especially pronounced in the Byzantine setting. As robust aggregation rules aim to reduce the impact of outliers, if a legitimate client’s local update significantly differs due to a unique data distribution, these rules may mistakenly ignore or minimize that contribution, compromising overall performance (El-Mhamdi et al., 2021; Karimireddy et al., 2022; Charikar et al., 2017; Liu et al., 2021). To counteract the effect of data heterogeneity, a pre-aggregation rule called Nearest Neighbor Mixing (NNM) is introduced in Allouah et al. (2023). By averaging each client’s update with a subset of its neighbors, NNM improves the performance of standard robust aggregation rules.

Zero-order optimization. Zero-order (ZO) optimization methods (Kiefer & Wolfowitz, 1952; Spall, 1992; Duchi et al., 2015; Ghadimi & Lan, 2013; Liu et al., 2020) bypass the need for explicit gradient computations through stochastic approximations. A typical ZO optimization step involves sampling a few random *perturbation vectors*, measuring the objective/loss function differences along these vectors, and then updating the model along the direction of

the perturbation vector proportionately to the corresponding function differences. Beyond their utility in black-box problems where explicit gradients are unavailable or computationally prohibitive, ZO methods have also been explored for backpropagation-free neural network training in memory-constrained settings (Salimans et al., 2017; Ilyas et al., 2018; Liu et al., 2020) and in federated learning (Fang et al., 2022; Qiu et al., 2023; Chen et al., 2023). In particular, ZO methods have proven attractive in fine-tuning scenarios, which exhibit low *intrinsic dimensionality* (Salimans et al., 2017; Malladi et al., 2023). In a preliminary version of this work (Neto et al., 2024), we introduced a specific version of CYBER-0 that ensures Byzantine resilience and communication efficiency in FL settings. The algorithm in (Neto et al., 2024) is theoretically proven to be resilient to Byzantine clients for convex optimization tasks under i.i.d. data.

Our contribution. We propose CYBER-0, a framework for communication-efficient, Byzantine-resilient FL that leverages ZO optimization with Byzantine-robust aggregation. Our general algorithm is designed to work with arbitrary robust aggregation rules, such as coordinate-wise trimmed mean (Yin et al., 2018) and Krum (Blanchard et al., 2017), that can be composed with heterogeneity-aware pre-processing steps such as NNM (Allouah et al., 2023). We prove the convergence of CYBER-0 under mild assumptions about general non-convex losses and bounded data heterogeneity. We measure heterogeneity by using bounded gradient divergence among clients and applying a pseudo-Lipschitz condition to the average loss, as proposed by Wang et al. (2025). We run comprehensive experiments for classification tasks on the MNIST dataset and fine-tuning RoBERTa-large (Liu, 2019) to three different tasks. Our experiments show that in the presence of state-of-the-art Byzantine attacks, CYBER-0 achieves accuracy comparable to gradient-based Byzantine-resilient FL methods while requiring significantly less communication, and low memory and computational cost compared to traditional gradient-based methods.

We formally describe CYBER-0 in Section 3.1 and give here the key technical novelties that we incorporate within. We describe these in further detail in Section 3.3.

• **Transformed robust aggregation via gradient embeddings:** Unlike full-gradient algorithms, in CYBER-0, the federator only has access to the ZO updates from clients, posing a challenge for the robust aggregation rule. To ensure that the global model updates lie in the space spanned by the perturbation vectors, CYBER-0 performs robust aggregation in the reduced-dimensional embedding of the ZO evaluations. Drawing on Johnson–Lindenstrauss embeddings (Johnson & Lindenstrauss, 1984), we show that the geometry of the original gradients is approximately preserved, so the robustness properties of existing schemes

carry over. This also substantially lowers federator-side computation improving the scalability.

• **Low-cost uplink and downlink communication via pseudorandom perturbation directions:** CYBER-0 leverages the structure of ZO updates enabling the clients and federator to *communicate only a handful of scalars* along random perturbation directions, rather than the full model parameters. A pseudorandom generation of these directions ensures synchronization across clients and federator via a shared seed, preserving significant communication savings.

• **Multiple local ZO epochs:** To further reduce the communication overhead, each client performs several local updates (epochs) before transmitting to the federator, thereby reducing the number of global epochs. We propose two methods: in one, the clients sample a new perturbation direction for each local epoch, and in the other, the clients use the same direction for all local epochs to further save on the communication cost. We provide theoretical and empirical convergence guarantees for the former and empirical convergence guarantees for the latter.

2 System Model and Preliminaries

Notation. The L_2 norm of a vector \mathbf{x} and the inner product of two vectors \mathbf{x} and \mathbf{y} are represented by $\|\mathbf{x}\|$ and $\langle \mathbf{x}, \mathbf{y} \rangle$, respectively. Let \mathbb{S}^d be the d -dimensional unit sphere, *i.e.*, $\mathbb{S}^d \triangleq \{\mathbf{x} \in \mathbb{R}^d : \|\mathbf{x}\|^2 = 1\}$. $\mathcal{U}(\mathbb{S}^d)$ denotes a uniform distribution over \mathbb{S}^d . For a natural number a , we let $[a] \triangleq \{1, \dots, a\}$. For column vectors $\mathbf{v}_i, i \in [a]$, we denote by $(\mathbf{v}_i)_{i=1}^a \triangleq (\mathbf{v}_1, \dots, \mathbf{v}_a)$ the horizontal stacking operation.

Learning objective. We consider an FL system with n clients and a federator. Each client $i \in [n]$ poses an individual dataset \mathcal{D}_i . The global dataset is denoted by the multiset $\mathcal{D} = \cup_{i \in [n]} \mathcal{D}_i$. Let $F : \mathbb{R}^d \times \mathcal{D} \rightarrow \mathbb{R}^+$ be a given loss function. Let $F(\mathbf{w}, \tilde{\mathcal{D}}) \triangleq \sum_{D \in \tilde{\mathcal{D}}} F(\mathbf{w}, D) / |\tilde{\mathcal{D}}|$ and $F_i(\mathbf{w}) \triangleq F(\mathbf{w}, \mathcal{D}_i)$ denote the average loss of \mathbf{w} on a subset $\tilde{\mathcal{D}}$ of \mathcal{D} and the average loss of \mathbf{w} on client i 's dataset, respectively. Given a set $\mathcal{A} \subseteq [n]$, we let $F_{\mathcal{A}}(\mathbf{w}) \triangleq \frac{1}{|\mathcal{A}|} \sum_{i \in \mathcal{A}} F_i(\mathbf{w})$ and $F_{\mathcal{A}}^* \triangleq \min_{\mathbf{w} \in \mathbb{R}^d} F_{\mathcal{A}}(\mathbf{w})$. The clients collectively wish to find a minimizer of $F_{[n]}(\mathbf{w})$.

All clients and the federator start with an initial model $\mathbf{w}^{(1)} \in \mathbb{R}^d$ and construct a sequence of models $\{\mathbf{w}^{(t)}\}_{t \in [T]}$, where T denotes the number of global epochs. In epoch t , client i observes the current global model $\mathbf{w}^{(t)}$, samples a *mini-batch* $\tilde{\mathcal{D}}_i$ of its local dataset and transmits an update to the federator. The federator aggregates all client updates, generates the new global model $\mathbf{w}^{(t+1)}$ and conveys it to all clients. For a mini-batch $\tilde{\mathcal{D}}_i$, we let $\mathbf{g}_i \triangleq \nabla F(\mathbf{w}^{(t)}, \tilde{\mathcal{D}}_i)$.

Adversarial model. We assume $b < n/2$ clients are Byzantine. We assume the strongest possible adversarial model, where all Byzantine clients can collaborate and have full knowledge of the learning algorithm, all countermea-

tures, and the results of honest clients. We refer to the set of honest clients as $\mathcal{H} \subseteq [n]$, where $|\mathcal{H}| = n - b$. The learning objective becomes finding a minimizer of $F_{\mathcal{H}}(\mathbf{w})$.

Zero-order gradient estimate. ZO gradient estimates are obtained by evaluating the loss function at points in the direction specified by the perturbation direction. In the following, we first define the two-point ZO estimate.¹

Definition 2.1 (Two-Point Zero-Order Estimate). Let $\mathbf{z} \in \mathbb{S}^d$, $\tilde{\mathcal{D}} \subseteq \mathcal{D} \setminus \emptyset$ and $\mathbf{w} \in \mathbb{R}^d$. The two-point ZO estimate of the gradient $\mathbf{g} \triangleq \nabla F(\mathbf{w}, \tilde{\mathcal{D}})$ along the perturbation direction \mathbf{z} is defined as $\mathbf{z}\mathbf{g}(\mathbf{w}, \mathbf{z}, \mu, \tilde{\mathcal{D}})$, where

$$\mathbf{z}\mathbf{g}(\mathbf{w}, \mathbf{z}, \mu, \tilde{\mathcal{D}}) \triangleq \begin{cases} d \frac{F(\mathbf{w} + \mu\mathbf{z}, \tilde{\mathcal{D}}) - F(\mathbf{w} - \mu\mathbf{z}, \tilde{\mathcal{D}})}{2\mu} & \mu > 0 \\ d \langle \nabla F(\mathbf{w}, \tilde{\mathcal{D}}), \mathbf{z} \rangle & \mu = 0 \end{cases}$$

Robust aggregation. In Byzantine-resilient FL schemes, the federator aggregates the clients' updates using a robust² aggregation rule $R(\cdot)$. To measure the robustness of an aggregation rule, we adopt the following notion introduced by Allouah et al. (2023).

Definition 2.2 ((b, κ) -Robust Aggregation). Let $\kappa \geq 0$ and $b < n/2$. For vectors $\mathbf{v}_1, \dots, \mathbf{v}_n$ and any set $\mathcal{H} \subset [n]$ of size $|\mathcal{H}| = n - b$, letting $\bar{\mathbf{v}}_{\mathcal{H}} = \frac{1}{|\mathcal{H}|} \sum_{i \in \mathcal{H}} \mathbf{v}_i$, an aggregation rule $R(\{\mathbf{v}_i\}_{i=1}^n)$ is (b, κ) -robust if

$$\|R(\{\mathbf{v}_i\}_{i=1}^n) - \bar{\mathbf{v}}_{\mathcal{H}}\|^2 \leq \frac{\kappa}{|\mathcal{H}|} \sum_{i \in \mathcal{H}} \|\mathbf{v}_i - \bar{\mathbf{v}}_{\mathcal{H}}\|^2.$$

The parameter κ measures the robustness of the aggregation rule against at most b Byzantine clients.

3 Overview of CYBER-0

3.1 Description of CYBER-0

CYBER-0 is stated in Algorithm 1. In the beginning, we assume that the federator and clients have access to a shared seed that lets all parties sample the same random vectors $\mathbf{z} \sim \mathcal{U}(\mathbb{S}^d)$ through a common pseudo-random number generator (PRNG). The federator and all clients set their initial model to $\mathbf{w}^{(1)}$. The algorithm operates over T global epochs, each consisting of K local epochs. Set a fixed $\mu \geq 0$ to be a parameter for the ZO estimator and let η be the learning rate. At the beginning of global epoch t , all clients and the federator have an identical global model $\mathbf{w}^{(t)}$, and each client i initializes a model $\mathbf{w}_{t,1}^i = \mathbf{w}^{(t)}$ for its local epochs. Global epoch t proceeds as follows:

¹Although the estimator in Definition 2.1 for $\mu = 0$ is, strictly speaking, not a zero-order estimate, when μ approaches 0, $\mathbf{z}\mathbf{g}(\mathbf{w}, \mathbf{z}, \mu, \mathcal{D})$ approaches $\langle \nabla F(\mathbf{w}, \mathcal{D}), \mathbf{z} \rangle$. Despite the focus of this work being on ZO optimization, our algorithm continues to work even in the $\mu = 0$ case, *i.e.*, when gradients are computed by first applying backpropagation and then projected in the direction specified by \mathbf{z} .

²When all clients are honest, a common choice of the robust aggregation rule is the average.

Algorithm 1 CYBER-0: Robust Efficient Zero-Order FL

Require: Shared seed for PRNG, $\mu \geq 0$, $\eta > 0$, $\nu > 0$, R .

- 1: Initialize and broadcast global model $\mathbf{w}^{(1)}$.
- 2: **for** $t = 1$ to T **do**
- 3: **for** each client $i \in [n]$ **in parallel do**
- 4: Initialize local model $\mathbf{w}_{t,1}^i = \mathbf{w}^{(t)}$.
- 5: **for** $\ell = 1$ to K **do**
- 6: Draw $\mathbf{z}_{t,\ell}^1, \dots, \mathbf{z}_{t,\ell}^\nu \sim \mathcal{U}(\mathbb{S}^d)$, let $\mathbf{Z}_{t,\ell} \triangleq (\mathbf{z}_{t,\ell}^r)_{r \in [\nu]}$
- 7: Compute $g_i(\mathbf{w}_{t,\ell}^i, \mathbf{Z}_{t,\ell}) \triangleq g(\mathbf{w}_{t,\ell}^i, \mathbf{z}_{t,\ell}^r, \mu, \mathcal{D}_i)$, $r \in [\nu]$ (cf. Definition 2.1)
- 8: Let $\mathbf{g}_i(\mathbf{w}_{t,\ell}^i, \mathbf{Z}_{t,\ell}) \triangleq \frac{1}{\nu} ((g_i(\mathbf{w}_{t,\ell}^i, \mathbf{z}_{t,\ell}^r))_{r=1}^\nu)^\top$
- 9: Update $\mathbf{w}_{t,\ell+1}^i = \mathbf{w}_{t,\ell}^i - \eta \mathbf{Z}_{t,\ell} \mathbf{g}_i(\mathbf{w}_{t,\ell}^i, \mathbf{Z}_{t,\ell})$
- 10: **end for**
- 11: Send $\{\mathbf{g}_i(\mathbf{w}_{t,\ell}^i, \mathbf{Z}_{t,\ell})\}_{\ell=1}^K$ to federator.
- 12: **end for**
- 13: Aggregate $R_{t,\ell} = R(\{\mathbf{g}_i(\mathbf{w}_{t,\ell}^i, \mathbf{Z}_{t,\ell})\}_{i=1}^n)$, $\ell \in [K]$
- 14: Update $\mathbf{w}^{(t+1)} = \mathbf{w}^{(t)} - \eta \sum_{\ell=1}^K \mathbf{Z}_{t,\ell} R_{t,\ell}$.
- 15: Broadcast $R_{t,\ell}$.
- 16: Clients recover $\mathbf{w}^{(t+1)}$ using $R_{t,\ell}$ and the known $\mathbf{Z}_{t,\ell}$.
- 17: **end for**

• **Sampling perturbation directions:** For each local epoch $\ell \in [K]$, all clients and the federator first generate $\nu \geq 1$ pseudorandom perturbations $\mathbf{z}_{t,\ell}^1, \dots, \mathbf{z}_{t,\ell}^\nu$. We consider two different settings:

– **Unbiased ZO estimator:** In this case, $\mathbf{z}_{t,\ell}^r \sim \mathcal{U}(\mathbb{S}^d)$ for each $\ell \in [K]$ and $r \in [\nu]$, as done in Algorithm 1.

– **Biased ZO estimator:** In a modified version (see Algorithm 5), we choose $\mathbf{z}_{t,1}^r \sim \mathcal{U}(\mathbb{S}^d)$ for each $r \in [\nu]$ and set $\mathbf{z}_{t,\ell}^r = \mathbf{z}_{t,1}^r$ for $\ell > 1$.

• **Local epochs (client-side):** For each local epoch ℓ , client i samples a mini-batch $\tilde{\mathcal{D}}_i$ and computes the two-point zero-order gradient estimate $\mathbf{z}_{t,\ell}^r g(\mathbf{w}_{t,\ell}^i, \mathbf{z}_{t,\ell}^r, \mu, \tilde{\mathcal{D}}_i)$ for each $r \in [\nu]$. Subsequently, it averages the ν different estimates thus obtained to compute a multi-point ZO estimate and updates its local model using this gradient estimate. Mathematically, let $\mathbf{w}_{t,\ell}^i$ be client i 's local model and let $g_i(\mathbf{w}_{t,\ell}^i, \mathbf{Z}_{t,\ell}) \triangleq g(\mathbf{w}_{t,\ell}^i, \mathbf{z}_{t,\ell}^r, \mu, \tilde{\mathcal{D}}_i)$. Let $\mathbf{Z}_{t,\ell} \in \mathbb{R}^{d \times \nu}$ denote the matrix $(\mathbf{z}_{t,\ell}^1, \dots, \mathbf{z}_{t,\ell}^\nu)$ and $\mathbf{g}_i(\mathbf{w}_{t,\ell}^i, \mathbf{Z}_{t,\ell}) \triangleq ((g_i(\mathbf{w}_{t,\ell}^i, \mathbf{z}_{t,\ell}^r))_{r=1}^\nu)^\top$. The clients update their model as $\mathbf{w}_{t,\ell+1}^i = \mathbf{w}_{t,\ell}^i - \eta \mathbf{Z}_{t,\ell} \mathbf{g}_i(\mathbf{w}_{t,\ell}^i, \mathbf{Z}_{t,\ell})$.

• **Client-to-federator model update:** At the end of local epoch K , each client i transmits its cumulative model update to the federator by specifying the projection along the perturbation directions. In the unbiased setting, this is performed at a communication cost of $K\nu$ scalars per client by transmitting $\{\mathbf{g}_i(\mathbf{w}_{t,\ell}^i, \mathbf{Z}_{t,\ell}) : \ell \in [K]\}$, while in the biased setting, this entails a communication cost of ν scalars per client by transmitting $\sum_{\ell=1}^K \mathbf{g}_i(\mathbf{w}_{t,\ell}^i, \mathbf{Z}_{t,\ell})$.

• **Transformed robust aggregation (federator side):**

Upon receiving the model updates from all clients, the federator performs robust aggregation on the model update vectors. Let $R : (\mathbb{R}^\nu)^n \rightarrow \mathbb{R}^\nu$ be a given robust aggregation rule. In the unbiased setting, the federator applies this on each local epoch separately, *i.e.*, it computes $R(\{\mathbf{g}_i(\mathbf{w}_{t,\ell}^i, \mathbf{Z}_{t,\ell})\}_{i \in [n]})$ for each ℓ , and updates the global model as $\mathbf{w}^{(t+1)} = \mathbf{w}^{(t)} - \eta \sum_{\ell=1}^K \mathbf{Z}_{t,\ell} R(\{\mathbf{g}_i(\mathbf{w}_{t,\ell}^i, \mathbf{Z}_{t,\ell})\}_{i \in [n]})$. In the biased setting, the robust aggregation is performed on the cumulative updates across all local epochs, *i.e.*, the federator updates the global model as $\mathbf{w}^{(t+1)} = \mathbf{w}^{(t)} - \eta \mathbf{Z}_{t,1} R(\{\sum_{\ell=1}^K \mathbf{g}_i(\mathbf{w}_{t,\ell}^i, \mathbf{Z}_{t,\ell})\}_{i \in [n]})$.

- **Global model broadcast:** Lastly, the federator conveys the updated model $\mathbf{w}^{(t+1)}$ by sending the projections of $\mathbf{w}^{(t+1)} - \mathbf{w}^{(t)}$ along the perturbation vectors $\{\mathbf{z}_{t,\ell}^r : \ell \in [K], r \in [\nu]\}$. Note that, all clients know the perturbation vectors and $\mathbf{w}^{(t)}$. Hence, they can recover $\mathbf{w}^{(t+1)}$ as the global model updates always lie in the subspace spanned by the current epoch’s perturbation vectors.

3.2 Choice of robust aggregation rule

CYBER-0 is compatible with arbitrary robust aggregation rules. In our theoretical analysis, the robustness guarantees of CYBER-0 depend on the parameters b and κ , which characterize the rule’s robustness (see Definition 2.2). Below, we outline three widely used aggregation rules from the literature that we employ in our experimental evaluation.

- **Coordinate-wise trimmed mean (CWTM):** CWTM is a simple yet effective aggregation rule that removes the $\lfloor \beta n \rfloor$ smallest and largest values on a per-coordinate basis, then averages the remaining values for a design parameter β . In our experiments, we set β to be b/n .

Definition 3.1 (CWTM (Yin et al., 2018)). Let $0 \leq \beta < 1/2$ be a design parameter, let $\mathcal{X} = \{\mathbf{v}_1, \dots, \mathbf{v}_n\}$ be a multiset of n vectors $\mathbf{v}_i = (v_{i,1}, \dots, v_{i,\nu}) \in \mathbb{R}^\nu$ and define \mathcal{X}_j as the multiset obtained from $v_{0,j}, \dots, v_{n,j}$ by removing the smallest and largest $\lfloor \beta n \rfloor$ elements. CWTM outputs a vector where the j -th entry is computed as $\frac{1}{n-2\lfloor \beta n \rfloor} \sum_{x \in \mathcal{X}_j} x$. Hence, $\text{CWTM}_\beta(\{\mathbf{v}_i\}_{i \in [n]}) = \frac{1}{n-2\lfloor \beta n \rfloor} (\sum_{x \in \mathcal{X}_1} x, \dots, \sum_{x \in \mathcal{X}_\nu} x)$.

- **Krum:** Krum selects a single vector from n candidate vectors by focusing on local geometric consistency to limit the influence of outliers. In our experiments, we set the Byzantine budget to b out of n clients.

Definition 3.2 (Krum (Blanchard et al., 2017)). Let $\mathcal{X} = \{\mathbf{v}_1, \dots, \mathbf{v}_n\}$ be a multiset of n vectors, and $d_{i,j}$ the Euclidean distance between \mathbf{v}_i and \mathbf{v}_j . Let \mathcal{C}_i be the set of indices of the $n - b - 2$ vectors closest to \mathbf{v}_i in Euclidean distance. Krum outputs the vector \mathbf{v}_{i^*} with $i^* = \arg \min_{i \in [n]} \sum_{j \in \mathcal{C}_i} d_{i,j}$.

- **Nearest neighbor mixing (NNM):** NNM is a pre-processing method that can be composed with standard robust aggregation rules to improve their Byzantine-resilience

under heterogeneous data. NNM mixes the clients’ gradients with their nearest neighbors as follows.

Definition 3.3 (NNM (Allouah et al., 2023)). Consider n vectors $\mathbf{v}_1, \dots, \mathbf{v}_n$ and a parameter b . For each \mathbf{v}_i , index the vectors into $\mathbf{v}_{i,1}, \dots, \mathbf{v}_{i,n}$ such that $\|\mathbf{v}_{i,1} - \mathbf{v}_i\|_2 \leq \dots \leq \|\mathbf{v}_{i,n} - \mathbf{v}_i\|_2$. NNM outputs the vectors $\bar{\mathbf{v}}_1, \dots, \bar{\mathbf{v}}_n$, where $\bar{\mathbf{v}}_i = \frac{1}{n-b} \sum_{j=1}^{n-b} \mathbf{v}_{i,j}$.

3.3 Innovations in CYBER-0

In the following, we mention a few challenges addressed by CYBER-0 and highlight its key technical novelties.

- **Transformed robust aggregation via embeddings:** Robust aggregation of the full gradients is well understood for achieving Byzantine resilience in FL. However, in CYBER-0 the federator only has access to the model updates along the random perturbations rather than full gradients.

A naive approach would be for the federator to first reconstruct approximate gradients from the ZO updates and then apply robust aggregation. However, in general, robust aggregation rules are non-linear, and the aggregate vector may lie outside the subspace spanned by the input vectors. For example, consider vectors $\mathbf{v}_1 = [2, 2, 0]^\top$, $\mathbf{v}_2 = [0, -1, -1]^\top$, and $\mathbf{v}_3 = [4, 0, -4]^\top$ that lie in the vector space \mathcal{V} spanned by $\{[1, 1, 0]^\top, [0, 1, 1]^\top\}$. Then, $\text{CWTM}_{1/3}(\mathbf{v}_1, \mathbf{v}_2, \mathbf{v}_3) = [2, 0, -1]^\top \notin \mathcal{V}$ (see Definition 3.1). In our context, this implies that the global model update $\mathbf{w}^{(t+1)} - \mathbf{w}^{(t)}$ does not necessarily lie in the subspace spanned by the perturbation vectors $\{\mathbf{z}_{t,\ell}^r : r \in [\nu], \ell \in [K]\}$. Thus, communicating the global model update requires either additional communication cost or projecting the global model update back onto the subspace, incurring additional variance and computation.

To address this issue, CYBER-0 introduces *transformed robust aggregation*, *i.e.*, robust aggregation of the clients’ model updates when viewed as vectors embedded in the perturbation space \mathbb{R}^ν . By directly aggregating in this lower dimensional perturbation space, CYBER-0 preserves communication savings (as the aggregated updates continue to belong to the perturbation space). A key challenge is to argue that performing the aggregation in the perturbation space and projecting the result back to the gradient space preserves the robustness guarantees from Definition 2.2. To prove this, we rely on Johnson–Lindenstrauss–style embeddings (Johnson & Lindenstrauss, 1984) to maintain the necessary geometric properties of robust aggregation. Thus, the aggregation remains both efficient and Byzantine-resilient, while limiting the attackers’ ability to manipulate the global update outside the chosen subspace.

- **Efficient downlink and uplink communication:** We leverage the structure of ZO updates and transformed robust aggregation to significantly reduce the communication cost on the uplink and the downlink. On the uplink, this is a consequence of having the clients perform local epochs and

transmit only the resulting scalar values for each perturbation direction. On the downlink, as the transformed robust aggregation outcome is guaranteed to lie in the span of the perturbation vectors, it is sufficient to only specify the projections along the perturbation directions. This reduces the communication burden to a handful of scalars, which is a major reduction compared to typical FL settings where the gradient dimension can range from 10^6 to 10^{12} .

- **Shared seed mechanism for synchronizing perturbations:** To ensure correct global model updates, the random perturbation directions must be synchronized between the federator and the clients. A naive, yet inefficient strategy would be to transmit the newly generated perturbation vectors in every round, but this negates any communication gains since their dimension matches that of the model. In CYBER-0, we address this challenge by adopting a lightweight shared seed protocol, inspired by [Salimans et al. \(2017\)](#), which enables both the clients and the federator to locally generate identical pseudorandom perturbations. Note that the (one-time) cost of sharing a common seed determined by the federator with all clients is negligible given that standard PRNGs, *e.g.*, in Tensorflow, have a cycle length in the order of 2^{128} ([Salmon et al., 2011](#)).

- **Multiple local epochs per client:** We show that CYBER-0 works well with each client performing multiple local epochs. This results in a reduction in the number of global epochs (and hence less frequent communication). Further, CYBER-0 also offers a design choice between the unbiased ZO estimator and the biased ZO estimator. The former is more amenable to theoretical analysis as $\mathbf{Z}_{t,\ell}$'s are independent across the local epochs. However, it has a communication cost of $K\nu$ per global epoch (both on each uplink as well as the downlink). The biased ZO estimator further reduces the communication cost by a factor of K by deliberately using the same perturbation vectors for each local iteration. This, however, introduces additional bias into the training process. We explore this tradeoff under varying numbers of local epochs in Appendix A.4.

- **Computation and memory efficiency:** While it is well established that ZO methods reduce the computation cost, especially when ν is small, the reduction in the memory requirements are especially impressive even when ν is large. [Malladi et al. \(2023\)](#) showed that ZO methods perform inference utilizing upto a factor of 12 lower memory compared to backpropagation. CYBER-0 inherits this property and can operate on resource constraint edge devices in fine-tuning tasks where classical approaches are intractable. The details can be found in Appendix A.1.

4 Experimental Evaluation

We evaluate CYBER-0 under a range of training tasks and Byzantine attacks. First, on logistic regression with MNIST, we compare CYBER-0 (with CWTM and Krum as trans-

formed robust aggregations) against standard FL (FedAvg) with (non-transformed) CWTM and Krum as robust aggregations, optionally combined with Nearest-Neighbor Mixing (NNM). Our results show that CYBER-0 achieves better worst-case accuracies than FedAvg, while requiring two orders of magnitude less communication (Figure 1(b)).

To highlight its real-world applicability, we follow [Malladi et al. \(2023\)](#) in fine-tuning RoBERTa-large ([Liu, 2019](#)) for various natural language processing (NLP) tasks. Here, CYBER-0 maintains competitive accuracies under a variety of attacks with communication savings of up to seven orders of magnitude (Figure 2).

4.1 Setup

Data Distribution. To model data heterogeneity, we base the data allocation according to the labels of the samples. First, we consider an i.i.d. scenario, where the data \mathcal{D}_i of each client stems from the same underlying distribution. Therefore, each client gets the same fraction of samples from a certain label. Detecting outliers arising from Byzantine behavior is usually less challenging in i.i.d. regimes as each honest client computes, on expectation, similar gradient. To model heterogeneous regimes, referred to as the non-i.i.d. scenario, for each label, we draw a distribution over the clients that determines the portion of samples each client gets from a given label. We employ a Dirichlet distribution, where the parameter α models the level of heterogeneity. For $\alpha \rightarrow \infty$, we recover the i.i.d. scenario from above. The difficulty of heterogeneous regimes increases with decreasing values for α . Hence, for the non-i.i.d. case, we focus on $\alpha \in \{0.1, 1\}$ as two challenging regimes.

Attack Models. We evaluate the robustness and efficiency of our method under a variety of established attacks, *i.e.*, *A Little is Enough* (ALIE) ([Baruch et al., 2019](#)), *Fall of Empires* (FOE) ([Xie et al., 2020](#)), *Sign Flipping* (SF) ([Allen-Zhu et al., 2021](#)) and *Label Flipping* (LF) ([Allen-Zhu et al., 2021](#)). We provide the details of the attacks in Appendix A.1. For CYBER-0, all attacks operate on the projected gradients $\mathbf{g}_i(\mathbf{w}_{t,\ell}^i, \mathbf{Z}_{t,\ell})$; while for the non-projected counterparts, the attacks operate on the gradients. This represents the strongest possible adversarial behavior. ALIE and FOE involve an optimization tailored to the used robust aggregation rule. On a high level, the manipulations are chosen to maximize the distance to the desired honest outcome of the aggregated gradient. When investigating robust aggregation rules R composed with NNM, we present two variants of ALIE and FOE, optimized to R , and optimized to $\text{NNM} \circ R$. We term the latter ALIE-NNM and FOE-NNM, and find they can reduce the benefits of NNM in certain cases. For fine-tuning tasks, we settle on CWTM as transformed robust aggregation, and additionally challenge our algorithm with a specifically tailored full-knowledge attack, inspired by [Fang](#)

Byzantine-Resilient Zero-Order Optimization for Communication-Efficient Heterogeneous Federated Learning

Table 1. Mean and standard deviation of maximum accuracies across seeds. The baseline FedAvg without robust aggregation nor Byzantine attacks achieves 91.0 ± 0.2

Algorithm	R. Agg.	NNM	ALIE	ALIE-NNM	FOE	FOE-NNM	SF	LF
CYBER-0	CWTM	No	87.4 ± 0.6	-	69.9 ± 4.8	-	71.2 ± 2.0	87.6 ± 0.6
CYBER-0	CWTM	Yes	90.3 ± 0.3	88.9 ± 1.3	74.0 ± 7.3	58.9 ± 4.9	59.2 ± 3.5	90.1 ± 0.6
CYBER-0	Krum	No	65.1 ± 8.9	-	34.7 ± 5.4	-	44.1 ± 11.9	66.3 ± 9.9
CYBER-0	Krum	Yes	90.6 ± 0.4	89.9 ± 0.4	70.4 ± 4.4	56.9 ± 6.0	58.2 ± 2.7	87.1 ± 3.5
FedAvg	CWTM	No	87.6 ± 0.7	-	41.7 ± 4.8	-	42.5 ± 7.9	80.8 ± 1.4
FedAvg	CWTM	Yes	90.6 ± 0.3	86.9 ± 1.2	76.8 ± 3.2	58.5 ± 2.8	67.3 ± 2.6	87.9 ± 3.5
FedAvg	Krum	No	75.7 ± 3.5	-	23.9 ± 13.5	-	50.0 ± 8.9	55.9 ± 6.9
FedAvg	Krum	Yes	88.6 ± 0.6	86.9 ± 1.1	73.0 ± 2.0	50.0 ± 4.1	57.7 ± 5.8	83.9 ± 4.6

et al. (2020) that targets maximizing the gradient deviation compared to the honest clients. Please see Appendix A.2 for details.

4.2 Comprehensive Study for Logistic Regression

We evaluate CYBER-0 compared to various baselines (cf. Allouah et al. (2023)) on ALIE, FOE, SF, and LF. We use $n = 40$ clients, from which $b = 10$ are Byzantine, and refer to Appendix A.3 for details of the experimental setup. CWTM is parameterized with $\beta = \frac{b}{n} = 0.25$. The parameter ν is set to $\nu = 64$. All results show averaged results over 5 runs with different seeds, including their standard deviations (shown after \pm in the tables, and with shaded areas in the plots). In Table 1, we provide results for all attacks on CYBER-0 combined with transformed CWTM and Krum, and FedAvg with CWTM and Krum. All variants are tested with and without NNM composition. If composed with NNM, we provide additionally the improved attacks described above, *i.e.*, ALIE-NNM and FOE-NNM. The worst-case performance of each robust aggregation across all attacks is highlighted in bold. With the exception of ALIE-NNM and FOE-NNM, the robustness against all attacks improves uniformly with the introduction of NNM.

CYBER-0 exhibits better worst-case robustness for all aggregation rules compared to standard Byzantine resilient FL and CYBER-0-CWTM outperforms the best of all state-of-the-art methods by more than 10 percent. We note that the goal of this section is not to optimize the absolute achieved accuracies of the presented schemes, but rather to provide a comprehensive overview and comparison for many attacks and robust aggregation rules.

We provide in Figure 1 a selection of plots showing the average accuracies as a function of global epochs and the communication cost. In Figure 1(a), we show for CYBER-0-CWTM the performance across all applicable attacks. The worst-case behavior is dominated by FOE. Figure 1(b) shows the significant performance improvements brought by CYBER-0 compared to its non-zero-order counterparts, and the reduction in communication cost by multiple orders of magnitude. While for Krum, the performance is improved

by more than 10%, the performance of CWTM is improved by more than 25% for the worst-case attack. In Figure 1(c), we show the performance improvements brought by both CYBER-0 and NNM against LF attack. The graphs of the remaining attacks are provided in Appendix A.6.

CYBER-0 allows for different strategies to conduct local epochs at the clients. Instead of the method presented in Algorithm 1, we present and compare in Appendix A.4 three different methods, exposing an efficiency-bias-variance trade-off. We further study the effect of the parameter ν in Appendix A.5 in standard, non-fine-tuning learning tasks.

4.3 Fine-Tuning Large Language Models

We follow the lines of Malladi et al. (2023) and investigate different fine-tuning tasks in the realm of NLP using the well-established RoBERTa-large (Liu, 2019). We conduct sentiment analysis on SST-2 (Socher et al., 2013), natural language inference (NLI) on the SNLI dataset (Bowman et al., 2015), and topic classification on TREC (Voorhees & Tice, 2000). We fix CWTM as a robust aggregation technique, as it was earlier shown to yield the best performance in CYBER-0. We average all results over three runs with different seeds. Due to space constraints, some of the results are shown in the Appendix.

Table 6 shows the results of CYBER-0-CWTM under ALIE, FOE, SF, and TMA for a non-i.i.d. data distribution with $\alpha = 1$, and compare the results to the baseline accuracy without attack. We set $n = 12$, $b = 3$ and $\nu = 1$. The rightmost column shows the worst-case accuracies over all attacks. It can be found that the worst-case attacks degrade the accuracy of fine-tuning on SST-2 by only approximately one percent, and that of SNLI and TREC by 7 – 8%. We plot in Figure 2 the evaluation accuracies throughout the fine-tuning process for all attacks, compared to the baseline. It can be clearly seen that FOE is the most challenging attack in this regime. For more plots, we refer the interested reader to Appendix A.7. Further, we perform the same study for an i.i.d. data distribution ($\alpha = \infty$), and find that CYBER-0 exhibits extremely stable performance under both i.i.d. and non-i.i.d. data. We refer the reader to Appendix A.7 for the

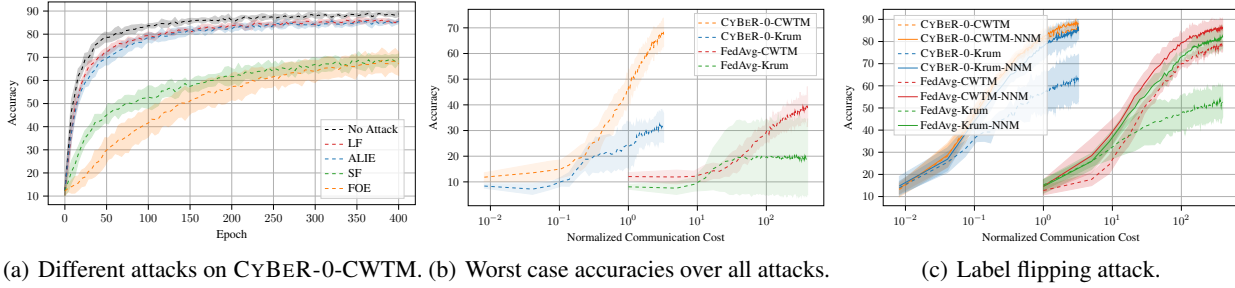


Figure 1. Performance of different robust aggregation rules against different attacks for logistic regression on MNIST.

results.

We give an extensive hyperparameter study for CYBER-0 in fine-tuning tasks. We run our experiments on SST-2 and RoBERTa-large, attacked by FOE. We use non-i.i.d. data with $\alpha = 0.1$. Please see Appendix A.8 for detailed results. We show the robustness of CYBER-0 under varying numbers of total and Byzantine clients with $\frac{b}{n} = 0.25$ and observe that the robustness increases with n . We study the stability of CYBER-0 under varying numbers ν of random perturbations, $n = 8$ and $b = 2$. For comparability, we fix the ratio $\nu T = 20000$ and observe very similar accuracies for $\nu \in \{1, 2, 4, 8\}$. Hence, the number of projections trades almost inversely with the number of global epochs T . A similar behavior is observed for a varying number of local epochs K , fixing the ratio KT . However, for large K and small T , we can see the negative impacts of local iterations. Lastly, we evaluate CYBER-0 under varying ratios of Byzantine clients, thereby fixing $n = 16$ for better flexibility, and using $\nu = 1$. While the performance reduction from $b = 2$ to $b = 4$ is negligible, we can observe a notable difference for $b = 6$, *i.e.*, when the number of Byzantine clients is close to $n/2$.

5 Convergence Analysis

We now turn our attention to theoretical guarantees on the convergence of CYBER-0. We provide a thorough theoretical analysis for arbitrary (b, κ) -robust aggregation rules, suitably transformed to account for ZO estimates, under het-

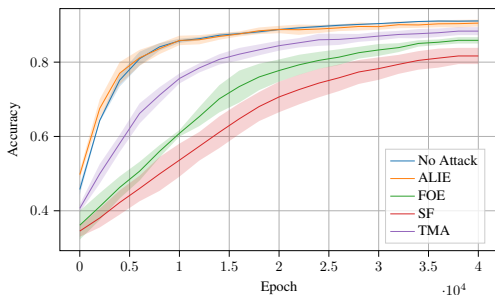


Figure 2. Accuracy over epochs for fine-tuning RoBERTa-large on TREC under different attack scenarios for non-i.i.d. data.

erogeneous data distribution and general non-convex loss functions. We employ the heterogeneity model introduced by Wang et al. (2025) in our analysis.

Challenges and novelty. While Allouah et al. (2023) provides a roadmap for analyzing robustness in non-convex regimes, the combination with ZO methods incurring bias and high variance poses particular challenges, especially given that, in expectation, the robust aggregation output does not necessarily equal the expectation of the honest clients’ gradient estimate. In addition to the challenges from the gradient estimates, the robust aggregation is here conducted on a transformed space instead of on estimated gradients themselves. We show, through a novel application of projection theorems to ZO methods, that such methods can converge even under adversarial attacks in harsh heterogeneous and non-convex settings. Although Fang et al. (2022) study the convergence of ZO FL methods in heterogeneous settings, the introduction of Byzantine resilience poses particular challenges, amplified by the new notion of heterogeneity (Wang et al., 2025). Even without robustness, the analysis of Wang et al. (2025) does not apply to ZO methods due to the bias and variance of the gradient estimates, which exhibit additional restrictions on the learning rate and incur a more complex analysis.

Tackling the above challenges, we believe that the combination of ZO optimization, Byzantine resilience, heterogeneity models, non-convexity, and transformed robust aggregation in gradient embedding spaces exhibits unique challenges interesting from a purely theoretical perspective. We make the following assumptions.

Assumption 5.1 (Lipschitz gradient). $\forall \mathbf{w}, \omega \in \mathbb{R}^d, i \in [n]$,

$$\|\nabla F_i(\mathbf{w}) - \nabla F_i(\omega)\| \leq L \|\mathbf{w} - \omega\|. \quad (1)$$

Assumption 5.2 (Bounded gradient variance). The variance of the clients’ gradient estimate is uniformly bounded as

$$\mathbb{E} \left[\|\mathbf{g}_i(\mathbf{w}) - \nabla F_i(\mathbf{w})\|^2 \right] \leq \sigma^2, \forall \mathbf{w}, i \in [n]. \quad (2)$$

Following Wang et al. (2025), we assume the following two properties to model the heterogeneity of the system.

Table 2. Mean and Standard Deviation of Maximum Accuracies Across Seeds

Dataset	ALIE	FOE	SF	TMA	No Attack	Worst Case
SST-2	93.3 ± 0.4	91.7 ± 1.5	91.6 ± 0.5	92.1 ± 1.2	92.9 ± 0.1	91.6
SNLI	80.8 ± 1.4	78.4 ± 2.1	76.1 ± 1.0	80.0 ± 0.7	84.3 ± 0.2	76.1
TREC	93.3 ± 1.2	91.7 ± 1.0	87.7 ± 2.9	92.2 ± 1.1	94.7 ± 0.7	87.7

Assumption 5.3 (Bounded gradient divergence). It holds

$$\|\nabla F_i(\mathbf{w}) - \nabla F_{\mathcal{H}}(\mathbf{w})\|^2 \leq \zeta^2, \forall i \in [n]. \quad (3)$$

Assumption 5.4 (Pseudo-Lipschitz on averaged gradients).

$$\left\| \frac{1}{n} \sum_{i=1}^n \nabla F_i(\mathbf{w}_i) - \nabla F_{\mathcal{H}}(\bar{\mathbf{w}}) \right\|^2 \leq \frac{D^2}{n} \sum_{i=1}^n \|\mathbf{w}_i - \bar{\mathbf{w}}\|^2 \quad (4)$$

For a given model \mathbf{w} , let $\nabla F_i^\mu \triangleq \mathbb{E}_{\mathbf{z} \sim \mathcal{U}(\mathbb{S}^d)}[\nabla F_i(\mathbf{w} + \mu \mathbf{z})]$ be a smoothed version of the gradient ∇F_i . Then, for the two-point zero-order estimate from Definition 2.1, we have the following well-known result (Flaxman et al., 2005).

Proposition 5.5. *The ZO estimate satisfies on expectation*

$$\mathbb{E}[\mathbf{Z}_{t,\ell} \mathbf{g}_i(\mathbf{w}_{t,\ell}^i, \mathbf{Z}_{t,\ell})] = \nabla F_i^\mu(\mathbf{w}_{t,\ell}^i).$$

Proposition 5.6 (Lemma 2, (Tang et al., 2020)). *It holds*

$$\|\nabla F_i^\mu(\mathbf{w}_{t,\ell}^i) - \nabla F_i(\mathbf{w}_{t,\ell}^i)\| \leq L\mu.$$

All proofs are deferred to Appendix B. Under the assumptions above, we present the following convergence guarantee for non-convex loss landscapes.

Let $\epsilon = \sqrt{\frac{64}{\nu} \log(\frac{2(|\mathcal{H}|-1)}{\delta})}$, and $\epsilon' \triangleq \frac{(1+\epsilon)}{(1-\epsilon)}$. Let c_1, c_2, c_3, c_4 and c_5 be as defined in (12)-(17) in Appendix B. These constants scale as follows: $c_1 = \Theta(\eta^2 K^3 \frac{d}{\nu} + \frac{d}{\nu} L^2 \eta^2 K (K + \frac{d}{|\mathcal{H}|\nu}))$, $c_2 = \Theta(\eta^2 K^3 (L + (\frac{d}{\nu} + \frac{d^2}{\nu^2 |\mathcal{H}|} L^2 K^2 \eta^2) (\zeta^2 + \sigma^2 + L^2 \mu d))$, $c_3 = \Theta(\frac{d}{\nu} (K^2 \epsilon' \kappa + \frac{K}{|\mathcal{H}|}) (1 + L^2 \eta^2 K (K + \frac{d}{|\mathcal{H}|\nu})) (1 + \frac{\nu}{d}))$, $c_4 = \Theta(K^2 L^2 \eta^2 (K^2 D^2 + \frac{1}{|\mathcal{H}|} \frac{d^2}{\nu^2} L^2) + K \epsilon' \kappa (D^2 + \zeta^2 + \frac{d}{\nu} L^2))$ and $c_5 = \Theta((\zeta^2 + \sigma^2 + L^2 \mu^2 d) ((K^2 \epsilon' \kappa) (\frac{d}{\nu} + \frac{d^2}{\nu^2 |\mathcal{H}|} L^2 K \eta^2)) + K^2 L (\epsilon' \kappa + \mu) + (K^2 \epsilon' \kappa) (\frac{d}{\nu} L^2 \eta^2 K^2 L \mu))$.

Theorem 5.7 (General non-convex landscapes). *Let $0 < \Delta < 1$ and suppose that Assumptions 5.1 to 5.4 hold. Consider CYBER-0 with a $(|\mathcal{H}|, \kappa)$ -robust aggregation rule. If (a) $\eta^2 \leq \min\{\frac{1}{72K^2L}, \frac{|\mathcal{H}|\nu}{96KdL^2}, 6\frac{D^2}{K^2} + 6\frac{\zeta^2}{K^2} + \frac{32d}{\nu K^2} L^2\}$, (b) $\nu \geq 64 \log(\frac{2(|\mathcal{H}|-1)TK}{\Delta})$, and (c) $c_3 + c_4 c_1 \leq \frac{1}{2}$ are satisfied, then the following convergence guarantee holds with probability $1 - \Delta$:*

$$\frac{1}{T} \sum_{t=1}^T \mathbb{E} \left[\|\nabla F_{\mathcal{H}}(\mathbf{w}_t)\|^2 \right] \leq \frac{4(F_{\mathcal{H}}(\mathbf{w}_1) - F_{\mathcal{H}}^*)}{\eta KT} + \eta / (2K) (c_4 c_2 + c_5).$$

Note that Theorem 5.7 requires $\nu = \Theta(d)$ in order for condition (c) to be satisfied. However, our empirical results demonstrate that CYBER-0 converges even when $\nu = 1$. To bridge the gap between our empirical finding and the analysis, we make the following additional assumption.³

Assumption 5.8 (Lipschitz Objective function). $\forall i \in [n]$,

$$\|F_i(\mathbf{w}) - F_i(\omega)\| \leq G \|\mathbf{w} - \omega\|, \forall \mathbf{w}, \omega \in \mathbb{R}^d. \quad (5)$$

Theorem 5.9 (Lipschitz objective functions). *Let $0 < \Delta < 1$, and suppose that Assumptions 5.1 to 5.4 hold. Consider CYBER-0 with $\mu > 0$ and a $(|\mathcal{H}|, \kappa)$ -robust aggregation rule. If (a) $\eta \leq \min\{\frac{1}{26KL}, \frac{1}{4K\sqrt{D^2+\zeta^2}}\}$, and (b) $\nu \geq 64 \log(\frac{2(|\mathcal{H}|-1)TK}{\Delta})$, the following convergence guarantee holds with probability at least $1 - \Delta$:*

$$\begin{aligned} \frac{1}{T} \sum_{t=1}^T \mathbb{E} \left[\|\nabla F_{\mathcal{H}}(\mathbf{w}_t)\|^2 \right] &\leq \frac{4(F_{\mathcal{H}}(\mathbf{w}_1) - F_{\mathcal{H}}^*)}{\eta TK} \\ &+ 2\eta K D^2 \left(\frac{\varphi^2 G^2 d}{L^2 \nu} + \frac{3}{L} \right) \left(13K + 24\epsilon' \kappa (1 + \frac{\zeta^2}{D^2}) + 4 \right) \\ &+ 2\eta \frac{\varphi^2 G^2 d}{\nu} \left(\frac{1}{5|\mathcal{H}|} + \frac{8}{|\mathcal{H}|^2} + 2K\epsilon' \kappa \right) + 12KL\eta (\kappa\epsilon' + \mu). \end{aligned}$$

6 Conclusion

In this work, we introduced CYBER-0, a Byzantine-resilient, communication-efficient FL framework that combines zero-order (ZO) optimization with arbitrary robust aggregation rules. CYBER-0 uses a shared-seed mechanism to generate identical pseudorandom perturbations at the clients and the federator. This enables ZO updates to be communicated using only a few scalars, thus drastically reduces the communication overhead.

A key novelty of our approach is the introduction of *transformed robust aggregation*, which operates directly in the perturbation space rather than on reconstructed gradients. This ensures compatibility of widely-used robust aggregation rules with ZO updates while retaining Byzantine resilience. Using Johnson-Lindenstrauss embeddings, we establish provable convergence guarantees under non-convex losses, even in adversarial and heterogeneous settings.

³In applications such as fine-tuning, Assumption 5.8 may be implied by Assumption 5.1. If it is known that the initial model \mathbf{w}_1 is within a distance Γ to a local optimal, then Assumption 5.8 is satisfied with $G = L\Gamma^2/2$.

Empirical evaluations on logistic regression (MNIST) and fine-tuning RoBERTa-large (NLP) demonstrate that the worst-case robustness of CYBER-0 is close to full-gradient Byzantine robust algorithms even though the communication costs are lower by up to seven orders of magnitude. Additionally, its low memory and computational footprint make it well-suited for resource-constrained edge devices.

Impact Statement

This paper presents work whose goal is to advance the field of Machine Learning. There are many potential societal consequences of our work, none which we feel must be specifically highlighted here.

References

- Allen-Zhu, Z., Ebrahimiaghazani, F., Li, J., and Alistarh, D. Byzantine-resilient non-convex stochastic gradient descent. In *International Conference on Learning Representations*, 2021.
- Allouah, Y., Farhadkhani, S., Guerraoui, R., Gupta, N., Pinot, R., and Stephan, J. Fixing by mixing: A recipe for optimal byzantine ml under heterogeneity. In *International Conference on Artificial Intelligence and Statistics*, pp. 1232–1300, 2023.
- Bagdasaryan, E., Poursaeed, O., and Shmatikov, V. Differential privacy has disparate impact on model accuracy. *Advances in neural information processing systems*, 32, 2019.
- Baruch, G., Baruch, M., and Goldberg, Y. A little is enough: Circumventing defenses for distributed learning. *Advances in Neural Information Processing Systems*, 32, 2019.
- Blanchard, P., El Mhamdi, E. M., Guerraoui, R., and Stainer, J. Machine learning with adversaries: Byzantine tolerant gradient descent. *Advances in neural information processing systems*, 30, 2017.
- Bowman, S. R., Angeli, G., Potts, C., and Manning, C. D. A large annotated corpus for learning natural language inference. In *Empirical Methods in Natural Language Processing*, pp. 632–642, 2015.
- Charikar, M., Steinhardt, J., and Valiant, G. Learning from untrusted data. In *ACM SIGACT Symposium on Theory of Computing*, pp. 47–60, 2017.
- Chen, J., Chen, H., Gu, B., and Deng, H. Fine-grained theoretical analysis of federated zeroth-order optimization. In *Neural Information Processing Systems*, 2023.
- Duchi, J. C., Jordan, M. I., Wainwright, M. J., and Wibisono, A. Optimal rates for zero-order convex optimization: The power of two function evaluations. *IEEE Transactions on Information Theory*, 61(5):2788–2806, 2015.
- Egger, M., Hofmeister, C., Wachter-Zeh, A., and Bitar, R. Private aggregation in wireless federated learning with heterogeneous clusters. In *IEEE International Symposium on Information Theory (ISIT)*, pp. 54–59, 2023.
- El-Mhamdi, E. M., Farhadkhani, S., Guerraoui, R., Guirguis, A., Hoang, L.-N., and Rouault, S. Collaborative learning in the jungle (decentralized, byzantine, heterogeneous, asynchronous and nonconvex learning). *Advances in neural information processing systems*, 34:25044–25057, 2021.
- Fang, M., Cao, X., Jia, J., and Gong, N. Local model poisoning attacks to byzantine-robust federated learning. In *USENIX security symposium*, pp. 1605–1622, 2020.
- Fang, W., Yu, Z., Jiang, Y., Shi, Y., Jones, C. N., and Zhou, Y. Communication-efficient stochastic zeroth-order optimization for federated learning. *IEEE Transactions on Signal Processing*, 70:5058–5073, 2022.
- Flaxman, A. D., Kalai, A. T., and McMahan, H. B. Online convex optimization in the bandit setting: gradient descent without a gradient. In *ACM-SIAM Symposium on Discrete Algorithms*, pp. 385–394, 2005.
- Gao, X., Jiang, B., and Zhang, S. On the information-adaptive variants of the admm: an iteration complexity perspective. *Journal of Scientific Computing*, 76:327–363, 2018.
- Ghadimi, S. and Lan, G. Stochastic first- and zeroth-order methods for nonconvex stochastic programming. *SIAM Journal on Optimization*, 23(4):2341–2368, 2013.
- Ilyas, A., Engstrom, L., Athalye, A., and Lin, J. Black-box adversarial attacks with limited queries and information. In *International Conference on Machine Learning*, pp. 2137–2146, 2018.
- Jahani-Nezhad, T., Maddah-Ali, M. A., Li, S., and Caire, G. SwiftAgg+: Achieving asymptotically optimal communication loads in secure aggregation for federated learning. *IEEE Journal on Selected Areas in Communications*, 41(4):977–989, 2023.
- Johnson, W. and Lindenstrauss, J. Extensions of lipschitz maps into a hilbert space. *Contemporary Mathematics*, 26:189–206, 01 1984.
- Karimireddy, S. P., Rebjock, Q., Stich, S., and Jaggi, M. Error feedback fixes SignSGD and other gradient compression schemes. In *International Conference on Machine Learning*, pp. 3252–3261, 2019.

- Karimireddy, S. P., He, L., and Jaggi, M. Byzantine-robust learning on heterogeneous datasets via bucketing. In *International Conference on Learning Representations*, 2022.
- Kiefer, J. and Wolfowitz, J. Stochastic Estimation of the Maximum of a Regression Function. *The Annals of Mathematical Statistics*, 23(3):462 – 466, 1952.
- Li, S., Cheng, Y., Wang, W., Liu, Y., and Chen, T. Learning to detect malicious clients for robust federated learning. *arXiv preprint arXiv:2002.00211*, 2020.
- Li, Y. Simple, unified analysis of johnson-lindenstrauss with applications. *arXiv preprint arXiv:2402.10232*, 2024.
- Liu, S., Chen, P.-Y., Kailkhura, B., Zhang, G., Hero III, A. O., and Varshney, P. K. A primer on zeroth-order optimization in signal processing and machine learning: Principals, recent advances, and applications. *IEEE Signal Processing Magazine*, 37(5):43–54, 2020.
- Liu, S., Gupta, N., and Vaidya, N. H. Approximate byzantine fault-tolerance in distributed optimization. In *ACM Symposium on Principles of Distributed Computing*, pp. 379–389, 2021.
- Liu, Y. Roberta: A robustly optimized bert pretraining approach. *arXiv preprint arXiv:1907.11692*, 364, 2019.
- M Abdelmoniem, A., Elzanaty, A., Alouini, M.-S., and Canini, M. An efficient statistical-based gradient compression technique for distributed training systems. *Proceedings of Machine Learning and Systems*, 3:297–322, 2021.
- Makkuva, A. V., Bondaschi, M., Vogels, T., Jaggi, M., Kim, H., and Gastpar, M. LASER: Linear compression in wireless distributed optimization. In *International Conference on Machine Learning*, 2024.
- Malladi, S., Gao, T., Nichani, E., Damian, A., Lee, J. D., Chen, D., and Arora, S. Fine-tuning language models with just forward passes. *Advances in Neural Information Processing Systems*, 36:53038–53075, 2023.
- McMahan, B., Moore, E., Ramage, D., Hampson, S., and y Arcas, B. A. Communication-efficient learning of deep networks from decentralized data. In *Artificial intelligence and statistics*, pp. 1273–1282, 2017.
- Neto, A. d. S. D., Egger, M., Bakshi, M., and Bitar, R. Communication-efficient byzantine-resilient federated zero-order optimization. *submitted to ICML 2024; arXiv preprint arXiv:2406.14362*, 2024.
- Qin, Z., Chen, D., Qian, B., Ding, B., Li, Y., and Deng, S. Federated full-parameter tuning of billion-sized language models with communication cost under 18 kilobytes. *arXiv preprint arXiv:2312.06353*, 2023.
- Qiu, Y., Shanbhag, U., and Yousefian, F. Zeroth-order methods for nondifferentiable, nonconvex, and hierarchical federated optimization. *Advances in Neural Information Processing Systems*, 36, 2023.
- Rodríguez-Barroso, N., Jiménez-López, D., Luzón, M. V., Herrera, F., and Martínez-Cámara, E. Survey on federated learning threats: Concepts, taxonomy on attacks and defences, experimental study and challenges. *Information Fusion*, 90:148–173, 2023.
- Salimans, T., Ho, J., Chen, X., Sidor, S., and Sutskever, I. Evolution strategies as a scalable alternative to reinforcement learning. *arXiv preprint arXiv:1703.03864*, 2017.
- Salmon, J. K., Moraes, M. A., Dror, R. O., and Shaw, D. E. Parallel random numbers: as easy as 1, 2, 3. In *International conference for high performance computing, networking, storage and analysis*, pp. 1–12, 2011.
- Schlegel, R., Kumar, S., Rosnes, E., and i Amat, A. G. CodedPaddedFL and CodedSecAgg: Straggler mitigation and secure aggregation in federated learning. *IEEE Transactions on Communications*, 2023.
- Shen, S., Tople, S., and Saxena, P. Auror: Defending against poisoning attacks in collaborative deep learning systems. In *Annual Conference on Computer Security Applications*, pp. 508–519, 2016.
- Socher, R., Perelygin, A., Wu, J., Chuang, J., Manning, C. D., Ng, A. Y., and Potts, C. Recursive deep models for semantic compositionality over a sentiment treebank. In *Conference on empirical methods in natural language processing*, pp. 1631–1642, 2013.
- Spall, J. Multivariate stochastic approximation using a simultaneous perturbation gradient approximation. *IEEE Transactions on Automatic Control*, 37(3):332–341, 1992.
- Tang, X., Panda, A., Nasr, M., Mahloujifar, S., and Mittal, P. Private fine-tuning of large language models with zeroth-order optimization. *CoRR*, 2024a.
- Tang, Y., Zhang, J., and Li, N. Distributed zero-order algorithms for nonconvex multiagent optimization. *IEEE Transactions on Control of Network Systems*, 8(1):269–281, 2020.
- Tang, Z., Wang, Y., and Chang, T.-H. z -SignFedAvg: A unified stochastic sign-based compression for federated learning. In *Proceedings of the AAAI Conference on Artificial Intelligence*, volume 38, pp. 15301–15309, 2024b.
- Truex, S., Baracaldo, N., Anwar, A., Steinke, T., Ludwig, H., Zhang, R., and Zhou, Y. A hybrid approach to privacy-preserving federated learning. In *ACM workshop on artificial intelligence and security*, pp. 1–11, 2019.

- Vogels, T., Karimireddy, S. P., and Jaggi, M. PowerSGD: Practical low-rank gradient compression for distributed optimization. *Advances in Neural Information Processing Systems*, 32, 2019.
- Voorhees, E. M. and Tice, D. M. Building a question answering test collection. In *Annual international ACM SIGIR conference on Research and development in information retrieval*, pp. 200–207, 2000.
- Wang, J., Liu, Q., Liang, H., Joshi, G., and Poor, H. V. A novel framework for the analysis and design of heterogeneous federated learning. *IEEE Transactions on Signal Processing*, 69:5234–5249, 2021.
- Wang, J., Wang, S., Chen, R.-R., and Ji, M. A new theoretical perspective on data heterogeneity in federated optimization. In *International Conference on Machine Learning*, 2025.
- Wei, K., Li, J., Ding, M., Ma, C., Yang, H. H., Farokhi, F., Jin, S., Quek, T. Q., and Poor, H. V. Federated learning with differential privacy: Algorithms and performance analysis. *IEEE Transactions on Information Forensics and Security*, 15:3454–3469, 2020.
- Wen, W., Xu, C., Yan, F., Wu, C., Wang, Y., Chen, Y., and Li, H. TernGrad: Ternary gradients to reduce communication in distributed deep learning. *Advances in neural information processing systems*, 30, 2017.
- Xie, C., Koyejo, O., and Gupta, I. Fall of empires: Breaking byzantine-tolerant sgd by inner product manipulation. In *Uncertainty in Artificial Intelligence*, pp. 261–270, 2020.
- Yin, D., Chen, Y., Kannan, R., and Bartlett, P. Byzantine-robust distributed learning: Towards optimal statistical rates. In *International conference on machine learning*, pp. 5650–5659, 2018.
- Zhao, Y., Li, M., Lai, L., Suda, N., Civin, D., and Chandra, V. Federated learning with non-iid data. *arXiv preprint arXiv:1806.00582*, 2018.
- Zhu, H., Xu, J., Liu, S., and Jin, Y. Federated learning on non-iid data: A survey. *Neurocomputing*, 465:371–390, 2021.
- Zhu, T. and Philip, S. Y. Applying differential privacy mechanism in artificial intelligence. In *IEEE International Conference on Distributed Computing Systems (ICDCS)*, pp. 1601–1609, 2019.

A Numerical Experiments

A.1 Experimental Details

A.1.1 SAMPLING OF PERTURBATION VECTORS

To sample the directions \mathbf{z} , for fine-tuning large language models (cf. Section 4.3) we use a practical approach similar to (Salimans et al., 2017; Malladi et al., 2023) that draws each coordinate independently from a standard Gaussian distribution. This minor modification has substantial practical implications by alleviating the allocation of the entire vector, and instead iteratively samples each model coordinate. Thereby, considerably reducing the memory footprint of our method.

A.1.2 RECONSTRUCTION OF THE SEED

Let s be a seed initially broadcast by the federator to all clients. Then, at each global and local iteration t and ℓ , the r -th random perturbation is sampled by setting the seed of the PRNG to $s' \triangleq (s, t, \ell, r)$. In this way, the perturbations $\mathbf{z}_{t,\ell}^r$ sampled by all clients will be equivalent. The client then compute the estimate according to Definition 2.1.

A.1.3 IN-PLACE MODEL PERTURBATION

Similar to (Salimans et al., 2017; Malladi et al., 2023), we use in-place perturbations of the model for memory efficient zero-order optimization throughout the training phase. In particular, client i employs Algorithms 2 and 3 to compute the zero-order estimate as $g_i(\mathbf{w}_{t,\ell}^i, \mathbf{z}_{t,\ell}^r) = \text{ZEROORDERESTIMATE}(\mathbf{w}_{t,\ell}^i, s', \mu, \mathcal{D}_i)$. Note that the function, instead of $\mathbf{z}_{t,\ell}^r$, takes as input the seed $s' = (s, t, \ell, r)$ used to reconstruct the projection $\mathbf{z}_{t,\ell}^r$.

Algorithm 2 PERTURB: Perturbing Model Parameters

Input: Model parameters \mathbf{w} , scaling factor μ , seed s'
Output: Perturbed model \mathbf{w}
 Initialize PRNG with seed s'
for $p = 1$ to d **do**
 Sample $z \sim \mathcal{N}(0, 1)$
 Perturb parameter $\mathbf{w}^{(p)} = \mathbf{w}^{(p)} + \mu \cdot z$
end for
Return: Perturbed model \mathbf{w}

Algorithm 3 ZEROORDERESTIMATE: Compute $g(\mathbf{w}, s', \mu, \mathcal{D})$ via Model Perturbation

Input: Model \mathbf{w} , seed s' , scaling factor μ , data \mathcal{D}
Output: Zero estimate $g(\mathbf{w}, s', \mu, \mathcal{D})$
Step 1: PERTURB(\mathbf{w}, μ, s') (cf. Algorithm 2)
 Compute $F_1 = F(\mathbf{w}^{(p)}, \mathcal{D})$
Step 2: PERTURB($\mathbf{w}, -2\mu, s'$)
 Compute $F_2 = F(\mathbf{w}^{(p)}, \mathcal{D})$
Step 3: PERTURB(\mathbf{w}, μ, s') {Reset the model}
Return: $g(\mathbf{w}, s', \mu, \mathcal{D}) = \frac{F_1 - F_2}{2\mu}$

A.2 Byzantine Attacks

We test and compare our algorithm using several state-of-the-art gradient attacks, i.e., *A little is enough* (ALIE) (Baruch et al., 2019), *Fall of Empires* (FOE) (Xie et al., 2020), *Sign Flipping* (SF) (Allen-Zhu et al., 2021), *Label Flipping* (LF) (Allen-Zhu et al., 2021), and a tailored trimmed mean attack (TMA) (cf. Algorithm 4). For all non-zero-order experiments, we conduct the attacks on the gradients $\mathbf{g}_i(\mathbf{w}_{t,\ell}^i)$. For the zero-order experiments, the attacks are conducted on the projected gradients, i.e., on $\mathbf{g}_i(\mathbf{w}_{t,\ell}^i, \mathbf{Z}_{t,\ell}) \triangleq \frac{1}{\nu} ((g_i(\mathbf{w}_{t,\ell}^i, \mathbf{z}_{t,\ell}^r))_{r=1}^\nu)^\top$, which we believe is the strongest attack scenario. Let in the following $\mathbf{g}_{t,\ell}^i$ denote the contribution of client i at global epoch t and local epoch ℓ . The attacks are summarized as follows. Let $\bar{\mathbf{g}}_{t,\ell} \triangleq \frac{1}{|\mathcal{H}|} \sum_{i \in \mathcal{H}} \mathbf{g}_{t,\ell}^i$ be the average of the honest clients gradients. For ALIE, FOE, and SF, the Byzantine clients

Algorithm 4 Transformed Trimmed-Mean Attack (TMA)

Require: $\beta, n, g_i(\mathbf{w}_{t,\ell}^i, \mathbf{z}_{t,\ell}^r) \forall i \in [n]$, honest clients \mathcal{H}

- 1: Compute $\bar{g}(\mathbf{w}_{t,\ell}^i, \mathbf{z}_{t,\ell}^r) = \frac{1}{n} \sum_{i=1}^n g_i(\mathbf{w}_{t,\ell}^i, \mathbf{z}_{t,\ell}^r)$
- 2: **for** Byzantine client $i \in [n] \setminus \mathcal{H}$ **do**
- 3: **if** $\bar{g}(\mathbf{w}_{t,\ell}^i, \mathbf{z}_{t,\ell}^r) > 0$ **then**
- 4: return $\lfloor \beta n \rfloor$ smallest value in $\{g_i(\mathbf{w}_{t,\ell}^i, \mathbf{z}_{t,\ell}^r)\}_{i \in \mathcal{H}}$
- 5: **else**
- 6: return $\lfloor \beta n \rfloor$ largest value in $\{g_i(\mathbf{w}_{t,\ell}^i, \mathbf{z}_{t,\ell}^r)\}_{i \in \mathcal{H}}$
- 7: **end if**
- 8: **end for**

$i \in \mathcal{B} \triangleq [n] \setminus \mathcal{H}$ compute their corrupted gradient as $\mathbf{g}_{t,\ell}^i = \bar{\mathbf{g}}_{t,\ell} + \omega \mathbf{a}_{t,\ell}$ for some optimized ω , where

- for ALIE, we have $\mathbf{a}_{t,\ell} = \sigma_{t,\ell}$, where $\sigma_{t,\ell}$ is the coordinate standard deviation of $\bar{\mathbf{g}}_{t,\ell}$,
- for FOE, we have $\mathbf{a}_{t,\ell} = -\bar{\mathbf{g}}_{t,\ell}$, and hence $\mathbf{g}_{t,\ell}^i = (1 - \omega)\bar{\mathbf{g}}_{t,\ell}$,
- for SF, we have $\mathbf{a}_{t,\ell} = -\bar{\mathbf{g}}_{t,\ell}$ for fixed $\omega = 2$, s.t. $\mathbf{g}_{t,\ell}^i = -\bar{\mathbf{g}}_{t,\ell}$.

For ALIE and FOE, similar to Allouah et al. (2023), we linearly optimize of potential choices of ω such that the L2 distance of the final aggregation $R_{t,\ell}$ to the honest clients' average $\bar{\mathbf{g}}_{t,\ell}$ is maximized. For LF, each Byzantine workers manipulates the labels of its local dataset. In particular, if for a Byzantine client $i \in \mathcal{B}$ a sample in \mathcal{D}_i is labeled ℓ , they instead train on the label $\ell' = 9 - \ell$ for a 10-class classification task.

The details of the tailored trimmed mean attack can be found in Algorithm 4.

A.3 Hyperparameters

We detail in the following Tables 3 and 4 the hyperparameters used through the experiments in Sections 4.2 and 4.3.

Table 3. Simulation Parameters and Hyperparameters for Section 4.2

MNIST	
Global Train Samples	60000
Number of Clients	40
Number of Byzantine Clients	10
Scaling Factor μ	0.001
Learning Rate η	0.01
Batch Size	64
Global Epochs T	400

Table 4. Simulation Parameters and Hyperparameters for Section 4.3

	SST-2	SNLI	TREC
Global Train Samples	512		
Scaling Factor μ	0.001		
Learning Rate η	10^{-6}		
Batch Size	64		
Global Epochs T	20,000	20,000	40,000

The numerical experiments were conducted on the following cluster of simulation servers.

Algorithm 5 CYBER-0: Robust Efficient Zero-Order FL with Biased ZO Estimator

Require: Shared seed for PRNG, $\mu \geq 0$, $\eta > 0$, $\nu > 0$, R .

- 1: Initialize and broadcast global model $\mathbf{w}^{(1)}$.
- 2: **for** $t = 1$ to T **do**
- 3: **for** each client $i \in [n]$ **in parallel do**
- 4: Initialize local model $\mathbf{w}_{t,1}^i = \mathbf{w}^{(t)}$.
- 5: Draw $\mathbf{z}_{t,1}^1, \dots, \mathbf{z}_{t,1}^\nu \sim \mathcal{U}(\mathbb{S}^d)$, let $\mathbf{Z}_{t,1} \triangleq (\mathbf{z}_{t,1}^r)_{r \in [\nu]}$
- 6: **for** $\ell = 1$ to K **do**
- 7: Compute $g_i(\mathbf{w}_{t,\ell}^i, \mathbf{z}_{t,1}^r) \triangleq g(\mathbf{w}_{t,\ell}^i, \mathbf{z}_{t,1}^r, \mu, \mathcal{D}_i)$, $r \in [\nu]$ (cf. Definition 2.1)
- 8: Let $\mathbf{g}_i(\mathbf{w}_{t,\ell}^i, \mathbf{Z}_{t,1}) \triangleq \frac{1}{\nu} ((g_i(\mathbf{w}_{t,\ell}^i, \mathbf{z}_{t,1}^r))_{r=1}^\nu)^\top$
- 9: Update $\mathbf{w}_{t,\ell+1}^i = \mathbf{w}_{t,\ell}^i - \eta \mathbf{Z}_{t,1} \mathbf{g}_i(\mathbf{w}_{t,\ell}^i, \mathbf{Z}_{t,1})$
- 10: **end for**
- 11: Send $\{\sum_{\ell=1}^K \mathbf{g}_i(\mathbf{w}_{t,\ell}^i, \mathbf{Z}_{t,1})\}$ to federator.
- 12: **end for**
- 13: Aggregate $R_t = R(\{\sum_{\ell=1}^K \mathbf{g}_i(\mathbf{w}_{t,\ell}^i, \mathbf{Z}_{t,\ell})\}_{i=1}^n)$
- 14: Update $\mathbf{w}^{(t+1)} = \mathbf{w}^{(t)} - \eta \sum_{\ell=1}^K \mathbf{Z}_{t,1} R_t$.
- 15: Broadcast R_t ; clients accordingly update using $\mathbf{Z}_{t,1}$
- 16: **end for**
- 17: Clients recover the updated global model $\mathbf{w}^{(t+1)}$ using known perturbations $\mathbf{Z}_{t,1}$.

CPU(s)	RAM	GPU(s)	VRAM
2x Intel Xeon Platinum 8176 (56 cores)	256 GB	2x NVIDIA GeForce GTX 1080 Ti	11 GB
2x AMD EPYC 7282 (32 cores)	512 GB	NVIDIA GeForce RTX 4090	24 GB
2x AMD EPYC 7282 (32 cores)	640 GB	NVIDIA GeForce RTX 4090	24 GB
2x AMD EPYC 7282 (32 cores)	448 GB	NVIDIA GeForce RTX 4080	16 GB
2x AMD EPYC 7282 (32 cores)	256 GB	NVIDIA GeForce RTX 4080	16 GB
HGX-A100 (96 cores)	1 TB	4x NVIDIA A100	80 GB
DGX-A100 (252 cores)	2 TB	8x NVIDIA Tesla A100	80 GB
DGX-1-V100 (76 cores)	512 GB	8x NVIDIA Tesla V100	16 GB
DGX-1-P100 (76 cores)	512 GB	8x NVIDIA Tesla P100	16 GB
HPE-P100 (28 cores)	256 GB	4x NVIDIA Tesla P100	16 GB

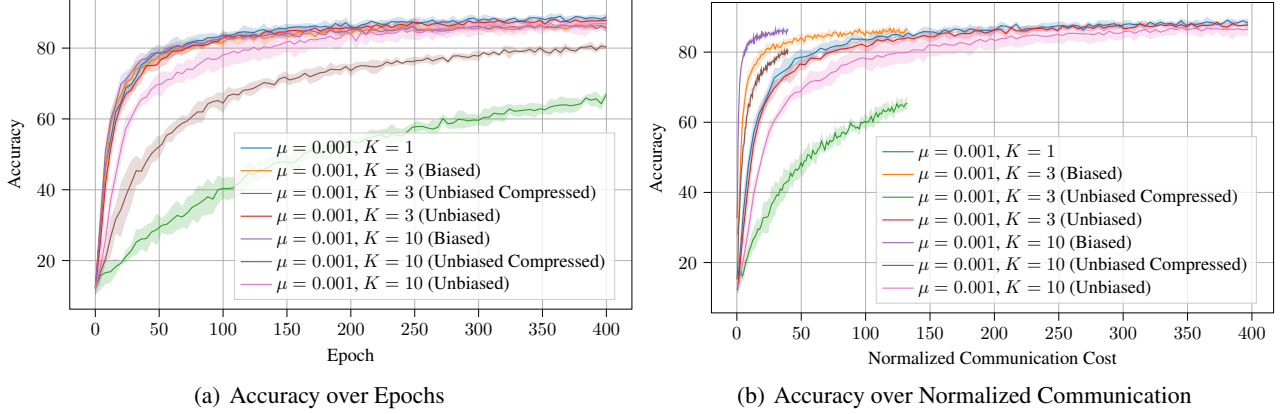
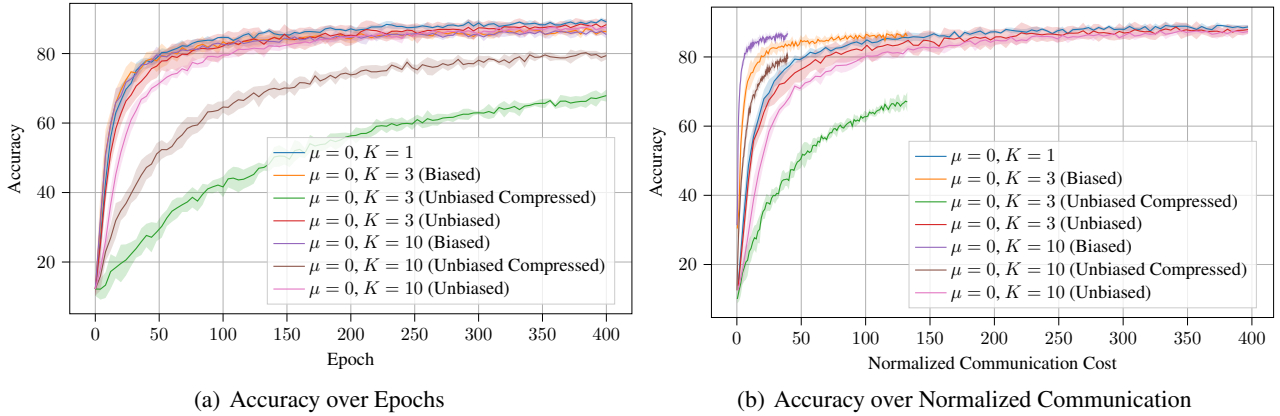
Table 5. System specifications of our simulation cluster.

A.4 Local Iterations

CYBER-0 offers different option to conduct local epochs at the clients. We term the approach for local epochs introduced in Algorithm 1 “Unbiased”.

A second approach is to follow Algorithm 1, but to replace the sending of $\{\mathbf{g}_i(\mathbf{w}_{t,\ell}^i, \mathbf{Z}_{t,\ell})\}_{\ell=1}^K$ from clients to the federator, followed by $R_{t,\ell} = R(\{\mathbf{g}_i(\mathbf{w}_{t,\ell}^i, \mathbf{Z}_{t,\ell})\}_{i=1}^n)$, $\ell \in [K]$ and $\mathbf{w}^{(t+1)} = \mathbf{w}^{(t)} - \eta \sum_{\ell=1}^K \mathbf{Z}_{t,\ell} R_{t,\ell}$. Instead of transmitting the results $\{\mathbf{g}_i(\mathbf{w}_{t,\ell}^i, \mathbf{Z}_{t,\ell})\}_{\ell=1}^K$ for all local epochs, the clients can instead reconstruct the aggregated local gradient updates as $\mathbf{g}_i = \sum_{\ell=1}^K \mathbf{Z}_{t,\ell} \mathbf{g}_i(\mathbf{w}_{t,\ell}^i, \mathbf{Z}_{t,\ell})$ and project this gradient approximation onto random directions \mathbf{Z}_t (known to the federator and all clients) according to Definition 2.1, and only transmit the result of $\mathbf{Z}_t^\top \mathbf{g}_i$ to the federator. The federator conducts the transformed aggregation on $R_{t,\ell} = R(\{\mathbf{Z}_t^\top \mathbf{g}_i\}_{i=1}^n)$ and updates the global model as $\mathbf{w}^{(t+1)} = \mathbf{w}^{(t)} - \eta \mathbf{Z}_t R_{t,\ell}$. This approach is by a factor of K more communication efficient. However, it can introduce significant additional variance, especially for small values of ν . This is because two randomly drawn vectors in high dimensions are likely almost orthogonal, and hence the subspaces resulting from \mathbf{Z}_t and $\{\mathbf{Z}_{t,\ell}\}_{\ell=1}^K$ might only be weakly dependent. However, for large values of ν , this approach might be beneficial due to the drastic savings in the cost of communication. We term this approach “Unbiased Compressed”.

A third approach, termed “Biased”, is to make the clients reuse the directions $\mathbf{Z}_{t,\ell}$ at each iteration, i.e., $\mathbf{Z}_{t,\ell} = \mathbf{Z}_{t,m}$


 Figure 3. Comparisons of Local Epoch Strategies for $\mu = 0.001$

 Figure 4. Comparisons of Local Epoch Strategies for $\mu = 0$

for $\ell \neq m \in [K]$. It suffices for the clients to communicate to the federator $\sum_{\ell=1}^K \mathbf{g}_i(\mathbf{w}_{t,\ell}^i, \mathbf{Z}_{t,\ell})$, thus reducing the communication cost by the same factor of K as for the second approach above. However, this strategy incurs bias in the local training process, since the gradient updates are not uniformly and independently chosen at each local iteration $\ell \in [K]$. We summarize this approach in Algorithm 5.

The above mentioned approaches expose an efficiency-bias-variance trade-off that we will examine in the following. In Figure 3(a), we provide a study for $\mu = 0.001$ in terms of accuracies over epochs. It can be observed that Unbiased Compressed local epochs are harmful, especially for small K . The larger K , the larger the space covered during the local training process, and the smaller the loss incurred by projection the approximated overall local gradient onto an independent subspace. Looking at the accuracies over the normalized communication cost in Figure 3, we can observe that Biased local epochs with reasonably large values of K can indeed significantly improve the performance when normalized by communication cost. The Unbiased approach, although reducing the number of packets to be transmitted, does not significantly improve the factual communication cost. Results for $\mu = 0$ in Figure 3(b) and Figure 4 exhibit the same trade offs.

A.5 Effect of Number of Perturbations

To highlight the effect of the number of perturbations ν on the convergence of zero-order optimization in standard learning tasks, we show in Figure 5 the performance of CYBER-0 compared to FedAvg (McMahan et al., 2017) for different values of perturbations ν . While $\nu = 1$ exhibits a substantial performance gap to FedAvg, this gap decreases with increasing ν , until nearly vanishing with $\nu = 64$.

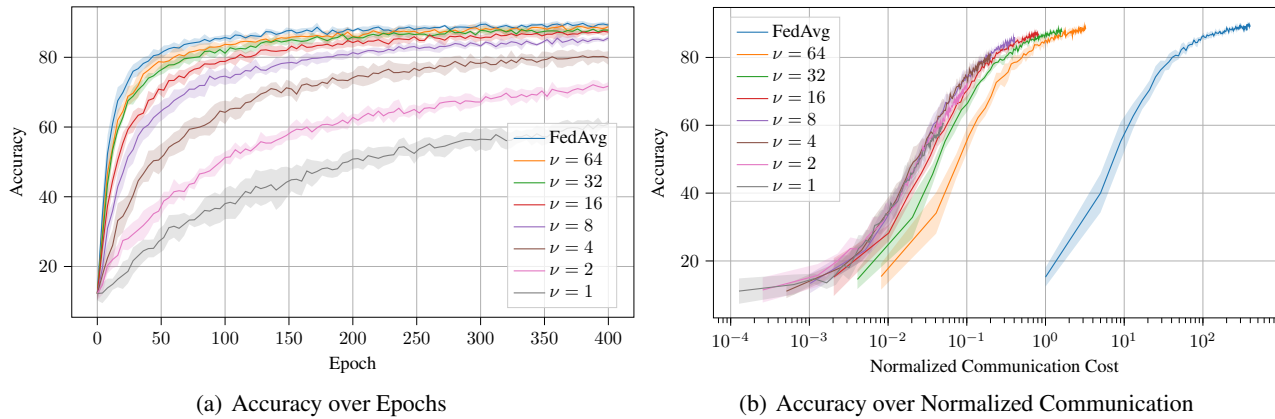


Figure 5. Comparison of Zero-Order Optimization for Different Values of ν Compared to the Baseline FedAvg.

A.6 Accuracies over Epochs for all Attacks on MNIST

We present in the following, extending the case of LF (cf. Figure 1(c)), the comparison of all countermeasures for ALIE, ALIE-NNM, FOE, FOE-NNM, and SF. We present the results for accuracies over epochs, and accuracies over normalized communication cost.

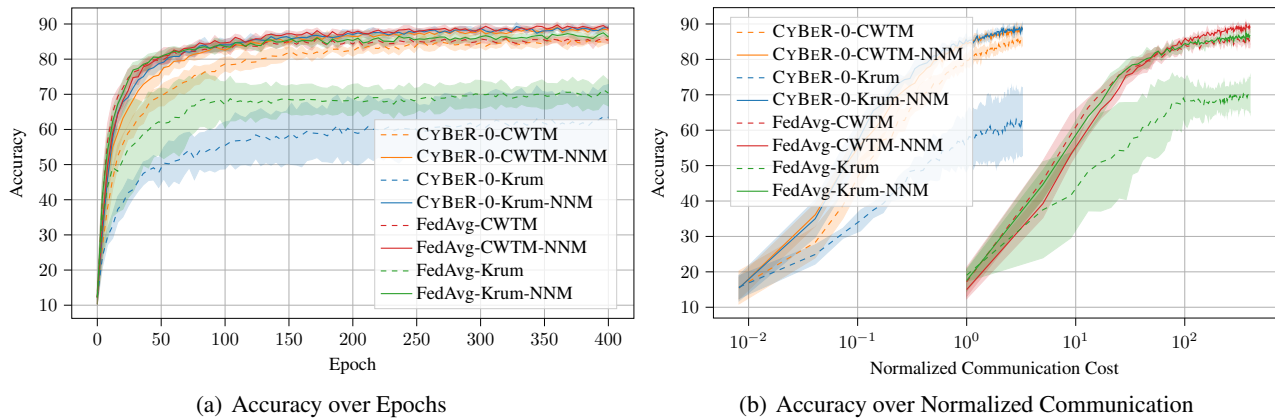


Figure 6. ALIE attack on logistic regression on MNIST.

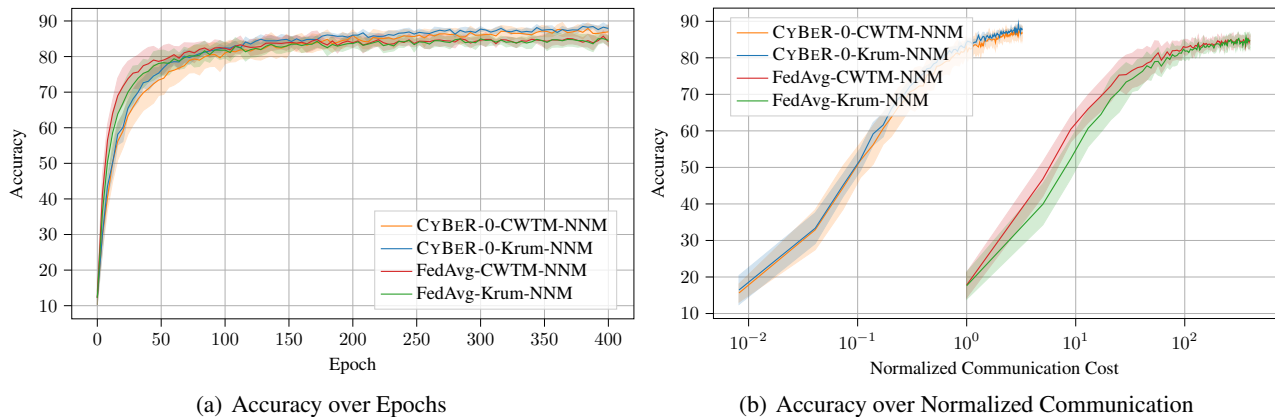


Figure 7. ALIE-NNM attack on logistic regression on MNIST.

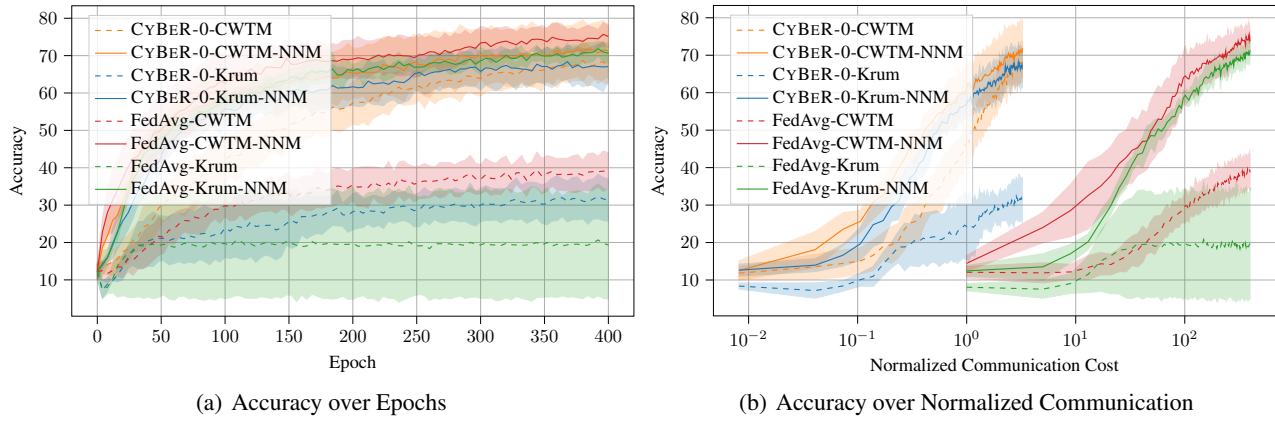


Figure 8. FOE attack on logistic regression on MNIST.

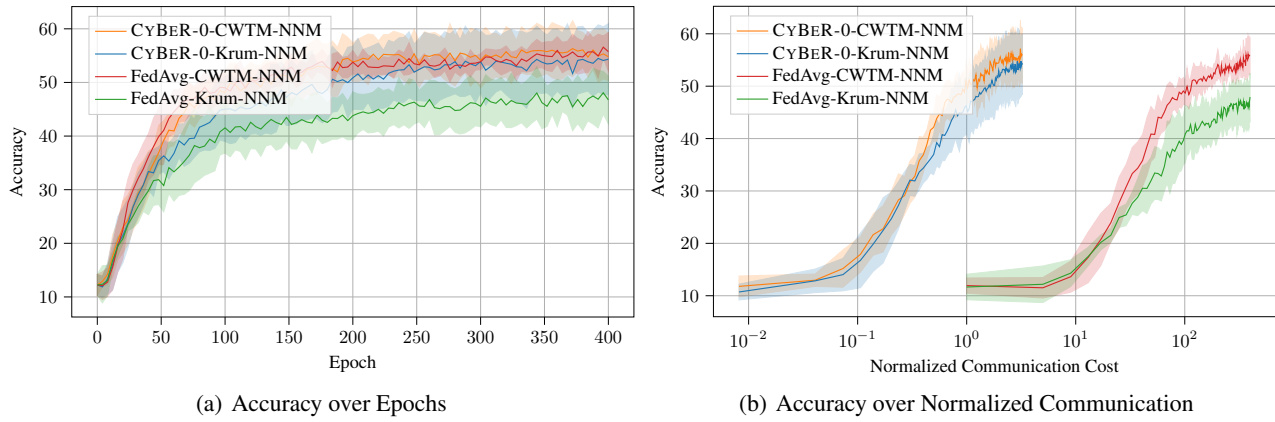


Figure 9. FOE-NNM attack on logistic regression on MNIST.

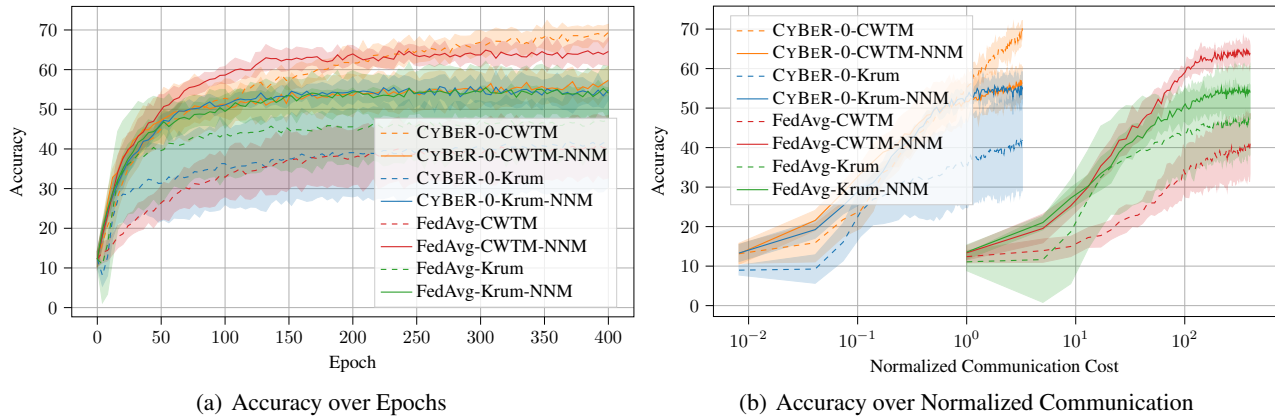


Figure 10. SF attack on logistic regression on MNIST.

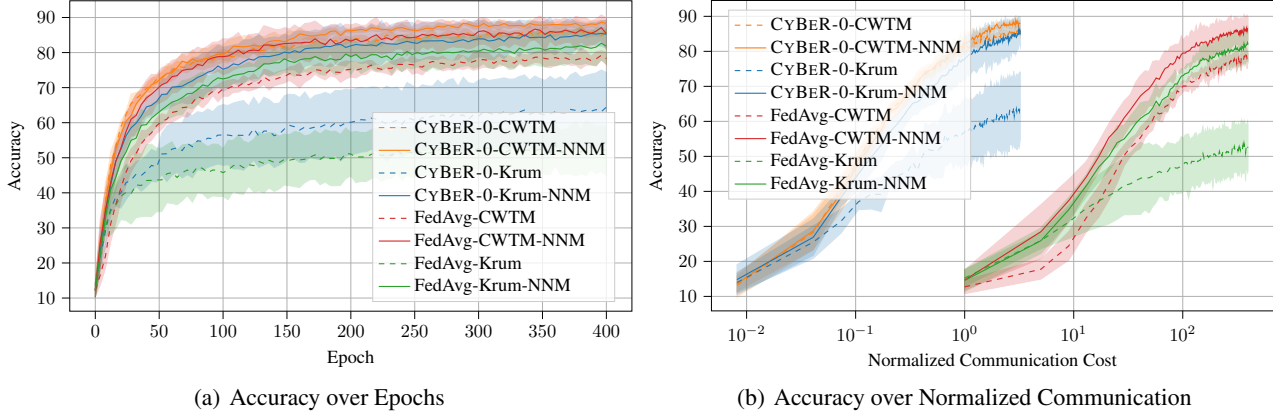


Figure 11. LF attack on logistic regression on MNIST.

A.7 Accuracies over Epochs for all Attacks on Fine-Tuning Tasks

We provide in Table 6 extensive results on an i.i.d. data distribution, analog to the non-i.i.d. results in Table 2. It can be found that our algorithm exhibits stable performance for both i.i.d. and non-i.i.d. distributions, and is not significantly affected by heterogeneity. Further, we provide in the following plots for the accuracies over the epochs for all attacks, datasets, and both i.i.d. and non-i.i.d. data distributions. CYBER-0 exhibits stable performance in all settings.

Dataset	ALIE	FOE	SF	TMA	No Attack	Worst Case
SST-2	93.0 ± 0.4	91.6 ± 0.2	91.9 ± 0.1	92.1 ± 0.6	92.9 ± 0.6	91.6
SNLI	83.5 ± 0.5	77.0 ± 0.8	78.7 ± 1.0	79.6 ± 0.9	84.9 ± 0.2	77.0
TREC	95.5 ± 0.3	88.5 ± 0.9	90.5 ± 0.8	91.4 ± 1.9	95.6 ± 0.4	88.5

Table 6. Mean and Standard Deviation of Maximum Accuracies Across Seeds

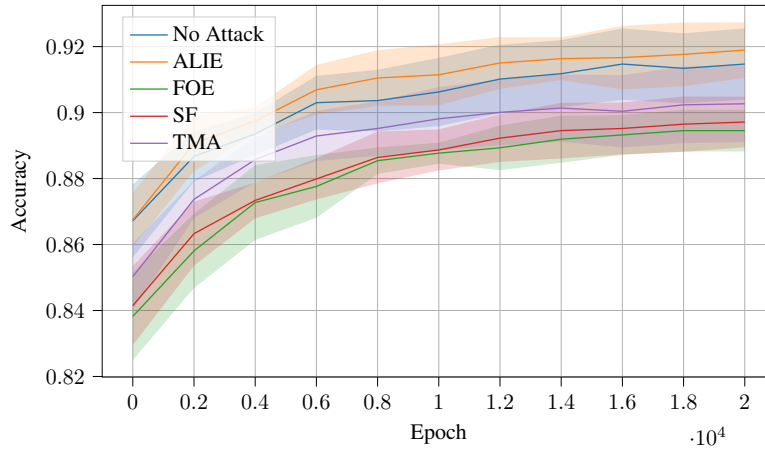


Figure 12. Accuracy comparison of different attacks on fine-tuning RoBERTa-large on SST-2 with i.i.d. data, compared to the baseline.

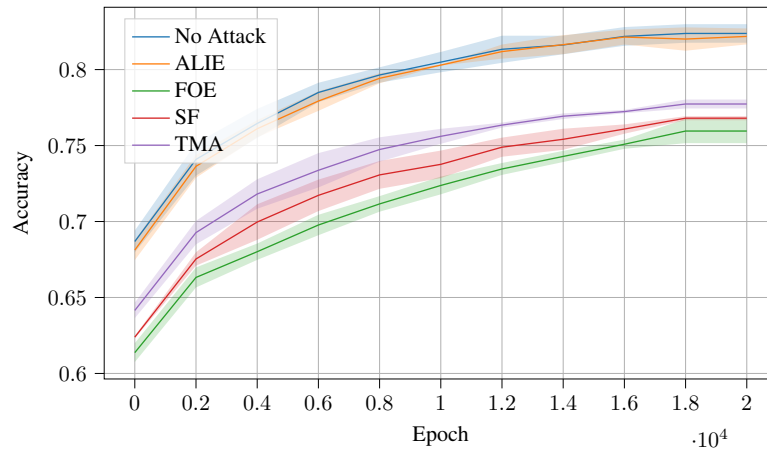


Figure 13. Accuracy comparison of different attacks on fine-tuning RoBERTa-large on SNLI with i.i.d. data, compared to the baseline.

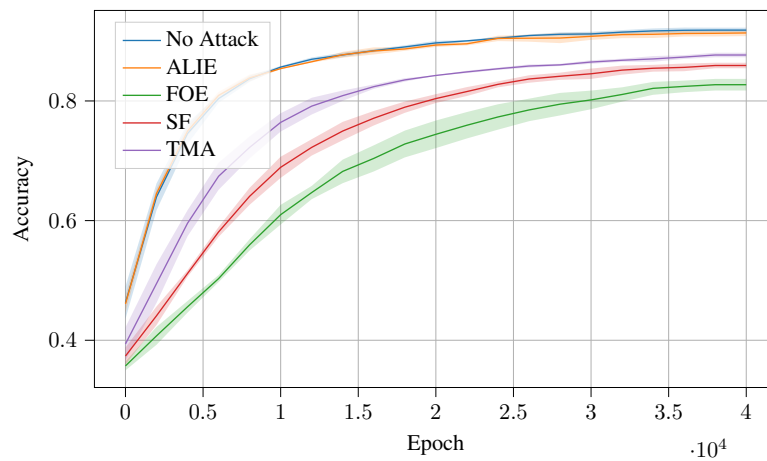


Figure 14. Accuracy comparison of different attacks on fine-tuning RoBERTa-large on SNLI with i.i.d. data, compared to the baseline.

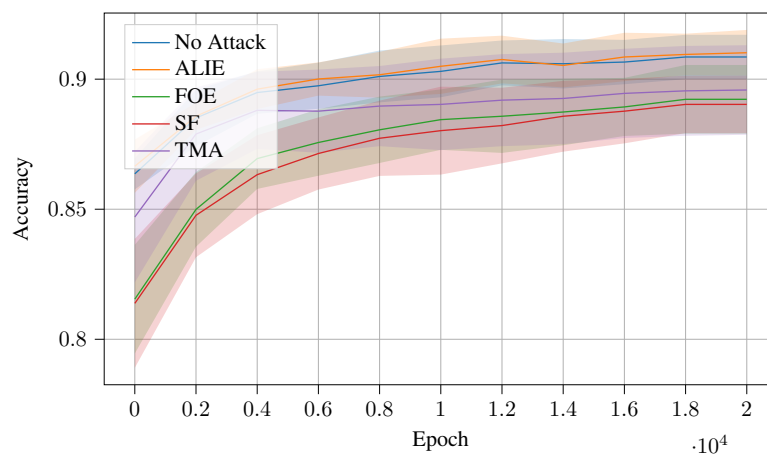


Figure 15. Accuracy comparison of different attacks on fine-tuning RoBERTa-large on SST-2 with non-i.i.d. data, compared to the baseline.

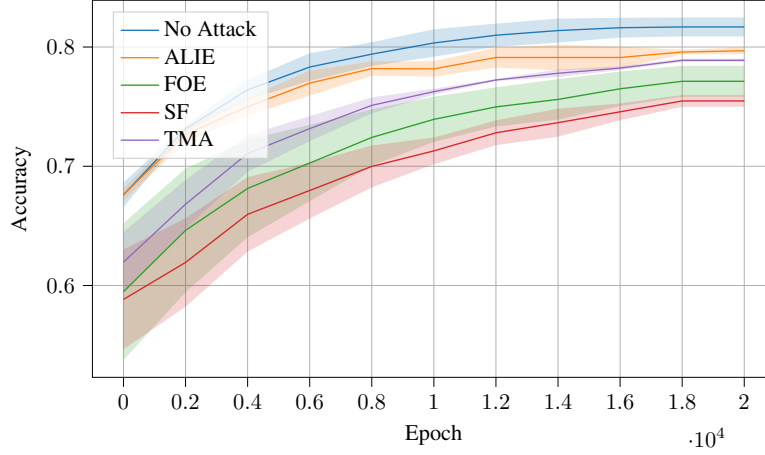


Figure 16. Accuracy comparison of different attacks on fine-tuning RoBERTa-large on SNLI with non-i.i.d. data, compared to the baseline.

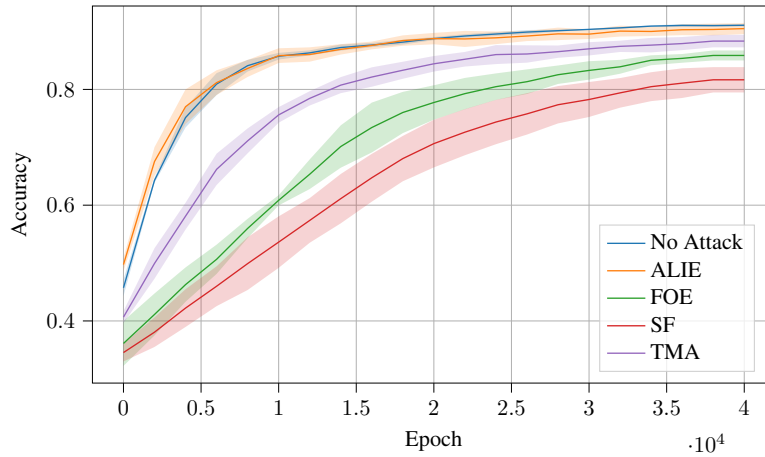


Figure 17. Accuracy comparison of different attacks on fine-tuning RoBERTa-large on SNLI with non-i.i.d. data, compared to the baseline.

A.8 Hyperparameter Study

We provide in the following tables Tables 7 to 10 a sensitivity analysis of CYBER-0 with respect to the number of global epochs T , the number of local epochs K , the number of perturbations ν , the number of clients n , and the number of Byzantine clients \mathcal{B} .

We run our experiments on SST-2 and RoBERTa-large, attacked by FOE. We use non-i.i.d. data with $\alpha = 0.1$. We first show in Table 7 the robustness of CYBER-0 under varying numbers of total and Byzantine clients with $\frac{b}{n} = 0.25$ and observe that the robustness increases with n . We fix $n = 8$, and $b = 2$ as the most challenging setting for the following experiments. We show in Table 8 the stability of CYBER-0 under varying number ν of random perturbations. For comparability, we fix the ratio $\nu T = 20000$ and observe very similar accuracies for $\nu \in \{1, 2, 4, 8\}$. Hence, the number of projections trades almost inversely with the number of global epochs T . A similar behavior can be observed in Table 9 for a varying number of local epochs K , fixing the ratio KT . However, for large K and small T , we can see the negative impacts of local iterations. Lastly, we evaluate CYBER-0 under varying ratios of Byzantine clients, thereby fixing $n = 16$ for better flexibility, and using $\nu = 1$. The results are depicted in Table 10, While the performance reduction from $b = 2$ to $b = 4$ is negligible, we can observe a notable difference for $b = 6$, i.e., when the number of Byzantine clients is close to $n/2$.

Table 7. Accuracy over n, b for $b/n = 0.25$

Clients n	Byzantine b	Acc \pm Std
8	2	0.86 ± 0.02
12	3	0.87 ± 0.06
16	4	0.89 ± 0.02
32	8	0.87 ± 0.03

 Table 8. Accuracy over T and ν .

Global epochs T	ν	Acc \pm Std
2500	8	0.87 ± 0.02
5000	4	0.88 ± 0.02
10000	2	0.86 ± 0.02
20000	1	0.86 ± 0.02

 Table 9. Accuracy over T and K .

Global epochs T	Local epochs K	Acc \pm Std
2000	10	0.81 ± 0.03
4000	5	0.86 ± 0.03
20000	1	0.86 ± 0.02

 Table 10. Accuracy over b/n for $n = 16$.

Clients n	Byzantine b	Acc \pm Std
16	2	0.90 ± 0.01
16	4	0.89 ± 0.02
16	6	0.78 ± 0.05

B Proofs

B.1 Proof of Theorem 5.7.

Sketch of Proof. We provide a brief proof outline in the following for the case when $\mu > 0$. The proof for $\mu = 0$ follows similar steps with some modifications, since $\left\| \left(\nabla F_i(\mathbf{w}_{t,\ell}^i) - \nabla F_i^\mu(\mathbf{w}_{t,\ell}^i) \right) \right\|^2 = 0$ by definition and the gradient estimate is bounded differently. We define the following quantities $\hat{\mathbf{w}}_{t,\ell} \triangleq \frac{1}{|\mathcal{H}|} \sum_{i \in \mathcal{H}} \mathbf{w}_{t,\ell}^i$ and $\bar{\mathbf{g}}_{\mathcal{H}}(\mathbf{w}_{t,\ell}^i, \mathbf{Z}_{t,\ell}) \triangleq \frac{1}{|\mathcal{H}|} \sum_{i \in \mathcal{H}} \mathbf{g}_i(\mathbf{w}_{t,\ell}^i, \mathbf{Z}_{t,\ell})$, and focus on the conceptual strategy and omit all factors. We first decompose the difference of two consecutive models into $\|\nabla F_{\mathcal{H}}(\mathbf{w}_t)\|^2$, $\left\| \sum_{\ell=1}^K R_{t,\ell} \mathbf{Z}_{t,\ell} \right\|^2$ and $\left\| K \nabla F_{\mathcal{H}}(\mathbf{w}_t) - \sum_{\ell=1}^K \mathbf{Z}_{t,\ell} R_{t,\ell} \right\|^2$. The former term is the quantity of interest. The second term can be made negative by an appropriate choice of the learning rate. On expectation and using Assumptions 5.1 and 5.4, the latter can be bounded by i) $\mathbb{E} \left[\|\mathbf{w}_t - \hat{\mathbf{w}}_{t,\ell}\|^2 \right]$, ii) $\mathbb{E} \left[\sum_{\ell=1}^K \left\| \mathbf{Z}_{t,\ell} \bar{\mathbf{g}}_{\mathcal{H}}(\mathbf{w}_{t,\ell}^i, \mathbf{Z}_{t,\ell}) - \mathbf{Z}_{t,\ell} R_{t,\ell} \right\|^2 \right]$, iii) $\mathbb{E} \left[\left\| \mathbf{w}_{t,\ell}^i - \hat{\mathbf{w}}_{t,\ell} \right\|^2 \right]$ and iv) $\mathbb{E} \left[\left\| \sum_{\ell=1}^K \left(\sum_{i \in \mathcal{H}} \frac{\nabla F_i(\mathbf{w}_{t,\ell}^i)}{|\mathcal{H}|} - \mathbf{Z}_{t,\ell} \bar{\mathbf{g}}_{\mathcal{H}}(\mathbf{w}_{t,\ell}^i, \mathbf{Z}_{t,\ell}) \right) \right\|^2 \right]$. Lemma B.1 (in turn requiring similar derivations as for the proof of Lemma B.2) relates the term ii) to $\mathbb{E} \left[\|\nabla F_{\mathcal{H}}(\mathbf{w}_t)\|^2 \right]$ and a term like iii). iv) can be bounded from above by $\left\| \left(\nabla F_i(\mathbf{w}_{t,\ell}^i) - \nabla F_i^\mu(\mathbf{w}_{t,\ell}^i) \right) \right\|^2$ and $\mathbb{E} \left[\left\| \sum_{\ell=1}^K \left(\nabla F_i^\mu(\mathbf{w}_{t,\ell}^i) - \mathbf{Z}_{t,\ell} \mathbf{g}_i(\mathbf{w}_{t,\ell}^i, \mathbf{Z}_{t,\ell}) \right) \right\|^2 \right]$. While the first is bounded by Proposition 5.6, the latter is bounded by Lemma B.2 (in turn requiring Assumption 5.2 and Lemmas B.1 and B.6 in terms of $\mathbb{E} \left[\|\nabla F_{\mathcal{H}}(\mathbf{w}_t)\|^2 \right]$ and terms like iii). ii) is bounded by a twice application of a particular Johnson-Lindenstrauss-type Lemma (Lemma B.5) and Lemma B.3 (which relies on (Wang et al., 2025, Lemma B.1) and Lemma B.2. All terms of the kind iii) are bounded using Lemma B.4 (that relies on Lemma B.3) in terms of $\mathbb{E} \left[\|\nabla F_{\mathcal{H}}(\mathbf{w}_t)\|^2 \right]$. By appropriate choices of the learning rates so that Lemma B.1 and Lemma B.4 hold and the term that multiplies the quantity $\mathbb{E} \left[\|\nabla F_{\mathcal{H}}(\mathbf{w}_t)\|^2 \right]$ of interest is negative and can hence be rearranged and bounded, the proof is completed by telescoping over all global iterations. \square

B.1.1 PROOF OF THEOREM 5.7 FOR $\mu > 0$

We start with proving convergence for $\mu > 0$, and apply similar steps to prove the result for $\mu = 0$ in Appendix B.1.2.

Proof. To prove the convergence of our algorithm for general non-convex functions with local iterations, byzantine resilience and heterogeneity, we rely on the following intermediate lemmas that we state in the following. We assume throughout that

Assumptions 5.1 to 5.4 hold, and the robust aggregator satisfies Definition 2.2.

Lemma B.1. *Let*

$$\begin{aligned} c_6 &\triangleq 5 \cdot 32\eta^2 K \left(K + \frac{d}{|\mathcal{H}|\nu} \right), \\ c_7 &\triangleq 5K\eta^2 \frac{d}{|\mathcal{H}|\nu} (32\zeta^2 + 8\sigma^2 + L^2\mu^2 d) + 5\eta^2 24K^2 L\mu, \text{ and} \\ c_8 &\triangleq 5 \cdot 32\eta^2 \left(KD^2 + \frac{1}{|\mathcal{H}|\nu} dL^2 \right). \end{aligned}$$

Let $\hat{\mathbf{w}}_{t,\ell} \triangleq \frac{1}{|\mathcal{H}|} \sum_{i \in \mathcal{H}} \mathbf{w}_{t,\ell}^i$. For a learning rate satisfying $24K\eta^2 L^2 \leq \frac{1}{3K}$ and $2\eta^2 \frac{1}{|\mathcal{H}|} \frac{4d}{\nu} 4L^2 \leq \frac{1}{3K}$, we have the following upper bound on the averaged local model divergence:

$$\mathbb{E} \left[\|\hat{\mathbf{w}}_{t,\ell} - \mathbf{w}_t\|^2 \right] \leq c_6 \mathbb{E} \left[\|\nabla F_{\mathcal{H}}(\mathbf{w}_t)\|^2 \right] + c_7 + c_8 \sum_{\ell'=1}^{\ell-1} \frac{1}{|\mathcal{H}|} \sum_{i \in \mathcal{H}} \mathbb{E} \left[\|\mathbf{w}_{t,\ell'}^i - \hat{\mathbf{w}}_{t,\ell'}\|^2 \right].$$

Lemma B.2. *Let*

$$\begin{aligned} c_9 &\triangleq \frac{16d}{\nu} L^2, \\ c_{10} &\triangleq \frac{80 \cdot 32d}{\nu} L^2 \eta^2 \left(KD^2 + \frac{1}{|\mathcal{H}|\nu} dL^2 \right), \\ c_{11} &\triangleq \frac{16d}{\nu} + \frac{80 \cdot 32d}{\nu} L^2 \eta^2 K \left(K + \frac{d}{|\mathcal{H}|\nu} \right), \text{ and} \\ c_{12} &\triangleq \left(\frac{d}{2\nu} + \frac{80d^2}{\nu^2 |\mathcal{H}|} L^2 K \eta^2 \right) (32\zeta^2 + 8\sigma^2 + L^2\mu^2 d) + \frac{80 \cdot 24d}{\nu} L^2 \eta^2 K^2 L\mu. \end{aligned}$$

We have the following bound on the gradient estimate variance based on multiple independent perturbations

$$\begin{aligned} &\mathbb{E} \left[\|\mathbf{Z}_{t,\ell} \mathbf{g}_i(\mathbf{w}_{t,\ell}^i, \mathbf{Z}_{t,\ell}) - \nabla F_i^\mu(\mathbf{w}_{t,\ell}^i)\|^2 \right] \\ &\leq c_9 \mathbb{E} \left[\|\mathbf{w}_{t,\ell}^i - \hat{\mathbf{w}}_{t,\ell}\|^2 \right] + c_{12} + c_{11} \mathbb{E} \left[\|\nabla F_{\mathcal{H}}(\mathbf{w}_t)\|^2 \right] + c_{10} \sum_{\ell'=1}^{\ell-1} \frac{1}{|\mathcal{H}|} \sum_{i \in \mathcal{H}} \mathbb{E} \left[\|\mathbf{w}_{t,\ell'}^i - \hat{\mathbf{w}}_{t,\ell'}\|^2 \right]. \end{aligned}$$

Lemma B.3. *Let*

$$\begin{aligned} c_{13} &\triangleq 6D^2 + 6\zeta^2 + 2c_9 + 2c_{10}K^2 = 6D^2 + 6\zeta^2 + 2\frac{4d}{\nu} 4L^2 + \frac{8d}{\nu} 4L^2 5 \cdot 32\eta^2 \left(KD^2 + \frac{1}{|\mathcal{H}|\nu} dL^2 \right) K^2, \\ c_{14} &\triangleq 2c_{12} = 2 \left(\frac{d}{2\nu} + \frac{80d^2}{\nu^2 |\mathcal{H}|} L^2 K \eta^2 \right) (32\zeta^2 + 8\sigma^2 + L^2\mu^2 d) + \frac{8d}{\nu} 4L^2 5\eta^2 24K^2 L\mu, \\ c_{15} &\triangleq 6L, \text{ and} \\ c_{16} &\triangleq 2c_{11} = \frac{8d}{\nu} 4 + \frac{8d}{\nu} 4L^2 5 \cdot 32\eta^2 K \left(K + \frac{d}{|\mathcal{H}|\nu} \right). \end{aligned}$$

Then the local gradient divergence is bounded from above by

$$\begin{aligned} &\sum_{m=1}^{\ell} \frac{1}{|\mathcal{H}|} \sum_{i \in \mathcal{H}} \mathbb{E} \left[\left\| \mathbf{Z}_{t,m} \mathbf{g}_i(\mathbf{w}_{t,\ell}^i, \mathbf{Z}_{t,\ell}) - \frac{1}{|\mathcal{H}|} \sum_{j \in \mathcal{H}} \mathbf{Z}_{t,m} \mathbf{g}_j(\mathbf{w}_{t,m}^j, \mathbf{Z}_{t,m}) \right\|^2 \right] \\ &\leq \sum_{m=1}^{\ell} \frac{1}{|\mathcal{H}|} \sum_{i \in \mathcal{H}} c_{13} \mathbb{E} \left[\|\hat{\mathbf{w}}_{t,m} - \mathbf{w}_{t,m}^i\|^2 \right] + \sum_{m=1}^{\ell} (c_{14} + c_{15}) + \sum_{m=1}^{\ell} c_{16} \mathbb{E} \left[\|\nabla F_{\mathcal{H}}(\mathbf{w}_t)\|^2 \right]. \end{aligned}$$

Lemma B.4. *Let*

$$c_1 \triangleq 4\eta^2 K^3 \frac{16d}{\nu} + \frac{4d}{\nu} 4L^2 5 \cdot 32\eta^2 K \left(K + \frac{d}{|\mathcal{H}|\nu} \right) \text{ and}$$

$$c_2 \triangleq 4\eta^2 K^3 \left(\left(\frac{d}{2\nu} + \frac{80d^2}{\nu^2 |\mathcal{H}|} L^2 K \eta^2 \right) (32\zeta^2 + 8\sigma^2 + L^2 \mu^2 d) + \frac{80 \cdot 24d}{\nu} L^2 \eta^2 K^2 L \mu \right) + 12\eta^2 K^3 L.$$

For a learning rate that satisfies $\eta \leq \sqrt{6 \frac{D^2}{K^2} + 6 \frac{\zeta^2}{K^2} + \frac{24d}{\nu K^2} L^2}$, we have the following upper bound on the local model divergence

$$\sum_{\ell=1}^K \frac{1}{|\mathcal{H}|} \sum_{i \in \mathcal{H}} \mathbb{E} \left[\|\mathbf{w}_{t,\ell}^i - \hat{\mathbf{w}}_{t,\ell}\|^2 \right] \leq c_1 \mathbb{E} \left[\|\nabla F_{\mathcal{H}}(\mathbf{w}_t)\|^2 \right] + c_2.$$

Now we are ready to prove Theorem 5.7. With $R_{t,\ell} \triangleq R \left(\{\mathbf{g}_i(\mathbf{w}_{t,\ell}^i, \mathbf{Z}_{t,\ell})\}_{i=1}^n \right)$, we have by Assumption 5.1 that

$$\begin{aligned} F_{\mathcal{H}}(\mathbf{w}_{t+1}) - F_{\mathcal{H}}(\mathbf{w}_t) &\leq \langle \nabla F_{\mathcal{H}}(\mathbf{w}_t), \mathbf{w}_{t+1} - \mathbf{w}_t \rangle + \frac{L}{2} \|\mathbf{w}_{t+1} - \mathbf{w}_t\|^2 \\ &= -\eta \left\langle \nabla F_{\mathcal{H}}(\mathbf{w}_t), \sum_{\ell=1}^K R_{t,\ell} \mathbf{Z}_{t,\ell}^r \right\rangle + \frac{\eta^2 L}{2} \left\| \sum_{\ell=1}^K R_{t,\ell} \mathbf{Z}_{t,\ell}^r \right\|^2 \end{aligned} \quad (6)$$

We first seek an upper bound to the first term:

$$\begin{aligned} &-\eta/K \left\langle K \nabla F_{\mathcal{H}}(\mathbf{w}_t), \sum_{\ell=1}^K R_{t,\ell} \mathbf{Z}_{t,\ell} \right\rangle \\ &= -\eta/(2K) \left(K^2 \|\nabla F_{\mathcal{H}}(\mathbf{w}_t)\|^2 + \left\| \sum_{\ell=1}^K R_{t,\ell} \mathbf{Z}_{t,\ell} \right\|^2 - \left\| K \nabla F_{\mathcal{H}}(\mathbf{w}_t) - \sum_{\ell=1}^K R_{t,\ell} \mathbf{Z}_{t,\ell} \right\|^2 \right). \end{aligned}$$

The leftmost term is the quantity of interest and will later be brought to the LHS of the equation. The prefactor of the middle term will, by an appropriate choice of the learning rate, be made small enough such that $c \triangleq \frac{\eta^2 L}{2} - \frac{\eta}{2K} \leq 0$, and hence we can bound the term $c \left\| \sum_{\ell=1}^K R_{t,\ell} \mathbf{Z}_{t,\ell} \right\|^2$ by 0. It remains to find a bound for the rightmost term $\left\| K \nabla F_{\mathcal{H}}(\mathbf{w}_t) - \sum_{\ell=1}^K R_{t,\ell} \mathbf{Z}_{t,\ell} \right\|^2$. Let $\bar{\mathbf{g}}_{\mathcal{H}}(\mathbf{w}_{t,\ell}^i, \mathbf{Z}_{t,\ell}) \triangleq \frac{1}{|\mathcal{H}|} \sum_{i \in \mathcal{H}} \mathbf{g}_i(\mathbf{w}_{t,\ell}^i, \mathbf{Z}_{t,\ell})$. By expansion, we can obtain

$$\begin{aligned} &\left\| K \nabla F_{\mathcal{H}}(\mathbf{w}_t) - \sum_{\ell=1}^K \mathbf{Z}_{t,\ell} R_{t,\ell} \right\|^2 \\ &= \left\| K \nabla F_{\mathcal{H}}(\mathbf{w}_t) + \sum_{\ell=1}^K \left(-\nabla F_{\mathcal{H}}(\hat{\mathbf{w}}_{t,\ell}) + \nabla F_{\mathcal{H}}(\hat{\mathbf{w}}_{t,\ell}) - \sum_{i \in \mathcal{H}} \frac{\nabla F_i(\mathbf{w}_{t,\ell}^i)}{|\mathcal{H}|} \right. \right. \\ &\quad \left. \left. + \sum_{i \in \mathcal{H}} \frac{\nabla F_i(\mathbf{w}_{t,\ell}^i)}{|\mathcal{H}|} - \mathbf{Z}_{t,\ell} \bar{\mathbf{g}}_{\mathcal{H}}(\mathbf{w}_{t,\ell}^i, \mathbf{Z}_{t,\ell}) + \mathbf{Z}_{t,\ell} \bar{\mathbf{g}}_{\mathcal{H}}(\mathbf{w}_{t,\ell}^i, \mathbf{Z}_{t,\ell}) - \mathbf{Z}_{t,\ell} R_{t,\ell} \right) \right\|^2 \\ &\leq 4K \sum_{\ell=1}^K \|\nabla F_{\mathcal{H}}(\mathbf{w}_t) - \nabla F_{\mathcal{H}}(\hat{\mathbf{w}}_{t,\ell})\|^2 + 4 \left\| \sum_{\ell=1}^K (\mathbf{Z}_{t,\ell} \bar{\mathbf{g}}_{\mathcal{H}}(\mathbf{w}_{t,\ell}^i, \mathbf{Z}_{t,\ell}) - \mathbf{Z}_{t,\ell} R_{t,\ell}) \right\|^2 \\ &\quad + 4K \sum_{\ell=1}^K \left\| \nabla F_{\mathcal{H}}(\hat{\mathbf{w}}_{t,\ell}) - \sum_{i \in \mathcal{H}} \frac{\nabla F_i(\mathbf{w}_{t,\ell}^i)}{|\mathcal{H}|} \right\|^2 + 4 \left\| \sum_{\ell=1}^K \left(\sum_{i \in \mathcal{H}} \frac{\nabla F_i(\mathbf{w}_{t,\ell}^i)}{|\mathcal{H}|} - \mathbf{Z}_{t,\ell} \bar{\mathbf{g}}_{\mathcal{H}}(\mathbf{w}_{t,\ell}^i, \mathbf{Z}_{t,\ell}) \right) \right\|^2 \\ &\stackrel{(a)}{\leq} 4K \sum_{\ell=1}^K L^2 \|\mathbf{w}_t - \hat{\mathbf{w}}_{t,\ell}\|^2 + 4 \left\| \sum_{\ell=1}^K (\mathbf{Z}_{t,\ell} \bar{\mathbf{g}}_{\mathcal{H}}(\mathbf{w}_{t,\ell}^i, \mathbf{Z}_{t,\ell}) - \mathbf{Z}_{t,\ell} R_{t,\ell}) \right\|^2 + 4K \sum_{\ell=1}^K \frac{D^2}{|\mathcal{H}|} \sum_{i \in \mathcal{H}} \|\mathbf{w}_{t,\ell}^i - \hat{\mathbf{w}}_{t,\ell}\|^2 \end{aligned}$$

$$+ 4 \left\| \sum_{\ell=1}^K \left(\sum_{i \in \mathcal{H}} \frac{\nabla F_i(\mathbf{w}_{t,\ell}^i)}{|\mathcal{H}|} - \mathbf{Z}_{t,\ell} \bar{\mathbf{g}}_{\mathcal{H}}(\mathbf{w}_{t,\ell}^i, \mathbf{Z}_{t,\ell}) \right) \right\|^2,$$

where (a) holds by Assumption 5.1 and Assumption 5.4. We take the expectation on both sides and obtain

$$\begin{aligned} & \mathbb{E} \left[\left\| K \nabla F_{\mathcal{H}}(\mathbf{w}_t) - \sum_{\ell=1}^K \mathbf{Z}_{t,\ell} R_{t,\ell} \right\|^2 \right] \\ & \leq 4K \sum_{\ell=1}^K L^2 \mathbb{E} \left[\|\mathbf{w}_t - \hat{\mathbf{w}}_{t,\ell}\|^2 \right] + 4\mathbb{E} \left[\sum_{\ell=1}^K \|\mathbf{Z}_{t,\ell} \bar{\mathbf{g}}_{\mathcal{H}}(\mathbf{w}_{t,\ell}^i, \mathbf{Z}_{t,\ell}) - \mathbf{Z}_{t,\ell} R_{t,\ell}\|^2 \right] \\ & + 4K \sum_{\ell=1}^K \frac{D^2}{|\mathcal{H}|} \sum_{i \in \mathcal{H}} \mathbb{E} \left[\|\mathbf{w}_{t,\ell}^i - \hat{\mathbf{w}}_{t,\ell}\|^2 \right] + 4\mathbb{E} \left[\left\| \sum_{\ell=1}^K \left(\sum_{i \in \mathcal{H}} \frac{\nabla F_i(\mathbf{w}_{t,\ell}^i)}{|\mathcal{H}|} - \mathbf{Z}_{t,\ell} \bar{\mathbf{g}}_{\mathcal{H}}(\mathbf{w}_{t,\ell}^i, \mathbf{Z}_{t,\ell}) \right) \right\|^2 \right]. \end{aligned} \quad (7)$$

We continue with bounding the individual terms, and start with the latter term.

$$\begin{aligned} & \mathbb{E} \left[\left\| \sum_{\ell=1}^K \left(\sum_{i \in \mathcal{H}} \frac{1}{|\mathcal{H}|} \nabla F_i(\mathbf{w}_{t,\ell}^i) - \mathbf{Z}_{t,\ell} \bar{\mathbf{g}}_{\mathcal{H}}(\mathbf{w}_{t,\ell}^i, \mathbf{Z}_{t,\ell}) \right) \right\|^2 \right] \\ & \leq 2\mathbb{E} \left[\left\| \sum_{\ell=1}^K \sum_{i \in \mathcal{H}} \frac{1}{|\mathcal{H}|} (\nabla F_i(\mathbf{w}_{t,\ell}^i) - \nabla F_i^\mu(\mathbf{w}_{t,\ell}^i)) \right\|^2 \right] + 2\mathbb{E} \left[\left\| \sum_{\ell=1}^K \sum_{i \in \mathcal{H}} \frac{1}{|\mathcal{H}|} (\nabla F_i^\mu(\mathbf{w}_{t,\ell}^i) - \mathbf{Z}_{t,\ell} \mathbf{g}_i(\mathbf{w}_{t,\ell}^i, \mathbf{Z}_{t,\ell})) \right\|^2 \right] \\ & \stackrel{(a)}{\leq} 2 \frac{K}{|\mathcal{H}|} \sum_{i \in \mathcal{H}} \sum_{\ell=1}^K \|\nabla F_i(\mathbf{w}_{t,\ell}^i) - \nabla F_i^\mu(\mathbf{w}_{t,\ell}^i)\|^2 + 2 \frac{1}{|\mathcal{H}|^2} \sum_{i \in \mathcal{H}} \mathbb{E} \left[\left\| \sum_{\ell=1}^K (\nabla F_i^\mu(\mathbf{w}_{t,\ell}^i) - \mathbf{Z}_{t,\ell} \mathbf{g}_i(\mathbf{w}_{t,\ell}^i, \mathbf{Z}_{t,\ell})) \right\|^2 \right] \\ & \stackrel{(b)}{\leq} 2K^2 L\mu + 2 \frac{1}{|\mathcal{H}|^2} \sum_{i \in \mathcal{H}} \sum_{\ell=1}^K \mathbb{E} \left[\|\nabla F_i^\mu(\mathbf{w}_{t,\ell}^i) - \mathbf{Z}_{t,\ell} \mathbf{g}_i(\mathbf{w}_{t,\ell}^i, \mathbf{Z}_{t,\ell})\|^2 \right] \\ & \stackrel{(c)}{\leq} 2K^2 L\mu + 2 \frac{1}{|\mathcal{H}|^2} \sum_{i \in \mathcal{H}} \sum_{\ell=1}^K \left(c_9 \mathbb{E} \left[\|\mathbf{w}_{t,\ell}^i - \hat{\mathbf{w}}_{t,\ell}\|^2 \right] + c_{12} \right. \\ & \quad \left. + c_{11} \mathbb{E} \left[\|\nabla F_{\mathcal{H}}(\mathbf{w}_t)\|^2 \right] + c_{10} \sum_{\ell'=1}^{\ell-1} \frac{1}{|\mathcal{H}|} \sum_{i \in \mathcal{H}} \mathbb{E} \left[\|\mathbf{w}_{t,\ell'}^i - \hat{\mathbf{w}}_{t,\ell'}\|^2 \right] \right) \\ & \stackrel{(d)}{\leq} 2K^2 L\mu + 2 \frac{1}{|\mathcal{H}|^2} \sum_{i \in \mathcal{H}} \sum_{\ell=1}^K \left(c_9 \mathbb{E} \left[\|\mathbf{w}_{t,\ell}^i - \hat{\mathbf{w}}_{t,\ell}\|^2 \right] + c_{12} \right. \\ & \quad \left. + c_{11} \mathbb{E} \left[\|\nabla F_{\mathcal{H}}(\mathbf{w}_t)\|^2 \right] + \frac{c_{10} K(K-1)}{|\mathcal{H}|} \sum_{i \in \mathcal{H}} \mathbb{E} \left[\|\mathbf{w}_{t,\ell}^i - \hat{\mathbf{w}}_{t,\ell}\|^2 \right] \right) \\ & = 2K^2 L\mu + 2 \frac{1}{|\mathcal{H}|^2} \sum_{i \in \mathcal{H}} \sum_{\ell=1}^K \left((c_9 + c_{10} K(K-1)) \mathbb{E} \left[\|\mathbf{w}_{t,\ell}^i - \hat{\mathbf{w}}_{t,\ell}\|^2 \right] + c_{12} + c_{11} \mathbb{E} \left[\|\nabla F_{\mathcal{H}}(\mathbf{w}_t)\|^2 \right] \right), \end{aligned} \quad (8)$$

where (a) is due to the independence of $\sum_{\ell=1}^K (\nabla F_i^\mu(\mathbf{w}_{t,\ell}^i) - \mathbf{Z}_{t,\ell} \mathbf{g}_i(\mathbf{w}_{t,\ell}^i, \mathbf{Z}_{t,\ell}))$ and $\sum_{\ell=1}^K (\nabla F_j^\mu(\mathbf{w}_{t,\ell}^j) - \mathbf{Z}_{t,\ell} \mathbf{g}_j(\mathbf{w}_{t,\ell}^j, \mathbf{Z}_{t,\ell}))$ for $i \neq j$. (b) follows from Proposition 5.5 and (Wang et al., 2021, Lemma 2). (c) is by the application of Lemma B.2. (d) holds since $\sum_{\ell=1}^K \sum_{\ell'=1}^{\ell-1} x_{\ell'} \leq \sum_{\ell=1}^K \sum_{\ell'=1}^{\ell} x_{\ell'} \leq \frac{K(K-1)}{2} \sum_{\ell} x_{\ell}$.

We continue with bounding the robustness term using a double-sided application of an extension of the Johnson-Lindenstrauss Lemma as stated in the following Lemma B.5 and the application of Lemma B.3.

Lemma B.5 (Proposition 8, (Li, 2024)). *Let $\mathbf{Z} = (\mathbf{z}_1, \dots, \mathbf{z}_\nu)^T \in \mathbb{R}^{\nu \times d}$ with $\mathbf{z}_r \sim \mathcal{U}(\mathbb{S}^d), \forall r \in [\nu]$. For a given vector $\mathbf{x} \in \mathbb{R}^d$, we have for $\epsilon > 0, \delta < 1/2$ with probability at least $1 - \delta$ that*

$$(1 - \epsilon) \|\mathbf{x}\|^2 \leq \|\mathbf{Z}\mathbf{x}\|^2 \leq (1 + \epsilon) \|\mathbf{x}\|^2$$

for $\nu \geq 64\epsilon^{-2} \log(2/\delta)$.

For the robustness term, we have

$$\begin{aligned} & \mathbb{E} \left[\left\| \sum_{\ell=1}^K \mathbf{Z}_{t,\ell} (R_{t,\ell} - \bar{\mathbf{g}}_{\mathcal{H}}(\mathbf{w}_{t,\ell}^i, \mathbf{Z}_{t,\ell})) \right\|^2 \right] \\ & \leq K \sum_{\ell=1}^K \|\mathbf{Z}_{t,\ell} (R_{t,\ell} - \bar{\mathbf{g}}_{\mathcal{H}}(\mathbf{w}_{t,\ell}^i, \mathbf{Z}_{t,\ell}))\|^2 \\ & \stackrel{(a)}{\leq} K \sum_{\ell=1}^K (1 + \epsilon) \frac{\kappa}{|\mathcal{H}|} \sum_{i \in \mathcal{H}} \mathbb{E} \left[\|\mathbf{g}_i(\mathbf{w}_{t,\ell}^i, \mathbf{Z}_{t,\ell}) - \bar{\mathbf{g}}_{\mathcal{H}}(\mathbf{w}_{t,\ell}^i, \mathbf{Z}_{t,\ell})\|^2 \right] \\ & \stackrel{(b)}{\leq} K \sum_{\ell=1}^K \frac{(1 + \epsilon)}{(1 - \epsilon)} \frac{\kappa}{|\mathcal{H}|} \sum_{i \in \mathcal{H}} \mathbb{E} \left[\|\mathbf{Z}_{t,\ell} (\mathbf{g}_i(\mathbf{w}_{t,\ell}^i, \mathbf{Z}_{t,\ell}) - \bar{\mathbf{g}}_{\mathcal{H}}(\mathbf{w}_{t,\ell}^i, \mathbf{Z}_{t,\ell}))\|^2 \right] \\ & \stackrel{(c)}{\leq} K \frac{(1 + \epsilon)}{(1 - \epsilon)} \kappa \left(\sum_{\ell=1}^K \frac{1}{|\mathcal{H}|} \sum_{i \in \mathcal{H}} c_{13} \mathbb{E} \left[\|\hat{\mathbf{w}}_{t,\ell} - \mathbf{w}_{t,\ell}^i\|^2 \right] + \sum_{\ell=1}^K (c_{14} + c_{15}) + \sum_{\ell=1}^K c_{16} \mathbb{E} \left[\|\nabla F_{\mathcal{H}}(\mathbf{w}_t)\|^2 \right] \right) \end{aligned} \quad (9)$$

where (a) and (b) are by the application of Lemma B.5 for in total $|\mathcal{H}| + 1$ projections. By a union bound over Lemma B.5, the distance preservation holds with probability $1 - \delta$ for $\epsilon \geq \sqrt{\frac{64}{\nu} \log(\frac{2(|\mathcal{H}|-1)}{\delta})}$. We choose the smallest possible ϵ . This must hold for each iteration, so the distance preservation holds w.p. at least $1 - K\delta$ for all local epochs. (c) is by Lemma B.3.

To bound the local model divergence from the global model, by Lemma B.1, we have

$$\begin{aligned} \sum_{\ell=1}^K \mathbb{E} \left[\|\hat{\mathbf{w}}_{t,\ell} - \mathbf{w}_t\|^2 \right] & \leq \sum_{\ell=1}^K c_6 \mathbb{E} \left[\|\nabla F_{\mathcal{H}}(\mathbf{w}_t)\|^2 \right] + \sum_{\ell=1}^K c_7 + \sum_{\ell=1}^K c_8 \sum_{\ell'=1}^{\ell-1} \frac{1}{|\mathcal{H}|} \sum_{i \in \mathcal{H}} \mathbb{E} \left[\|\mathbf{w}_{t,\ell'}^i - \hat{\mathbf{w}}_{t,\ell'}\|^2 \right] \\ & \leq \sum_{\ell=1}^K c_6 \mathbb{E} \left[\|\nabla F_{\mathcal{H}}(\mathbf{w}_t)\|^2 \right] + \sum_{\ell=1}^K c_7 + \sum_{\ell=1}^K \frac{c_8 K(K-1)}{|\mathcal{H}|} \sum_{i \in \mathcal{H}} \mathbb{E} \left[\|\mathbf{w}_{t,\ell}^i - \hat{\mathbf{w}}_{t,\ell}\|^2 \right], \end{aligned} \quad (10)$$

where the latter follows since $\sum_{\ell=1}^K \sum_{\ell'=1}^{\ell-1} x_{\ell'} \leq \sum_{\ell=1}^K \sum_{\ell'=1}^{\ell} x_{\ell'} \leq \frac{K(K-1)}{2} \sum_{\ell} x_{\ell}$.

Plugging (8), (9), and (10) into (7), we obtain

$$\begin{aligned} & \mathbb{E} \left[\left\| K \nabla F_{\mathcal{H}}(\mathbf{w}_t) - \sum_{\ell=1}^K \mathbf{Z}_{t,\ell} R_{t,\ell} \right\|^2 \right] \\ & \leq 4KL^2 \left(\sum_{\ell=1}^K c_6 \mathbb{E} \left[\|\nabla F_{\mathcal{H}}(\mathbf{w}_t)\|^2 \right] + \sum_{\ell=1}^K c_7 + \sum_{\ell=1}^K \frac{c_8 K(K-1)}{|\mathcal{H}|} \sum_{i \in \mathcal{H}} \mathbb{E} \left[\|\mathbf{w}_{t,\ell}^i - \hat{\mathbf{w}}_{t,\ell}\|^2 \right] \right) \\ & + 4 \left(K \frac{(1 + \epsilon)}{(1 - \epsilon)} \kappa \left(\sum_{\ell=1}^K \frac{1}{|\mathcal{H}|} \sum_{i \in \mathcal{H}} c_{13} \mathbb{E} \left[\|\hat{\mathbf{w}}_{t,\ell} - \mathbf{w}_{t,\ell}^i\|^2 \right] + \sum_{\ell=1}^K (c_{14} + c_{15}) + \sum_{\ell=1}^K c_{16} \mathbb{E} \left[\|\nabla F_{\mathcal{H}}(\mathbf{w}_t)\|^2 \right] \right) \right) \\ & + 4K \sum_{\ell=1}^K \frac{D^2}{|\mathcal{H}|} \sum_{i \in \mathcal{H}} \mathbb{E} \left[\|\mathbf{w}_{t,\ell}^i - \hat{\mathbf{w}}_{t,\ell}\|^2 \right] \end{aligned}$$

$$\begin{aligned}
 & + 4 \left(2K^2 L \mu + 2 \frac{1}{|\mathcal{H}|^2} \sum_{i \in \mathcal{H}} \sum_{\ell=1}^K \left((c_9 + c_{10} K (K-1)) \mathbb{E} \left[\|\mathbf{w}_{t,\ell}^i - \hat{\mathbf{w}}_{t,\ell}\|^2 \right] + c_{12} + c_{11} \mathbb{E} \left[\|\nabla F_{\mathcal{H}}(\mathbf{w}_t)\|^2 \right] \right) \right) \\
 & \leq c'_3 \mathbb{E} \left[\|\nabla F_{\mathcal{H}}(\mathbf{w}_t)\|^2 \right] + c'_4 \sum_{\ell=1}^K \frac{1}{|\mathcal{H}|} \sum_{i \in \mathcal{H}} \mathbb{E} \left[\|\hat{\mathbf{w}}_{t,\ell} - \mathbf{w}_{t,\ell}^i\|^2 \right] + c'_5 \\
 & \leq c'_3 \mathbb{E} \left[\|\nabla F_{\mathcal{H}}(\mathbf{w}_t)\|^2 \right] + c'_4 c_1 \mathbb{E} \left[\|\nabla F_{\mathcal{H}}(\mathbf{w}_t)\|^2 \right] + c'_4 c_2 + c'_5, \\
 & \leq (c'_3 + c'_4 c_1) \mathbb{E} \left[\|\nabla F_{\mathcal{H}}(\mathbf{w}_t)\|^2 \right] + c'_4 c_2 + c'_5, \tag{11}
 \end{aligned}$$

where the penultimate step is by the application of Lemma B.4, and the constants read and can be bounded as

$$\begin{aligned}
 c'_3 & \triangleq 4KL^2 \sum_{\ell=1}^K c_6 + 4K \frac{(1+\epsilon)}{(1-\epsilon)} \kappa \sum_{\ell=1}^K c_{16} + 4 \cdot 2 \frac{1}{|\mathcal{H}|^2} \sum_{i \in \mathcal{H}} \sum_{\ell=1}^K c_{11} \\
 & \leq 4K^2 L^2 c_6 + \left(8K^2 \frac{(1+\epsilon)}{(1-\epsilon)} \kappa + 8 \frac{1}{|\mathcal{H}|} K \right) c_{11} \\
 & \leq c_3 \triangleq 4K^2 L^2 5 \cdot 32\eta^2 K \left(K + \frac{d}{|\mathcal{H}|\nu} \right) + \left(8K^2 \frac{(1+\epsilon)}{(1-\epsilon)} \kappa + 8 \frac{1}{|\mathcal{H}|} K \right) \left(\frac{16d}{\nu} + \frac{80 \cdot 32d}{\nu} L^2 \eta^2 K \left(K + \frac{d}{|\mathcal{H}|\nu} \right) \right) \\
 c'_4 & \triangleq 4KL^2 c_8 K (K-1) + 4K \frac{(1+\epsilon)}{(1-\epsilon)} \kappa c_{13} + 4KD^2 + 4 \cdot 2 \frac{1}{|\mathcal{H}|} (c_9 + c_{10} K (K-1)) \\
 & \leq 4K^3 L^2 c_8 + 4K \frac{(1+\epsilon)}{(1-\epsilon)} \kappa c_{13} + 4KD^2 + 8 \frac{1}{|\mathcal{H}|} (c_9 + c_{10} K^2) \\
 & \leq 4K^3 L^2 c_8 + 8K \frac{(1+\epsilon)}{(1-\epsilon)} \kappa (3D^2 + 3\zeta^2 + c_9 + c_{10} K^2) + 4KD^2 + 8 \frac{1}{|\mathcal{H}|} (c_9 + c_{10} K^2) \\
 & \leq 4K^3 L^2 c_8 + 8K \frac{(1+\epsilon)}{(1-\epsilon)} \kappa (3D^2 + 3\zeta^2) + 4KD^2 + 8 \left(\frac{1}{|\mathcal{H}|} + K \frac{(1+\epsilon)}{(1-\epsilon)} \kappa \right) (c_9 + c_{10} K^2) \\
 & \leq 20 \cdot 32K^3 L^2 \eta^2 \left(KD^2 + \frac{1}{|\mathcal{H}|} \frac{d}{\nu} L^2 \right) + 8K \frac{(1+\epsilon)}{(1-\epsilon)} \kappa (3D^2 + 3\zeta^2) + 4KD^2 \\
 & + 8 \left(\frac{1}{|\mathcal{H}|} + K \frac{(1+\epsilon)}{(1-\epsilon)} \kappa \right) \left(\frac{16d}{\nu} L^2 + \frac{80 \cdot 32d}{\nu} L^2 \eta^2 \left(KD^2 + \frac{1}{|\mathcal{H}|} \frac{d}{\nu} L^2 \right) K^2 \right) \\
 & \leq c_4 \triangleq 20 \cdot 32K^2 L^2 \eta^2 \left(KD^2 + \frac{1}{|\mathcal{H}|} \frac{d}{\nu} L^2 \right) \left(K + \frac{4d}{\nu} \right) \\
 & \quad + 8K \frac{(1+\epsilon)}{(1-\epsilon)} \kappa \left(3D^2 + 3\zeta^2 + \frac{16d}{\nu} L^2 \right) + 4KD^2 + 8 \frac{1}{|\mathcal{H}|} \frac{16d}{\nu} L^2 \\
 c'_5 & \triangleq 4KL^2 \sum_{\ell=1}^K c_7 + 4K \frac{(1+\epsilon)}{(1-\epsilon)} \kappa \sum_{\ell=1}^K (c_{14} + c_{15}) + 4 \cdot 2K^2 L \mu + 4 \cdot 2 \frac{1}{|\mathcal{H}|^2} \sum_{i \in \mathcal{H}} \sum_{\ell=1}^K c_{12} \\
 & \leq 4K^2 L^2 c_7 + 4K^2 \frac{(1+\epsilon)}{(1-\epsilon)} \kappa (c_{14} + c_{15}) + 8K^2 L \mu + 8 \frac{1}{|\mathcal{H}|} K c_{12} \\
 & \leq 4K^2 L^2 c_7 + 4K^2 \frac{(1+\epsilon)}{(1-\epsilon)} \kappa (2c_{12} + 6L) + 8K^2 L \mu + 8 \frac{1}{|\mathcal{H}|} K c_{12} \\
 & \leq 4K^2 L^2 c_7 + 4K^2 \frac{(1+\epsilon)}{(1-\epsilon)} \kappa 6L + 8K^2 L \mu + \left(8 \frac{1}{|\mathcal{H}|} K + 8K^2 \frac{(1+\epsilon)}{(1-\epsilon)} \kappa \right) c_{12} \\
 & \leq 4K^2 L^2 \left(5K \eta^2 \frac{d}{|\mathcal{H}|\nu} (32\zeta^2 + 8\sigma^2 + L^2 \mu^2 d) + 5\eta^2 24K^2 L \mu \right) + 4K^2 \frac{(1+\epsilon)}{(1-\epsilon)} \kappa 6L + 8K^2 L \mu \\
 & + \left(8 \frac{1}{|\mathcal{H}|} K + 8K^2 \frac{(1+\epsilon)}{(1-\epsilon)} \kappa \right) \left(\left(\frac{d}{2\nu} + \frac{80d^2}{\nu^2 |\mathcal{H}|} L^2 K \eta^2 \right) (32\zeta^2 + 8\sigma^2 + L^2 \mu^2 d) + \frac{80 \cdot 24d}{\nu} L^2 \eta^2 K^2 L \mu \right)
 \end{aligned}$$

$$\leq c_5 \triangleq (32\zeta^2 + 8\sigma^2 + L^2\mu^2d) \left(20K^3L^2\eta^2 \frac{d}{|\mathcal{H}|\nu} + \left(8\frac{1}{|\mathcal{H}|}K + 8K^2\frac{(1+\epsilon)}{(1-\epsilon)}\kappa \right) \left(\frac{d}{2\nu} + \frac{80d^2}{\nu^2|\mathcal{H}|}L^2K\eta^2 \right) \right) \\ + 4K^2L^25\eta^224K^2L\mu + 4K^2\frac{(1+\epsilon)}{(1-\epsilon)}\kappa6L + 8K^2L\mu + \left(8\frac{1}{|\mathcal{H}|}K + 8K^2\frac{(1+\epsilon)}{(1-\epsilon)}\kappa \right) \left(\frac{80 \cdot 24d}{\nu}L^2\eta^2K^2L\mu \right)$$

By taking the expectation over (6) and replacing $\mathbb{E} \left[\left\| K\nabla F_{\mathcal{H}}(\mathbf{w}_t) - \sum_{\ell=1}^K \mathbf{Z}_{t,\ell} R_{t,\ell} \right\|^2 \right]$ by (11), we can write

$$\mathbb{E} [F_{\mathcal{H}}(\mathbf{w}_{t+1})] - \mathbb{E} [F_{\mathcal{H}}(\mathbf{w}_t)] \\ \leq -\eta/(2)K\mathbb{E} \left[\|\nabla F_{\mathcal{H}}(\mathbf{w}_t)\|^2 \right] + \left(\frac{\eta^2L}{2} - \frac{\eta}{2K} \right) \mathbb{E} \left[\left\| \sum_{\ell=1}^K R_{t,\ell} \mathbf{Z}_{t,\ell} \right\|^2 \right] + \eta/(2K)\mathbb{E} \left[\left\| K\nabla F_{\mathcal{H}}(\mathbf{w}_t) - \sum_{\ell=1}^K R_{t,\ell} \mathbf{Z}_{t,\ell} \right\|^2 \right] \\ \stackrel{(a)}{\leq} -\eta/(2)K\mathbb{E} \left[\|\nabla F_{\mathcal{H}}(\mathbf{w}_t)\|^2 \right] + \eta/(2K) \left((c_3 + c_4c_1)\mathbb{E} \left[\|\nabla F_{\mathcal{H}}(\mathbf{w}_t)\|^2 \right] + c_4c_2 + c_5 \right) \\ \stackrel{(b)}{\leq} -\frac{\eta K}{4}\mathbb{E} \left[\|\nabla F_{\mathcal{H}}(\mathbf{w}_t)\|^2 \right] + \eta/(2K)(c_4c_2 + c_5),$$

where (a) holds when $\eta \leq \frac{1}{KL}$ and (b) assumes that $\frac{\eta}{2K}(c_3 + c_4c_1) \leq \frac{\eta K}{4}$.

Reordering and telescoping over t , we obtain

$$\frac{1}{T} \sum_{t=1}^T \mathbb{E} \left[\|\nabla F_{\mathcal{H}}(\mathbf{w}_t)\|^2 \right] \leq \frac{4(\mathbb{E} [F_{\mathcal{H}}(\mathbf{w}_1)] - \mathbb{E} [F_{\mathcal{H}}(\mathbf{w}_{T+1})])}{T\eta K} + \eta/(2K)(c_4c_2 + c_5)$$

with probability $1 - \delta KT$ by a union bound argument over all global iterations T . We let $\Delta \triangleq \delta KT$, and obtain $\epsilon \geq \sqrt{\frac{64}{\nu} \log(\frac{2(|\mathcal{H}|-1)}{\delta})} = \sqrt{\frac{64}{\nu} \log(\frac{2(|\mathcal{H}|-1)TK}{\Delta})}$. Since it is required to satisfy $\epsilon < 1$, the proof holds for $\nu \geq 64 \log(\frac{2(|\mathcal{H}|-1)TK}{\Delta})$. Noting that $F_{\mathcal{H}}(\mathbf{w}_{T+1}) \geq F_{\mathcal{H}}^*$ by definition concludes the proof. The requirements on the learning rate are summarized as follows:

- $24K\eta^2L^2 \leq \frac{1}{3K} \rightarrow \eta \leq \frac{1}{\sqrt{72K^2L}}$
- $2\eta^2 \frac{1}{|\mathcal{H}|} \frac{4d}{\nu} 4L^2 \leq \frac{1}{3K} \rightarrow \eta \leq \sqrt{\frac{|\mathcal{H}|\nu}{96KdL^2}}$
- $\eta \leq \sqrt{6\frac{D^2}{K^2} + 6\frac{\zeta^2}{K^2} + \frac{32d}{\nu K^2}L^2}$

The constants are summarized as

$$c_1 \triangleq 4\eta^2K^3\frac{16}{\nu} + \frac{4d}{\nu}4L^25 \cdot 32\eta^2K \left(K + \frac{d}{|\mathcal{H}|\nu} \right) \\ c_2 \triangleq 4\eta^2K^3 \left(\left(\frac{d}{2\nu} + \frac{80d^2}{\nu^2|\mathcal{H}|}L^2K\eta^2 \right) (32\zeta^2 + 8\sigma^2 + L^2\mu^2d) + \frac{80 \cdot 24d}{\nu}L^2\eta^2K^2L\mu \right) + 12\eta^2K^3L \\ c_3 \triangleq 4K^2L^25 \cdot 32\eta^2K \left(K + \frac{d}{|\mathcal{H}|\nu} \right) + \left(8K^2\frac{(1+\epsilon)}{(1-\epsilon)}\kappa + 8\frac{1}{|\mathcal{H}|}K \right) \left(\frac{16d}{\nu} + \frac{80 \cdot 32d}{\nu}L^2\eta^2K \left(K + \frac{d}{|\mathcal{H}|\nu} \right) \right) \\ c_4 \triangleq 20 \cdot 32K^2L^2\eta^2 \left(KD^2 + \frac{1}{|\mathcal{H}|}\frac{d}{\nu}L^2 \right) \left(K + \frac{4d}{\nu} \right) + 8K\frac{(1+\epsilon)}{(1-\epsilon)}\kappa \left(3D^2 + 3\zeta^2 + \frac{16d}{\nu}L^2 \right) + 4KD^2 + 8\frac{1}{|\mathcal{H}|}\frac{16d}{\nu}L^2 \\ c_5 \triangleq (32\zeta^2 + 8\sigma^2 + L^2\mu^2d) \left(20K^3L^2\eta^2 \frac{d}{|\mathcal{H}|\nu} + \left(8\frac{1}{|\mathcal{H}|}K + 8K^2\frac{(1+\epsilon)}{(1-\epsilon)}\kappa \right) \left(\frac{d}{2\nu} + \frac{80d^2}{\nu^2|\mathcal{H}|}L^2K\eta^2 \right) \right) + 4K^2L^25\eta^224K^2L\mu \\ + 4K^2\frac{(1+\epsilon)}{(1-\epsilon)}\kappa6L + 8K^2L\mu + \left(8\frac{1}{|\mathcal{H}|}K + 8K^2\frac{(1+\epsilon)}{(1-\epsilon)}\kappa \right) \left(\frac{80 \cdot 24d}{\nu}L^2\eta^2K^2L\mu \right),$$

and, with $\epsilon' \triangleq \frac{(1+\epsilon)}{(1-\epsilon)}$, can be approximated by

$$c_1 = \Theta \left(\eta^2 K^3 \frac{d}{\nu} + \frac{d}{\nu} L^2 \eta^2 K \left(K + \frac{d}{|\mathcal{H}| \nu} \right) \right) \quad (12)$$

$$c_2 = \Theta \left(\eta^2 K^3 \left(L + \left(\frac{d}{\nu} + \frac{d^2}{\nu^2 |\mathcal{H}|} L^2 K^2 \eta^2 \right) (\zeta^2 + \sigma^2 + L^2 \mu d) \right) \right) \quad (13)$$

$$c_3 = \Theta \left(\frac{d}{\nu} \left(K^2 \epsilon' \kappa + \frac{K}{|\mathcal{H}|} \right) \left(1 + L^2 \eta^2 K \left(K + \frac{d}{|\mathcal{H}| \nu} \right) \left(1 + \frac{\nu}{d} \right) \right) \right) \quad (14)$$

$$c_4 = \Theta \left(K^2 L^2 \eta^2 \left(K^2 D^2 + \frac{1}{|\mathcal{H}|} \frac{d^2}{\nu^2} L^2 \right) + K \epsilon' \kappa \left(D^2 + \zeta^2 + \frac{d}{\nu} L^2 \right) \right) \quad (15)$$

$$c_5 = \Theta \left((\zeta^2 + \sigma^2 + L^2 \mu^2 d) \left((K^2 \epsilon' \kappa) \left(\frac{d}{\nu} + \frac{d^2}{\nu^2 |\mathcal{H}|} L^2 K \eta^2 \right) \right) \right) \quad (16)$$

$$+ K^2 L (\epsilon' \kappa + \mu) + (K^2 \epsilon' \kappa) \left(\frac{d}{\nu} L^2 \eta^2 K^2 L \mu \right). \quad (17)$$

□

We now continue to prove all intermediate Lemmas B.1 to B.4.

Proof of Lemma B.1. By definition, $\mathbb{E} \left[\|\hat{\mathbf{w}}_{t,1} - \mathbf{w}_t\|^2 \right] = 0$. For $\ell \in \{2, \dots, K\}$, we have

$$\begin{aligned} & \mathbb{E} \left[\|\hat{\mathbf{w}}_{t,\ell} - \mathbf{w}_t\|^2 \right] \\ &= \mathbb{E} \left[\left\| \hat{\mathbf{w}}_{t,\ell-1} - \frac{\eta}{|\mathcal{H}|} \sum_{i \in \mathcal{H}} \mathbf{Z}_{t,\ell-1} \mathbf{g}_i(\mathbf{w}_{t,\ell-1}^i, \mathbf{Z}_{t,\ell-1}) - \mathbf{w}_t \right\|^2 \right] \\ &= \mathbb{E} \left[\left\| \hat{\mathbf{w}}_{t,\ell-1} - \mathbf{w}_t - \eta \left(\frac{1}{|\mathcal{H}|} \sum_{i \in \mathcal{H}} \mathbf{Z}_{t,\ell-1} \mathbf{g}_i(\mathbf{w}_{t,\ell-1}^i, \mathbf{Z}_{t,\ell-1}) - \frac{1}{|\mathcal{H}|} \sum_{i \in \mathcal{H}} \nabla F_i^\mu(\mathbf{w}_{t,\ell-1}^i) + \frac{1}{|\mathcal{H}|} \sum_{i \in \mathcal{H}} \nabla F_i^\mu(\mathbf{w}_{t,\ell-1}^i) \right. \right. \right. \\ & \quad \left. \left. - \frac{1}{|\mathcal{H}|} \sum_{i \in \mathcal{H}} \nabla F_i(\mathbf{w}_{t,\ell-1}^i) + \frac{1}{|\mathcal{H}|} \sum_{i \in \mathcal{H}} \nabla F_i(\mathbf{w}_{t,\ell-1}^i) - \nabla F_{\mathcal{H}}(\hat{\mathbf{w}}_{t,\ell-1}) + \nabla F_{\mathcal{H}}(\hat{\mathbf{w}}_{t,\ell-1}) - \nabla F_{\mathcal{H}}(\mathbf{w}_t) + \nabla F_{\mathcal{H}}(\mathbf{w}_t) \right) \right\|^2 \right] \\ &\leq (1 + \frac{1}{\tau}) \mathbb{E} \left[\|\hat{\mathbf{w}}_{t,\ell-1} - \mathbf{w}_t\|^2 \right] + \\ &(1 + \tau) \mathbb{E} \left[\left\| -\eta \left(\frac{1}{|\mathcal{H}|} \sum_{i \in \mathcal{H}} \mathbf{Z}_{t,\ell-1} \mathbf{g}_i(\mathbf{w}_{t,\ell-1}^i, \mathbf{Z}_{t,\ell-1}) - \frac{1}{|\mathcal{H}|} \sum_{i \in \mathcal{H}} \nabla F_i^\mu(\mathbf{w}_{t,\ell-1}^i) + \frac{1}{|\mathcal{H}|} \sum_{i \in \mathcal{H}} \nabla F_i^\mu(\mathbf{w}_{t,\ell-1}^i) \right. \right. \right. \\ & \quad \left. \left. - \frac{1}{|\mathcal{H}|} \sum_{i \in \mathcal{H}} \nabla F_i(\mathbf{w}_{t,\ell-1}^i) + \frac{1}{|\mathcal{H}|} \sum_{i \in \mathcal{H}} \nabla F_i(\mathbf{w}_{t,\ell-1}^i) - \nabla F_{\mathcal{H}}(\hat{\mathbf{w}}_{t,\ell-1}) + \nabla F_{\mathcal{H}}(\hat{\mathbf{w}}_{t,\ell-1}) - \nabla F_{\mathcal{H}}(\mathbf{w}_t) + \nabla F_{\mathcal{H}}(\mathbf{w}_t) \right) \right\|^2 \right] \\ &\stackrel{(b)}{\leq} (1 + \frac{1}{\tau}) \mathbb{E} \left[\|\hat{\mathbf{w}}_{t,\ell-1} - \mathbf{w}_t\|^2 \right] \\ & \quad + 2(1 + \tau) \eta^2 \mathbb{E} \left[\left\| \frac{1}{|\mathcal{H}|} \sum_{i \in \mathcal{H}} \nabla F_i^\mu(\mathbf{w}_{t,\ell-1}^i) - \frac{1}{|\mathcal{H}|} \sum_{i \in \mathcal{H}} \nabla F_i(\mathbf{w}_{t,\ell-1}^i) + \frac{1}{|\mathcal{H}|} \sum_{i \in \mathcal{H}} \nabla F_i(\mathbf{w}_{t,\ell-1}^i) - \nabla F_{\mathcal{H}}(\hat{\mathbf{w}}_{t,\ell-1}) \right. \right. \\ & \quad \left. \left. + \nabla F_{\mathcal{H}}(\hat{\mathbf{w}}_{t,\ell-1}) - \nabla F_{\mathcal{H}}(\mathbf{w}_t) + \nabla F_{\mathcal{H}}(\mathbf{w}_t) \right\|^2 \right] \\ & \quad + 2\eta^2 \frac{1}{|\mathcal{H}|^2} \sum_{i \in \mathcal{H}} \mathbb{E} \left[\left\| \mathbf{Z}_{t,\ell-1} \mathbf{g}_i(\mathbf{w}_{t,\ell-1}^i, \mathbf{Z}_{t,\ell-1}) - \nabla F_i^\mu(\mathbf{w}_{t,\ell-1}^i) \right\|^2 \right] \end{aligned}$$

$$\begin{aligned}
 &\leq \left(1 + \frac{1}{\tau}\right) \mathbb{E} \left[\|\hat{\mathbf{w}}_{t,\ell-1} - \mathbf{w}_t\|^2 \right] + 8(1 + \tau)\eta^2 \mathbb{E} \left[\left\| \frac{1}{|\mathcal{H}|} \sum_{i \in \mathcal{H}} \nabla F_i^\mu(\mathbf{w}_{t,\ell-1}^i) - \frac{1}{|\mathcal{H}|} \sum_{i \in \mathcal{H}} \nabla F_i(\mathbf{w}_{t,\ell-1}^i) \right\|^2 \right] \\
 &\quad + 8(1 + \tau)\eta^2 \mathbb{E} \left[\|\nabla F_{\mathcal{H}}(\mathbf{w}_t)\|^2 \right] \\
 &\quad + 8(1 + \tau)\eta^2 \mathbb{E} \left[\left\| \frac{1}{|\mathcal{H}|} \sum_{i \in \mathcal{H}} \nabla F_i(\mathbf{w}_{t,\ell-1}^i) - \nabla F_{\mathcal{H}}(\hat{\mathbf{w}}_{t,\ell-1}) \right\|^2 \right] + 8(1 + \tau)\eta^2 \mathbb{E} \left[\|\nabla F_{\mathcal{H}}(\hat{\mathbf{w}}_{t,\ell-1}) - \nabla F_{\mathcal{H}}(\mathbf{w}_t)\|^2 \right] \\
 &\quad + 2\eta^2 \frac{1}{|\mathcal{H}|^2} \sum_{i \in \mathcal{H}} \mathbb{E} \left[\|\mathbf{Z}_{t,\ell-1} \mathbf{g}_i(\mathbf{w}_{t,\ell-1}^i, \mathbf{Z}_{t,\ell-1}) - \nabla F_i^\mu(\mathbf{w}_{t,\ell-1}^i)\|^2 \right]
 \end{aligned} \tag{18}$$

$$\begin{aligned}
 &\stackrel{(c)}{\leq} \left(1 + \frac{1}{\tau}\right) \mathbb{E} \left[\|\hat{\mathbf{w}}_{t,\ell-1} - \mathbf{w}_t\|^2 \right] + 8(1 + \tau)\eta^2 L\mu + 8(1 + \tau)\eta^2 \mathbb{E} \left[\|\nabla F_{\mathcal{H}}(\mathbf{w}_t)\|^2 \right] \\
 &\quad + 8(1 + \tau)\eta^2 \frac{D^2}{|\mathcal{H}|} \sum_{i \in \mathcal{H}} \mathbb{E} \left[\|\mathbf{w}_{t,\ell-1}^i - \hat{\mathbf{w}}_{t,\ell-1}\|^2 \right] + 8(1 + \tau)\eta^2 L^2 \mathbb{E} \left[\|\hat{\mathbf{w}}_{t,\ell-1} - \mathbf{w}_t\|^2 \right] \\
 &\quad + 2\eta^2 \frac{1}{|\mathcal{H}|^2} \sum_{i \in \mathcal{H}} \frac{4d}{\nu} \left(4L^2 \mathbb{E} \left[\|\mathbf{w}_{t,\ell-1}^i - \hat{\mathbf{w}}_{t,\ell-1}\|^2 \right] + 4\zeta^2 + 4L^2 \mathbb{E} \left[\|\hat{\mathbf{w}}_{t,\ell-1} - \mathbf{w}_t\|^2 \right] + 4\mathbb{E} \left[\|\nabla F_{\mathcal{H}}(\mathbf{w}_t)\|^2 \right] \right) \\
 &\quad + 2\eta^2 \frac{1}{|\mathcal{H}|} \frac{4d}{\nu} \sigma^2 + 2\eta^2 \frac{1}{|\mathcal{H}|} \frac{L^2 \mu^2 d^2}{2\nu} \\
 &\stackrel{(d)}{\leq} \left(\left(1 + \frac{1}{\tau}\right) + 8(1 + \tau)\eta^2 L^2 + 2\eta^2 \frac{1}{|\mathcal{H}|} \frac{4d}{\nu} 4L^2 \right) \mathbb{E} \left[\|\hat{\mathbf{w}}_{t,\ell-1} - \mathbf{w}_t\|^2 \right] + 8(1 + \tau)\eta^2 L\mu \\
 &\quad + \left(8(1 + \tau)\eta^2 + 2\eta^2 \frac{1}{|\mathcal{H}|} \frac{4d}{\nu} 4 \right) \mathbb{E} \left[\|\nabla F_{\mathcal{H}}(\mathbf{w}_t)\|^2 \right] \\
 &\quad + \left(8(1 + \tau)\eta^2 \frac{D^2}{|\mathcal{H}|} + 2\eta^2 \frac{1}{|\mathcal{H}|^2} \frac{4d}{\nu} 4L^2 \right) \sum_{i \in \mathcal{H}} \mathbb{E} \left[\|\mathbf{w}_{t,\ell-1}^i - \hat{\mathbf{w}}_{t,\ell-1}\|^2 \right] + 2\eta^2 \frac{1}{|\mathcal{H}|} \frac{4d}{\nu} 4\zeta^2 \\
 &\quad + 2\eta^2 \frac{1}{|\mathcal{H}|} \frac{4d}{\nu} \sigma^2 + 2\eta^2 \frac{1}{|\mathcal{H}|} \frac{L^2 \mu^2 d^2}{2\nu}
 \end{aligned}$$

where (a) is by independence for $i \neq j$, and (b) is because $\|\mathbf{x} + \mathbf{y}\|^2 = (1 + 1/\tau) \|\mathbf{x}\|^2 + (1 + \tau) \|\mathbf{y}\|^2$, $\tau > 0$. (c) follows from Assumption 5.1, Assumption 5.4 and an intermediate step in the proof of Lemma B.2.

To ensure the bound holds uniformly for all $\ell \in [K]$, we now choose $\tau = 3K - 1$ and the learning rate small enough so that $\left(\left(1 + \frac{1}{\tau}\right) + 8(1 + \tau)\eta^2 L^2 + 2\eta^2 \frac{1}{|\mathcal{H}|} \frac{4d}{\nu} 4L^2 \right) \leq 1 + \frac{1}{K-1}$, i.e., that $8(1 + \tau)\eta^2 L^2 \leq \frac{1}{3K}$ and $2\eta^2 \frac{1}{|\mathcal{H}|} \frac{4d}{\nu} 4L^2 \leq \frac{1}{3K}$. With this choice of the learning rate, we have

$$\begin{aligned}
 &\mathbb{E} \left[\|\hat{\mathbf{w}}_{t,\ell} - \mathbf{w}_t\|^2 \right] \\
 &\leq \left(1 + \frac{1}{K-1}\right) \mathbb{E} \left[\|\hat{\mathbf{w}}_{t,\ell-1} - \mathbf{w}_t\|^2 \right] + 8(1 + \tau)\eta^2 L\mu + \left(8(1 + \tau)\eta^2 + 2\eta^2 \frac{1}{|\mathcal{H}|} \frac{4d}{\nu} 4 \right) \mathbb{E} \left[\|\nabla F_{\mathcal{H}}(\mathbf{w}_t)\|^2 \right] \\
 &\quad + \left(8(1 + \tau)\eta^2 \frac{D^2}{|\mathcal{H}|} + 2\eta^2 \frac{1}{|\mathcal{H}|^2} \frac{4d}{\nu} 4L^2 \right) \sum_{i \in \mathcal{H}} \mathbb{E} \left[\|\mathbf{w}_{t,\ell-1}^i - \hat{\mathbf{w}}_{t,\ell-1}\|^2 \right] + 2\eta^2 \frac{1}{|\mathcal{H}|} \frac{4d}{\nu} 4\zeta^2 + 2\eta^2 \frac{1}{|\mathcal{H}|} \frac{4d}{\nu} \sigma^2 + 2\eta^2 \frac{1}{|\mathcal{H}|} \frac{L^2 \mu^2 d^2}{2\nu} \\
 &\stackrel{(d)}{\leq} c'_6(\ell) \mathbb{E} \left[\|\nabla F_{\mathcal{H}}(\mathbf{w}_t)\|^2 \right] + c'_7(\ell) + c'_8 \sum_{\ell'=1}^{\ell-1} \sum_{i \in \mathcal{H}} \mathbb{E} \left[\|\mathbf{w}_{t,\ell'}^i - \hat{\mathbf{w}}_{t,\ell'}\|^2 \right],
 \end{aligned}$$

where (e) is by the recursive application of (d) and the fact that $(1 + \frac{1}{K})^\ell \leq (1 + \frac{1}{\ell})^\ell \leq e$ for all $\ell \in [K]$. This concludes the proof. The constants are given as

$$c'_6(\ell) \triangleq 5(\ell - 1) \left(8(1 + \tau)\eta^2 + 2\eta^2 \frac{1}{|\mathcal{H}|} \frac{4d}{\nu} 4 \right) \leq c_6 \triangleq 5 \cdot 32\eta^2 K \left(K + \frac{d}{|\mathcal{H}| \nu} \right)$$

$$\begin{aligned}
 c'_7(\ell) &\triangleq 5(\ell - 1) \left(2\eta^2 \frac{1}{|\mathcal{H}|} \frac{4d}{\nu} 4\zeta^2 + 2\eta^2 \frac{1}{|\mathcal{H}|} \frac{4d}{\nu} \sigma^2 + 2\eta^2 \frac{1}{|\mathcal{H}|} \frac{L^2 \mu^2 d^2}{2\nu} + 8(1 + \tau)\eta^2 L\mu \right) \\
 &\leq c_7 \triangleq 5K\eta^2 \frac{d}{|\mathcal{H}|\nu} (32\zeta^2 + 8\sigma^2 + L^2 \mu^2 d) + 5\eta^2 24K^2 L\mu \\
 c'_8 &\triangleq 5 \left(8(1 + \tau)\eta^2 D^2 + 2\eta^2 \frac{1}{|\mathcal{H}|} \frac{4d}{\nu} 4L^2 \right) \leq c_8 \triangleq 5 \cdot 32\eta^2 \left(KD^2 + \frac{1}{|\mathcal{H}|} \frac{d}{\nu} L^2 \right)
 \end{aligned}$$

□

Proof of Lemma B.2. For the proof of the zero-order approximated gradient variance, we rely on the following intermediate lemma.

Lemma B.6. *The second moment of the gradient estimate can be bounded from above as*

$$\mathbb{E} \left[\|\mathbf{z}g(\mathbf{w}, \mathbf{z}, \mu, \mathcal{D})\|^2 \right] \leq 2d \|\nabla F_{\mathcal{H}}(\mathbf{w}, \mathcal{D})\|^2 + \frac{L^2 \mu^2 d^2}{2}.$$

Proof.

$$\begin{aligned}
 \mathbb{E} \left[\|\mathbf{z}g(\mathbf{w}, \mathbf{z}, \mu, \mathcal{D})\|^2 \right] &= \mathbb{E} \left[\left\| d \frac{F(\mathbf{w} + \mu\mathbf{z}) - F(\mathbf{w} - \mu\mathbf{z})}{2\mu} \right\|^2 \right] \\
 &= \mathbb{E} \left[\left\| d \frac{F(\mathbf{w} + \mu\mathbf{z}) - F(\mathbf{w}) + F(\mathbf{w}) - F(\mathbf{w} - \mu\mathbf{z})}{2\mu} \right\|^2 \right] \\
 &\leq \frac{1}{2} \mathbb{E} \left[\left\| d \frac{F(\mathbf{w} + \mu\mathbf{z}) - F(\mathbf{w})}{\mu} \right\|^2 \right] + \frac{1}{2} \mathbb{E} \left[\left\| d \frac{F(\mathbf{w} - \mu\mathbf{z}) - F(\mathbf{w})}{\mu} \right\|^2 \right] \\
 &= \mathbb{E} \left[\left\| d \frac{F(\mathbf{w} + \mu\mathbf{z}) - F(\mathbf{w})}{\mu} \right\|^2 \right] \\
 &\leq 2d \|\nabla F_{\mathcal{H}}(\mathbf{w})\|^2 + \frac{L^2 \mu^2 d^2}{2},
 \end{aligned}$$

where the penultimate step holds by symmetry and the last step is from (Gao et al., 2018, Lemma 4.1). □

We bound the zero-order approximated gradient variance as follows: Since $\mathbb{E} \left[\|Z - \mathbb{E}[Z]\|^2 \right] \leq \mathbb{E} \left[\|Z\|^2 \right]$, and $\mathbb{E} \left[\mathbf{z}_{t,\ell}^r g_i(\mathbf{w}_{t,\ell}^i, \mathbf{z}_{t,\ell}^r) \right] = \nabla F_i^\mu(\mathbf{w}_{t,\ell}^i)$, we have

$$\begin{aligned}
 \mathbb{E} \left[\left\| \mathbf{Z}_{t,\ell} \mathbf{g}_i(\mathbf{w}_{t,\ell}^i, \mathbf{Z}_{t,\ell}) - \nabla F_i^\mu(\mathbf{w}_{t,\ell}^i) \right\|^2 \right] &= \mathbb{E} \left[\left\| \frac{1}{\nu} \sum_{r=1}^{\nu} \mathbf{z}_{t,\ell}^r g_i(\mathbf{w}_{t,\ell}^i, \mathbf{z}_{t,\ell}^r) - \nabla F_i^\mu(\mathbf{w}_{t,\ell}^i) \right\|^2 \right] \\
 &\stackrel{(a)}{=} \frac{1}{\nu^2} \sum_{r=1}^{\nu} \mathbb{E} \left[\left\| \mathbf{z}_{t,\ell}^r g_i(\mathbf{w}_{t,\ell}^i, \mathbf{z}_{t,\ell}^r) - \nabla F_i^\mu(\mathbf{w}_{t,\ell}^i) \right\|^2 \right] \\
 &\leq \frac{1}{\nu^2} \sum_{r=1}^{\nu} \mathbb{E} \left[\left\| \mathbf{z}_{t,\ell}^r g_i(\mathbf{w}_{t,\ell}^i, \mathbf{z}_{t,\ell}^r) \right\|^2 \right] \\
 &\stackrel{(b)}{\leq} \frac{2d}{\nu^2} \sum_{r=1}^{\nu} \mathbb{E} \left[\mathbb{E} \left[\left\| \mathbf{g}_i(\mathbf{w}_{t,\ell}^i) \right\|^2 \right] \right] + \frac{L^2 \mu^2 d^2}{2\nu} \\
 &\leq \frac{2d}{\nu^2} \sum_{r=1}^{\nu} \mathbb{E} \left[\mathbb{E} \left[\left\| \mathbf{g}_i(\mathbf{w}_{t,\ell}^i) - \nabla F_i(\mathbf{w}_{t,\ell}^i) + \nabla F_i(\mathbf{w}_{t,\ell}^i) \right\|^2 \right] \right] + \frac{L^2 \mu^2 d^2}{2\nu} \\
 &\leq \frac{2d}{\nu^2} \sum_{r=1}^{\nu} \mathbb{E} \left[2\mathbb{E} \left[\left\| \mathbf{g}_i(\mathbf{w}_{t,\ell}^i) - \nabla F_i(\mathbf{w}_{t,\ell}^i) \right\|^2 \right] + 2\left\| \nabla F_i(\mathbf{w}_{t,\ell}^i) \right\|^2 \right] + \frac{L^2 \mu^2 d^2}{2\nu}
 \end{aligned}$$

$$\stackrel{(c)}{\leq} \frac{4d}{\nu^2} \sum_{r=1}^{\nu} \mathbb{E} \left[\|\nabla F_i(\mathbf{w}_{t,\ell}^i)\|^2 \right] + \frac{4d}{\nu} \sigma^2 + \frac{L^2 \mu^2 d^2}{2\nu} \quad (19)$$

where (a) is due to the independence of $\mathbf{z}_{t,\ell}^r g_i(\mathbf{w}_{t,\ell}^i, \mathbf{z}_{t,\ell}^r)$ and $\mathbf{z}_{t,\ell}^{r'} g_i(\mathbf{w}_{t,\ell}^i, \mathbf{z}_{t,\ell}^{r'})$ for $r \neq r'$. (b) is by Lemma B.6. (c) follows from Assumption 5.2.

$$\begin{aligned} \mathbb{E} \left[\|\nabla F_i(\mathbf{w}_{t,\ell}^i)\|^2 \right] &= \mathbb{E} \left[\|\nabla F_i(\mathbf{w}_{t,\ell}^i) - \nabla F_i(\hat{\mathbf{w}}_{t,\ell}) + \nabla F_i(\hat{\mathbf{w}}_{t,\ell}) - \nabla F_{\mathcal{H}}(\hat{\mathbf{w}}_{t,\ell}) + \nabla F_{\mathcal{H}}(\hat{\mathbf{w}}_{t,\ell}) - \nabla F_{\mathcal{H}}(\mathbf{w}_t) + \nabla F_{\mathcal{H}}(\mathbf{w}_t)\|^2 \right] \\ &\leq 4\mathbb{E} \left[\|\nabla F_i(\mathbf{w}_{t,\ell}^i) - \nabla F_i(\hat{\mathbf{w}}_{t,\ell})\|^2 \right] + 4\mathbb{E} \left[\|\nabla F_i(\hat{\mathbf{w}}_{t,\ell}) - \nabla F_{\mathcal{H}}(\hat{\mathbf{w}}_{t,\ell})\|^2 \right] \\ &\quad + 4\mathbb{E} \left[\|\nabla F_{\mathcal{H}}(\hat{\mathbf{w}}_{t,\ell}) - \nabla F_{\mathcal{H}}(\mathbf{w}_t)\|^2 \right] + 4\mathbb{E} \left[\|\nabla F_{\mathcal{H}}(\mathbf{w}_t)\|^2 \right] \\ &\leq 4L^2 \mathbb{E} \left[\|\mathbf{w}_{t,\ell}^i - \hat{\mathbf{w}}_{t,\ell}\|^2 \right] + 4\zeta^2 + 4L^2 \mathbb{E} \left[\|\hat{\mathbf{w}}_{t,\ell} - \mathbf{w}_t\|^2 \right] + 4\mathbb{E} \left[\|\nabla F_{\mathcal{H}}(\mathbf{w}_t)\|^2 \right]. \end{aligned}$$

Substituting the result in (19), we obtain

$$\begin{aligned} \mathbb{E} \left[\|\mathbf{Z}_{t,\ell} \mathbf{g}_i(\mathbf{w}_{t,\ell}^i, \mathbf{Z}_{t,\ell}) - \nabla F_i^\mu(\mathbf{w}_{t,\ell}^i)\|^2 \right] &= \mathbb{E} \left[\left\| \frac{1}{\nu} \sum_{r=1}^{\nu} \mathbf{z}_{t,\ell}^r g_i(\mathbf{w}_{t,\ell}^i, \mathbf{z}_{t,\ell}^r) - \nabla F_i^\mu(\mathbf{w}_{t,\ell}^i) \right\|^2 \right] \\ &\leq \frac{4d}{\nu^2} \sum_{r=1}^{\nu} \left(4L^2 \mathbb{E} \left[\|\mathbf{w}_{t,\ell}^i - \hat{\mathbf{w}}_{t,\ell}\|^2 \right] + 4\zeta^2 + 4L^2 \mathbb{E} \left[\|\hat{\mathbf{w}}_{t,\ell} - \mathbf{w}_t\|^2 \right] + 4\mathbb{E} \left[\|\nabla F_{\mathcal{H}}(\mathbf{w}_t)\|^2 \right] \right) + \frac{4d}{\nu} \sigma^2 + \frac{L^2 \mu^2 d^2}{2\nu} \\ &= \frac{4d}{\nu} \left(4L^2 \mathbb{E} \left[\|\mathbf{w}_{t,\ell}^i - \hat{\mathbf{w}}_{t,\ell}\|^2 \right] + 4\zeta^2 + 4L^2 \mathbb{E} \left[\|\hat{\mathbf{w}}_{t,\ell} - \mathbf{w}_t\|^2 \right] + 4\mathbb{E} \left[\|\nabla F_{\mathcal{H}}(\mathbf{w}_t)\|^2 \right] \right) + \frac{4d}{\nu} \sigma^2 + \frac{L^2 \mu^2 d^2}{2\nu} \\ &\leq \frac{4d}{\nu} \left(4L^2 \mathbb{E} \left[\|\mathbf{w}_{t,\ell}^i - \hat{\mathbf{w}}_{t,\ell}\|^2 \right] + 4\zeta^2 + 4\mathbb{E} \left[\|\nabla F_{\mathcal{H}}(\mathbf{w}_t)\|^2 \right] \right) + \frac{4d}{\nu} \sigma^2 + \frac{L^2 \mu^2 d^2}{2\nu} \\ &\quad + \frac{4d}{\nu} 4L^2 \left(c_6 \mathbb{E} \left[\|\nabla F_{\mathcal{H}}(\mathbf{w}_t)\|^2 \right] + c_7 + c_8 \sum_{\ell'=1}^{\ell-1} \frac{1}{|\mathcal{H}|} \sum_{i \in \mathcal{H}} \mathbb{E} \left[\|\mathbf{w}_{t,\ell'}^i - \hat{\mathbf{w}}_{t,\ell'}\|^2 \right] \right) \\ &\leq c'_9 \mathbb{E} \left[\|\mathbf{w}_{t,\ell}^i - \hat{\mathbf{w}}_{t,\ell}\|^2 \right] + c'_{12} + c'_{11} \mathbb{E} \left[\|\nabla F_{\mathcal{H}}(\mathbf{w}_t)\|^2 \right] + c'_{10} \sum_{\ell'=1}^{\ell-1} \frac{1}{|\mathcal{H}|} \sum_{i \in \mathcal{H}} \mathbb{E} \left[\|\mathbf{w}_{t,\ell'}^i - \hat{\mathbf{w}}_{t,\ell'}\|^2 \right], \end{aligned}$$

where the latter is by Lemma B.1, and we have

$$\begin{aligned} c'_9 &\triangleq c_9 \triangleq \frac{4d}{\nu} 4L^2 \\ c'_{10} &\triangleq \frac{4d}{\nu} 4L^2 c_8 \leq c_{10} \triangleq \frac{4d}{\nu} 4L^2 5 \cdot 32\eta^2 \left(KD^2 + \frac{1}{|\mathcal{H}|} \frac{d}{\nu} L^2 \right) \\ c'_{11} &\triangleq \frac{4d}{\nu} 4 + \frac{4d}{\nu} 4L^2 c_6 \leq c_{11} \triangleq \frac{4d}{\nu} 4 + \frac{4d}{\nu} 4L^2 5 \cdot 32\eta^2 K \left(K + \frac{d}{|\mathcal{H}|\nu} \right) \\ c'_{12} &\triangleq \frac{4d}{\nu} 4\zeta^2 + \frac{4d}{\nu} \sigma^2 + \frac{L^2 \mu^2 d^2}{2\nu} + \frac{4d}{\nu} 4L^2 c_7 \\ &\leq \frac{d}{2\nu} (32\zeta^2 + 8\sigma^2 + L^2 \mu^2 d) + \frac{4d}{\nu} 4L^2 \left(5K\eta^2 \frac{d}{|\mathcal{H}|\nu} (32\zeta^2 + 8\sigma^2 + L^2 \mu^2 d) + 5\eta^2 24K^2 L\mu \right) \\ &\leq c_{12} \triangleq \left(\frac{d}{2\nu} + \frac{80d^2}{\nu^2 |\mathcal{H}|} L^2 K \eta^2 \right) (32\zeta^2 + 8\sigma^2 + L^2 \mu^2 d) + \frac{4d}{\nu} 4L^2 5\eta^2 24K^2 L\mu. \end{aligned}$$

This concludes the proof. \square

Proof of Lemma B.3. We start with stating an intermediate lemma proven by Wang et al. (2025).

Lemma B.7 (Extracted from Lemma B.1, (Wang et al., 2025)). *The following holds for the divergence of the local gradients:*

$$\left\| \frac{1}{|\mathcal{H}|} \sum_{j \in \mathcal{H}} \nabla F_j(\mathbf{w}_{t,\ell}^j) - \nabla F_i(\mathbf{w}_{t,\ell}^i) \right\|^2 \leq 3 \frac{D^2}{|\mathcal{H}|} \sum_{j \in \mathcal{H}} \|\hat{\mathbf{w}}_{t,\ell} - \mathbf{w}_{t,\ell}^j\|^2 + 3L + 3\zeta^2 \|\hat{\mathbf{w}}_{t,\ell} - \mathbf{w}_{t,\ell}^i\|^2.$$

Following similar lines as in the proof of (Wang et al., 2025, Lemma B.2), for some local iteration $m \in [\ell]$, we have

$$\begin{aligned}
 & \mathbb{E} \left[\left\| \mathbf{Z}_{t,m} \mathbf{g}_i(\mathbf{w}_{t,\ell}^i, \mathbf{Z}_{t,\ell}) - \frac{1}{|\mathcal{H}|} \sum_{j \in \mathcal{H}} \mathbf{Z}_{t,m} \mathbf{g}_j(\mathbf{w}_{t,m}^j, \mathbf{Z}_{t,m}) \right\|^2 \right] \\
 &= \mathbb{E} \left[\left\| \mathbf{Z}_{t,m} \mathbf{g}_i(\mathbf{w}_{t,m}^i, \mathbf{Z}_{t,m}) - \nabla F_i(\mathbf{w}_{t,m}^i) + \nabla F_i(\mathbf{w}_{t,m}^i) \right. \right. \\
 &\quad \left. \left. - \frac{1}{|\mathcal{H}|} \sum_{j \in \mathcal{H}} \nabla F_j(\mathbf{w}_{t,m}^j) + \frac{1}{|\mathcal{H}|} \sum_{j \in \mathcal{H}} \nabla F_j(\mathbf{w}_{t,m}^j) - \frac{1}{|\mathcal{H}|} \sum_{j \in \mathcal{H}} \mathbf{Z}_{t,m} \mathbf{g}_j(\mathbf{w}_{t,m}^j, \mathbf{Z}_{t,m}) \right\|^2 \right] \\
 &\leq 2 \mathbb{E} \left[\left\| \nabla F_i(\mathbf{w}_{t,m}^i) - \frac{1}{|\mathcal{H}|} \sum_{j \in \mathcal{H}} \nabla F_j(\mathbf{w}_{t,m}^j) \right\|^2 \right] \\
 &\quad + 2 \mathbb{E} \left[\left\| \mathbf{Z}_{t,m} \mathbf{g}_i(\mathbf{w}_{t,m}^i, \mathbf{Z}_{t,m}) - \nabla F_i(\mathbf{w}_{t,m}^i) + \frac{1}{|\mathcal{H}|} \sum_{j \in \mathcal{H}} \nabla F_j(\mathbf{w}_{t,m}^j) - \frac{1}{|\mathcal{H}|} \sum_{j \in \mathcal{H}} \mathbf{Z}_{t,m} \mathbf{g}_j(\mathbf{w}_{t,m}^j, \mathbf{Z}_{t,m}) \right\|^2 \right] \\
 &\stackrel{(a)}{\leq} 2 \mathbb{E} \left[\left\| \nabla F_i(\mathbf{w}_{t,m}^i) - \frac{1}{|\mathcal{H}|} \sum_{j \in \mathcal{H}} \nabla F_j(\mathbf{w}_{t,m}^j) \right\|^2 \right] \\
 &\quad + 2 \mathbb{E} \left[\left\| \mathbf{Z}_{t,m} \mathbf{g}_i(\mathbf{w}_{t,m}^i, \mathbf{Z}_{t,m}) - \nabla F_i(\mathbf{w}_{t,m}^i) \right\|^2 \right] \\
 &\leq 2 \mathbb{E} \left[3 \frac{D^2}{|\mathcal{H}|} \sum_{j \in \mathcal{H}} \left\| \hat{\mathbf{w}}_{t,m} - \mathbf{w}_{t,m}^j \right\|^2 + 3L + 3\zeta^2 \left\| \hat{\mathbf{w}}_{t,m} - \mathbf{w}_{t,m}^i \right\|^2 \right] \\
 &\quad + 2 \mathbb{E} \left[\left\| \mathbf{Z}_{t,m} \mathbf{g}_i(\mathbf{w}_{t,m}^i, \mathbf{Z}_{t,m}) - \nabla F_i(\mathbf{w}_{t,m}^i) \right\|^2 \right], \tag{20}
 \end{aligned}$$

where (a) is since $\frac{1}{|\mathcal{H}|} \sum_{i \in \mathcal{H}} \left\| \mathbf{x}_i - \frac{1}{|\mathcal{H}|} \sum_{j \in \mathcal{H}} \mathbf{x}_j \right\|^2 = \frac{1}{|\mathcal{H}|} \sum_{j \in \mathcal{H}} \|\mathbf{x}_j\|^2 - \left\| \frac{1}{|\mathcal{H}|} \sum_{j \in \mathcal{H}} \mathbf{x}_j \right\|^2 \leq \frac{1}{|\mathcal{H}|} \sum_{i \in \mathcal{H}} \|\mathbf{x}_i\|^2$ for $\mathbf{x}_i \in \mathbb{R}^d, \forall i$, where we set $\mathbf{x}_i = \mathbf{Z}_{t,m} \mathbf{g}_i(\mathbf{w}_{t,m}^i, \mathbf{Z}_{t,m}) - \nabla F_i(\mathbf{w}_{t,m}^i)$.

Summing over all benign clients, we obtain

$$\begin{aligned}
 & \sum_{m=1}^{\ell} \frac{1}{|\mathcal{H}|} \sum_{i \in \mathcal{H}} \mathbb{E} \left[\left\| \mathbf{Z}_{t,m} \mathbf{g}_i(\mathbf{w}_{t,\ell}^i, \mathbf{Z}_{t,\ell}) - \frac{1}{|\mathcal{H}|} \sum_{j \in \mathcal{H}} \mathbf{Z}_{t,m} \mathbf{g}_j(\mathbf{w}_{t,m}^j, \mathbf{Z}_{t,m}) \right\|^2 \right] \\
 &\stackrel{(a)}{\leq} 2 \sum_{m=1}^{\ell} \mathbb{E} \left[\left(3 \frac{D^2}{|\mathcal{H}|} + 3 \frac{\zeta^2}{|\mathcal{H}|} \right) \sum_{i \in \mathcal{H}} \left\| \hat{\mathbf{w}}_{t,m} - \mathbf{w}_{t,m}^i \right\|^2 + 3L \right] \\
 &\quad + 2 \sum_{m=1}^{\ell} \frac{1}{|\mathcal{H}|} \sum_{i \in \mathcal{H}} \left(c_9 \mathbb{E} \left[\left\| \mathbf{w}_{t,m}^i - \hat{\mathbf{w}}_{t,m} \right\|^2 \right] + c_{12} + c_{11} \mathbb{E} \left[\left\| \nabla F_{\mathcal{H}}(\mathbf{w}_t) \right\|^2 \right] + c_{10} \sum_{\ell'=1}^{m-1} \sum_{i \in \mathcal{H}} \mathbb{E} \left[\left\| \mathbf{w}_{t,\ell'}^i - \hat{\mathbf{w}}_{t,\ell'} \right\|^2 \right] \right) \\
 &\leq 2 \sum_{m=1}^{\ell} \frac{1}{|\mathcal{H}|} \sum_{i \in \mathcal{H}} \left((3D^2 + 3\zeta^2 + c_9) \mathbb{E} \left[\left\| \mathbf{w}_{t,m}^i - \hat{\mathbf{w}}_{t,m} \right\|^2 \right] + c_{12} + 3L \right. \\
 &\quad \left. + c_{11} \mathbb{E} \left[\left\| \nabla F_{\mathcal{H}}(\mathbf{w}_t) \right\|^2 \right] + c_{10} \sum_{\ell'=1}^{m-1} \sum_{i \in \mathcal{H}} \mathbb{E} \left[\left\| \mathbf{w}_{t,\ell'}^i - \hat{\mathbf{w}}_{t,\ell'} \right\|^2 \right] \right) \\
 &\leq 2 \sum_{m=1}^{\ell} \frac{1}{|\mathcal{H}|} \sum_{i \in \mathcal{H}} \left((3D^2 + 3\zeta^2 + c_9) \mathbb{E} \left[\left\| \mathbf{w}_{t,m}^i - \hat{\mathbf{w}}_{t,m} \right\|^2 \right] + c_{12} + 3L \right)
 \end{aligned}$$

$$\begin{aligned}
 & + c_{11} \mathbb{E} \left[\|\nabla F_{\mathcal{H}}(\mathbf{w}_t)\|^2 \right] + c_{10} \ell(\ell-1) \frac{1}{|\mathcal{H}|} \sum_{i \in \mathcal{H}} \mathbb{E} \left[\|\mathbf{w}_{t,m}^i - \hat{\mathbf{w}}_{t,m}\|^2 \right] \\
 & \leq \sum_{m=1}^{\ell} \frac{1}{|\mathcal{H}|} \sum_{i \in \mathcal{H}} c'_{13}(\ell) \mathbb{E} \left[\|\hat{\mathbf{w}}_{t,m} - \mathbf{w}_{t,m}^i\|^2 \right] + \sum_{m=1}^{\ell} (c_{14} + c_{15}) + \sum_{m=1}^{\ell} c_{16} \mathbb{E} \left[\|\nabla F_{\mathcal{H}}(\mathbf{w}_t)\|^2 \right],
 \end{aligned}$$

where (a) is due to Lemma B.2 and (b) is since $\sum_{m=1}^{\ell} \sum_{\ell'=1}^m x_m \leq \frac{\ell(\ell-1)}{2} \sum_m x_m$. Thereby,

$$\begin{aligned}
 c'_{13}(\ell) & \triangleq 2(3D^2 + 3\zeta^2 + c_9 + c_{10}\ell(\ell-1)) \leq c_{13} \triangleq 6D^2 + 6\zeta^2 + 2c_9 + 2c_{10}K^2 \\
 c_{14} & \triangleq 2c_{12} \\
 c_{15} & \triangleq 6L \\
 c_{16} & \triangleq 2c_{11}.
 \end{aligned}$$

This concludes the proof. \square

Proof of Lemma B.4. From Lemma B.3, we have

$$\begin{aligned}
 & \sum_{\ell=1}^K \frac{1}{|\mathcal{H}|} \sum_{i \in \mathcal{H}} \mathbb{E} \left[\|\mathbf{w}_{t,\ell}^i - \hat{\mathbf{w}}_{t,\ell}\|^2 \right] = \sum_{\ell=1}^K \frac{1}{|\mathcal{H}|} \sum_{i \in \mathcal{H}} \mathbb{E} \left[\left\| \eta \sum_{m=1}^{\ell} \left(\mathbf{z}_{t,m} \mathbf{g}_i(\mathbf{w}_{t,\ell}^i, \mathbf{z}_{t,\ell}) - \frac{1}{|\mathcal{H}|} \sum_{j \in \mathcal{H}} \mathbf{z}_{t,m} \mathbf{g}_j(\mathbf{w}_{t,m}^j, \mathbf{z}_{t,m}) \right) \right\|^2 \right] \\
 & \leq \eta^2 \sum_{\ell=1}^K \ell \sum_{m=1}^{\ell} \frac{1}{|\mathcal{H}|} \sum_{i \in \mathcal{H}} \mathbb{E} \left[\left\| \mathbf{z}_{t,m} \mathbf{g}_i(\mathbf{w}_{t,\ell}^i, \mathbf{z}_{t,\ell}) - \frac{1}{|\mathcal{H}|} \sum_{j \in \mathcal{H}} \mathbf{z}_{t,m} \mathbf{g}_j(\mathbf{w}_{t,m}^j, \mathbf{z}_{t,m}) \right\|^2 \right] \\
 & = \eta^2 \sum_{\ell=1}^K \ell \sum_{m=1}^{\ell} \sum_{i \in \mathcal{H}} \frac{1}{|\mathcal{H}|} c_{13} \mathbb{E} \left[\|\hat{\mathbf{w}}_{t,m} - \mathbf{w}_{t,m}^i\|^2 \right] + \eta^2 \sum_{\ell=1}^K \ell \sum_{m=1}^{\ell} c_{14} + \eta^2 \sum_{\ell=1}^K \ell \sum_{m=1}^{\ell} c_{15} + \eta^2 \sum_{\ell=1}^K \ell \sum_{m=1}^{\ell} c_{16} \mathbb{E} \left[\|\nabla F_{\mathcal{H}}(\mathbf{w}_t)\|^2 \right] \\
 & \leq \eta^2 \sum_{\ell=1}^K \frac{1}{|\mathcal{H}|} \sum_{i \in \mathcal{H}} K^2 c_{13} \mathbb{E} \left[\|\hat{\mathbf{w}}_{t,\ell} - \mathbf{w}_{t,\ell}^i\|^2 \right] + \eta^2 \sum_{\ell=1}^K \ell \sum_{m=1}^{\ell} c_{14} + \eta^2 \sum_{\ell=1}^K \ell \sum_{m=1}^{\ell} c_{15} + \eta^2 \sum_{\ell=1}^K \ell \sum_{m=1}^{\ell} c_{16} \mathbb{E} \left[\|\nabla F_{\mathcal{H}}(\mathbf{w}_t)\|^2 \right].
 \end{aligned}$$

We rewrite the equation as

$$(1 - \eta^2 K^2 c_{13}) \sum_{\ell=1}^K \frac{1}{|\mathcal{H}|} \sum_{i \in \mathcal{H}} \mathbb{E} \left[\|\mathbf{w}_{t,\ell}^i - \hat{\mathbf{w}}_{t,\ell}\|^2 \right] \leq \eta^2 \sum_{\ell=1}^K \ell \sum_{m=1}^{\ell} c_{14} + \eta^2 \sum_{\ell=1}^K \ell \sum_{m=1}^{\ell} c_{15} + \eta^2 \sum_{\ell=1}^K \ell \sum_{m=1}^{\ell} c_{16} \mathbb{E} \left[\|\nabla F_{\mathcal{H}}(\mathbf{w}_t)\|^2 \right]$$

and choose the learning rate small enough so that $(1 - \eta^2 K^2 c_{13}) \geq \frac{1}{2}$. Letting $c_{13} = 6D^2 + 6\zeta^2 + \frac{32d}{\nu} L^2 + \frac{160 \cdot 32d}{\nu} L^2 \eta^2 \left(KD^2 + \frac{1}{|\mathcal{H}|} \frac{d}{\nu} L^2 \right) K^2$, we require that $\eta \leq \sqrt{6 \frac{D^2}{K^2} + 6 \frac{\zeta^2}{K^2} + \frac{32d}{\nu K^2} L^2 + \frac{160 \cdot 32d}{\nu} L^2 \eta^2 \left(KD^2 + \frac{1}{|\mathcal{H}|} \frac{d}{\nu} L^2 \right)}$.

Since $\frac{160 \cdot 32d}{\nu} L^2 \eta^2 \left(KD^2 + \frac{1}{|\mathcal{H}|} \frac{d}{\nu} L^2 \right) \geq 0$, it suffices to let $\eta \leq \sqrt{6 \frac{D^2}{K^2} + 6 \frac{\zeta^2}{K^2} + \frac{32d}{\nu K^2} L^2}$. Hence, we obtain

$$\sum_{\ell=1}^K \frac{1}{|\mathcal{H}|} \sum_{i \in \mathcal{H}} \mathbb{E} \left[\|\mathbf{w}_{t,\ell}^i - \hat{\mathbf{w}}_{t,\ell}\|^2 \right] \leq c'_2 + c'_1 \mathbb{E} \left[\|\nabla F_{\mathcal{H}}(\mathbf{w}_t)\|^2 \right],$$

where

$$\begin{aligned}
 c'_1 & \triangleq 2\eta^2 \sum_{\ell=1}^K \ell \sum_{m=1}^{\ell} c_{16} \leq 2\eta^2 K^3 c_{16} \leq c_1 \triangleq 4\eta^2 K^3 c_{11}, \\
 c'_2 & \triangleq 2\eta^2 \sum_{\ell=1}^K \ell \sum_{m=1}^{\ell} c_{14} + 2\eta^2 \sum_{\ell=1}^K \ell \sum_{m=1}^{\ell} c_{15} \leq c_2 \triangleq 4\eta^2 K^3 c_{12} + 12\eta^2 K^3 L.
 \end{aligned}$$

\square

B.1.2 PROOF OF THEOREM 5.7 FOR $\mu = 0$

Proof. For the proof of the projected gradient variance, we rely on the following intermediate lemma.

Lemma B.8. *The second moment of the projected gradient according to Definition 2.1 for $\mu = 0$ is bounded as*

$$\mathbb{E} \left[\|\mathbf{z}g(\mathbf{w}, \mathbf{z}, \mu, \mathcal{D})\|^2 \right] \leq d \|\nabla F(\mathbf{w}, \mathcal{D})\|^2.$$

Proof of Lemma B.8.

$$\begin{aligned} \mathbb{E} \left[\|\mathbf{z}g(\mathbf{w}, \mathbf{z}, \mu, \mathcal{D})\|^2 \right] &= \mathbb{E} \left[\|d\mathbf{z} \langle \nabla F(\mathbf{w}, \mathcal{D}), \mathbf{z} \rangle\|^2 \right] \\ &= \mathbb{E} \left[\|d\mathbf{z}\mathbf{z}^T \nabla F(\mathbf{w}, \mathcal{D})\|^2 \right] \\ &= \mathbb{E} \left[d^2 \nabla F(\mathbf{w}, \mathcal{D})^T \mathbf{z}\mathbf{z}^T \mathbf{z}\mathbf{z}^T \nabla F(\mathbf{w}, \mathcal{D}) \right] \\ &= d^2 \nabla F(\mathbf{w}, \mathcal{D})^T \mathbb{E} [\mathbf{z}\mathbf{z}^T] \nabla F(\mathbf{w}, \mathcal{D}) \\ &= d \nabla F(\mathbf{w}, \mathcal{D})^T \nabla F(\mathbf{w}, \mathcal{D}) \\ &= d \|\nabla F(\mathbf{w}, \mathcal{D})\|^2, \end{aligned}$$

where the penultimate step is by (Gao et al., 2018, Lemma 7.3), which states that $\mathbb{E} [\mathbf{z}\mathbf{z}^T] = \frac{1}{d}\mathbf{I}$, for \mathbf{I} being the identity matrix. \square

Accordingly, the bound in Lemma B.6 for the zero-order estimate is an upper bound to the result of Lemma B.8 when choosing $\mu = 0$ in Lemma B.6. Further, we observe that Proposition 5.6 still holds for $\mu = 0$, due to a non-zero bias in the gradient projection case. Since those are the only two intermediate results where the case of gradient projection differs from the zero-order estimate, the result established in Theorem 5.7 holds for the gradient projection case when choosing $\mu = 0$. \square

B.2 Proof of Theorem 5.9

Proof. We assume for all that follows that the objective F exhibits a G -Lipschitz behavior. Similar to the proof of Theorem 5.7, we first state necessary intermediate lemmas, which we prove in the sequel. All lemmas hold under Assumptions 5.1 to 5.4 and 5.8 and a robust aggregator according to Definition 2.2.

Lemma B.9. *Let*

$$\begin{aligned} c_6 &\triangleq 5 \cdot 16\eta^2 K^2 \\ c_7 &\triangleq 5K\eta^2 \frac{\varphi^2 G^2 d}{|\mathcal{H}|^\nu} + 5\eta^2 16K^2 L\mu \\ c_8 &\triangleq 5 \cdot 16\eta^2 (KD^2) \end{aligned}$$

For a learning rate satisfying $\eta \leq \sqrt{\frac{1}{32L^2K^2}}$, we have the following upper bound on the averaged local model divergence:

$$\mathbb{E} \left[\|\hat{\mathbf{w}}_{t,\ell} - \mathbf{w}_t\|^2 \right] \leq c_6 \mathbb{E} \left[\|\nabla F_{\mathcal{H}}(\mathbf{w}_t)\|^2 \right] + c_7 + c_8 \sum_{\ell'=1}^{\ell-1} \frac{1}{|\mathcal{H}|} \sum_{i \in \mathcal{H}} \mathbb{E} \left[\|\mathbf{w}_{t,\ell'}^i - \hat{\mathbf{w}}_{t,\ell'}\|^2 \right]$$

Lemma B.10. *The following holds for the gradient estimate variance*

$$\mathbb{E} \left[\|\mathbf{Z}_{t,\ell} \mathbf{g}_i(\mathbf{w}_{t,\ell}^i, \mathbf{Z}_{t,\ell}) - \nabla F_i^\mu(\mathbf{w}_{t,\ell}^i)\|^2 \right] \leq \frac{\varphi^2 G^2 d}{\nu}$$

Lemma B.11. *Let*

$$c_{13} \triangleq 6D^2 + 6\zeta^2$$

$$c_{14} \triangleq 2 \frac{\varphi^2 G^2 d}{\nu}$$

$$c_{15} \triangleq 6L$$

Then

$$\begin{aligned} & \sum_{m=1}^{\ell} \frac{1}{|\mathcal{H}|} \sum_{i \in \mathcal{H}} \mathbb{E} \left[\left\| \mathbf{Z}_{t,m} \mathbf{g}_i(\mathbf{w}_{t,\ell}^i, \mathbf{Z}_{t,\ell}) - \frac{1}{|\mathcal{H}|} \sum_{j \in \mathcal{H}} \mathbf{Z}_{t,m} \mathbf{g}_j(\mathbf{w}_{t,m}^j, \mathbf{Z}_{t,m}) \right\|^2 \right] \\ & \leq \sum_{m=1}^{\ell} \frac{1}{|\mathcal{H}|} \sum_{i \in \mathcal{H}} c_{13} \mathbb{E} \left[\|\hat{\mathbf{w}}_{t,m} - \mathbf{w}_{t,m}^i\|^2 \right] + \sum_{m=1}^{\ell} (c_{14} + c_{15}) \end{aligned}$$

Lemma B.12. Let

$$c_2 \triangleq 4\eta^2 K^3 \frac{\varphi^2 G^2 d}{\nu} + 12\eta^2 K^3 L.$$

For a learning rate that satisfies $\eta \leq \sqrt{\frac{1}{12K^2(D^2 + \zeta^2)}}$, we have

$$\sum_{\ell=1}^K \frac{1}{|\mathcal{H}|} \sum_{i \in \mathcal{H}} \mathbb{E} \left[\|\mathbf{w}_{t,\ell}^i - \hat{\mathbf{w}}_{t,\ell}\|^2 \right] \leq c_2$$

To proof Theorem 5.9, we first follow the same lines as in the proof of Theorem 5.7, arriving at Equation (7). We continue with bounding the individual terms.

$$\begin{aligned} & \mathbb{E} \left[\left\| \sum_{\ell=1}^K \left(\sum_{i \in \mathcal{H}} \frac{1}{|\mathcal{H}|} \nabla F_i(\mathbf{w}_{t,\ell}^i) - \mathbf{Z}_{t,\ell} \bar{\mathbf{g}}_{\mathcal{H}}(\mathbf{w}_{t,\ell}^i, \mathbf{Z}_{t,\ell}) \right) \right\|^2 \right] \\ & \leq 2\mathbb{E} \left[\left\| \sum_{\ell=1}^K \sum_{i \in \mathcal{H}} \frac{1}{|\mathcal{H}|} (\nabla F_i(\mathbf{w}_{t,\ell}^i) - \nabla F_i^\mu(\mathbf{w}_{t,\ell}^i)) \right\|^2 \right] + 2\mathbb{E} \left[\left\| \sum_{\ell=1}^K \sum_{i \in \mathcal{H}} \frac{1}{|\mathcal{H}|} (\nabla F_i^\mu(\mathbf{w}_{t,\ell}^i) - \mathbf{Z}_{t,\ell} \mathbf{g}_i(\mathbf{w}_{t,\ell}^i, \mathbf{Z}_{t,\ell})) \right\|^2 \right] \\ & \stackrel{(a)}{\leq} 2 \frac{K}{|\mathcal{H}|} \sum_{i \in \mathcal{H}} \sum_{\ell=1}^K \|\nabla F_i(\mathbf{w}_{t,\ell}^i) - \nabla F_i^\mu(\mathbf{w}_{t,\ell}^i)\|^2 + 2 \frac{1}{|\mathcal{H}|^2} \sum_{i \in \mathcal{H}} \mathbb{E} \left[\left\| \sum_{\ell=1}^K (\nabla F_i^\mu(\mathbf{w}_{t,\ell}^i) - \mathbf{Z}_{t,\ell} \mathbf{g}_i(\mathbf{w}_{t,\ell}^i, \mathbf{Z}_{t,\ell})) \right\|^2 \right] \\ & \stackrel{(b)}{\leq} 2K^2 L\mu + 2 \frac{1}{|\mathcal{H}|^2} \sum_{i \in \mathcal{H}} \sum_{\ell=1}^K \mathbb{E} \left[\|\nabla F_i^\mu(\mathbf{w}_{t,\ell}^i) - \mathbf{Z}_{t,\ell} \mathbf{g}_i(\mathbf{w}_{t,\ell}^i, \mathbf{Z}_{t,\ell})\|^2 \right] \\ & \stackrel{(c)}{\leq} 2K^2 L\mu + 2 \frac{1}{|\mathcal{H}|^2} \sum_{i \in \mathcal{H}} \sum_{\ell=1}^K \frac{\varphi^2 G^2 d}{\nu} \\ & \stackrel{(c)}{\leq} 2K^2 L\mu + 2 \frac{1}{|\mathcal{H}|} K \frac{\varphi^2 G^2 d}{\nu} \tag{21} \end{aligned}$$

where (a) is due to the independence of $\sum_{\ell=1}^K (\nabla F_i^\mu(\mathbf{w}_{t,\ell}^i) - \mathbf{Z}_{t,\ell} \mathbf{g}_i(\mathbf{w}_{t,\ell}^i, \mathbf{Z}_{t,\ell}))$ and $\sum_{\ell=1}^K (\nabla F_j^\mu(\mathbf{w}_{t,\ell}^j) - \mathbf{Z}_{t,\ell} \mathbf{g}_j(\mathbf{w}_{t,\ell}^j, \mathbf{Z}_{t,\ell}))$ for $i \neq j$. (b) follows from Proposition 5.5 and (Wang et al., 2021, Lemma 2). (c) is by the application of Lemma B.10.

We continue with bounding the robustness term using as the main ingredient a double-sided application of an extended Johnson-Lindenstrauss Lemma as stated in Lemma B.5 and the application of Lemma B.11. We have

$$\mathbb{E} \left[\left\| \sum_{\ell=1}^K \mathbf{Z}_{t,\ell} (R_{t,\ell} - \bar{\mathbf{g}}_{\mathcal{H}}(\mathbf{w}_{t,\ell}^i, \mathbf{Z}_{t,\ell})) \right\|^2 \right]$$

$$\begin{aligned}
 &\leq K \sum_{\ell=1}^K \|\mathbf{Z}_{t,\ell} (R_{t,\ell} - \bar{\mathbf{g}}_{\mathcal{H}}(\mathbf{w}_{t,\ell}^i, \mathbf{Z}_{t,\ell}))\|^2 \\
 &\stackrel{(a)}{\leq} K \sum_{\ell=1}^K (1+\epsilon) \frac{\kappa}{|\mathcal{H}|} \sum_{i \in \mathcal{H}} \mathbb{E} \left[\|\mathbf{g}_i(\mathbf{w}_{t,\ell}^i, \mathbf{Z}_{t,\ell}) - \bar{\mathbf{g}}_{\mathcal{H}}(\mathbf{w}_{t,\ell}^i, \mathbf{Z}_{t,\ell})\|^2 \right] \\
 &\stackrel{(b)}{\leq} K \sum_{\ell=1}^K \frac{(1+\epsilon)}{(1-\epsilon)} \frac{\kappa}{|\mathcal{H}|} \sum_{i \in \mathcal{H}} \mathbb{E} \left[\|\mathbf{Z}_{t,\ell}(\mathbf{g}_i(\mathbf{w}_{t,\ell}^i, \mathbf{Z}_{t,\ell}) - \bar{\mathbf{g}}_{\mathcal{H}}(\mathbf{w}_{t,\ell}^i, \mathbf{Z}_{t,\ell}))\|^2 \right] \\
 &\stackrel{(c)}{\leq} K \frac{(1+\epsilon)}{(1-\epsilon)} \kappa \left(\sum_{\ell=1}^K \frac{1}{|\mathcal{H}|} \sum_{i \in \mathcal{H}} c_{13} \mathbb{E} \left[\|\hat{\mathbf{w}}_{t,\ell} - \mathbf{w}_{t,\ell}^i\|^2 \right] + \sum_{\ell=1}^K (c_{14} + c_{15}) \right) \tag{22}
 \end{aligned}$$

where (a) and (b) are by the application of Lemma B.5 for in total $|\mathcal{H}| + 1$ projections. By a union bound over Lemma B.5, the distance preservation holds with probability $1 - \delta$ for $\epsilon \geq \sqrt{\frac{64}{\nu} \log(\frac{2(|\mathcal{H}|-1)}{\delta})}$. We choose the smallest possible ϵ . This must hold for each iteration, so the distance preservation holds w.p. at least $1 - K\delta$ for all local epochs. (c) is by Lemma B.3.

To bound the local model divergence from the global model, by Lemma B.1, we have

$$\begin{aligned}
 \sum_{\ell=1}^K \mathbb{E} \left[\|\hat{\mathbf{w}}_{t,\ell} - \mathbf{w}_t\|^2 \right] &\leq \sum_{\ell=1}^K c_6 \mathbb{E} \left[\|\nabla F_{\mathcal{H}}(\mathbf{w}_t)\|^2 \right] + \sum_{\ell=1}^K c_7 + \sum_{\ell=1}^K c_8 \sum_{\ell'=1}^{\ell-1} \frac{1}{|\mathcal{H}|} \sum_{i \in \mathcal{H}} \mathbb{E} \left[\|\mathbf{w}_{t,\ell'}^i - \hat{\mathbf{w}}_{t,\ell'}\|^2 \right] \\
 &\leq \sum_{\ell=1}^K c_6 \mathbb{E} \left[\|\nabla F_{\mathcal{H}}(\mathbf{w}_t)\|^2 \right] + \sum_{\ell=1}^K c_7 + \sum_{\ell=1}^K \frac{c_8 K(K-1)}{|\mathcal{H}|} \sum_{i \in \mathcal{H}} \mathbb{E} \left[\|\mathbf{w}_{t,\ell}^i - \hat{\mathbf{w}}_{t,\ell}\|^2 \right], \tag{23}
 \end{aligned}$$

where the latter follows since $\sum_{\ell=1}^K \sum_{\ell'=1}^{\ell-1} x_{\ell'} \leq \sum_{\ell=1}^K \sum_{\ell'=1}^{\ell} x_{\ell'} \leq \frac{K(K-1)}{2} \sum_{\ell} x_{\ell}$.

Plugging (8), (22), and (23) into (7), we obtain

$$\begin{aligned}
 &\mathbb{E} \left[\left\| K \nabla F_{\mathcal{H}}(\mathbf{w}_t) - \sum_{\ell=1}^K \mathbf{Z}_{t,\ell} R_{t,\ell} \right\|^2 \right] \\
 &\leq 4KL^2 \left(\sum_{\ell=1}^K c_6 \mathbb{E} \left[\|\nabla F_{\mathcal{H}}(\mathbf{w}_t)\|^2 \right] + \sum_{\ell=1}^K c_7 + \sum_{\ell=1}^K \frac{c_8 K(K-1)}{|\mathcal{H}|} \sum_{i \in \mathcal{H}} \mathbb{E} \left[\|\mathbf{w}_{t,\ell}^i - \hat{\mathbf{w}}_{t,\ell}\|^2 \right] \right) \\
 &\quad + 4 \left(K \frac{(1+\epsilon)}{(1-\epsilon)} \kappa \left(\sum_{\ell=1}^K \frac{1}{|\mathcal{H}|} \sum_{i \in \mathcal{H}} c_{13} \mathbb{E} \left[\|\hat{\mathbf{w}}_{t,\ell} - \mathbf{w}_{t,\ell}^i\|^2 \right] + \sum_{\ell=1}^K (c_{14} + c_{15}) \right) \right) \\
 &\quad + 4K \sum_{\ell=1}^K \frac{D^2}{|\mathcal{H}|} \sum_{i \in \mathcal{H}} \mathbb{E} \left[\|\mathbf{w}_{t,\ell}^i - \hat{\mathbf{w}}_{t,\ell}\|^2 \right] + 4 \left(2K^2 L \mu + 2 \frac{1}{|\mathcal{H}|} K \frac{\varphi^2 G^2 d}{\nu} \right) \\
 &\leq c'_3 \mathbb{E} \left[\|\nabla F_{\mathcal{H}}(\mathbf{w}_t)\|^2 \right] + c'_4 \sum_{\ell=1}^K \frac{1}{|\mathcal{H}|} \sum_{i \in \mathcal{H}} \mathbb{E} \left[\|\hat{\mathbf{w}}_{t,\ell} - \mathbf{w}_{t,\ell}^i\|^2 \right] + c'_5 \\
 &\leq c'_3 \mathbb{E} \left[\|\nabla F_{\mathcal{H}}(\mathbf{w}_t)\|^2 \right] + c'_4 c_2 + c'_5, \tag{24}
 \end{aligned}$$

where

$$\begin{aligned}
 c'_3 &\triangleq 4KL^2 \sum_{\ell=1}^K c_6 \leq c_3 \triangleq 4K^4 L^2 5 \cdot 16\eta^2 \\
 c'_4 &\triangleq 4KL^2 c_8 K(K-1) + 4K \frac{(1+\epsilon)}{(1-\epsilon)} \kappa c_{13} + 4KD^2 \\
 &\leq 4KL^2 5 \cdot 16\eta^2 (KD^2) K(K-1) + 4K \kappa \frac{(1+\epsilon)}{(1-\epsilon)} 6(D^2 + \zeta^2) + 4KD^2
 \end{aligned}$$

$$\begin{aligned}
 &\leq c_4 \triangleq 20 \cdot 16K^4 L^2 \eta^2 D^2 + 4K \frac{(1+\epsilon)}{(1-\epsilon)} \kappa 6(D^2 + \zeta^2) + 4KD^2 \\
 c'_5 &\triangleq 4KL^2 \sum_{\ell=1}^K c_7 + 4K \frac{(1+\epsilon)}{(1-\epsilon)} \kappa \sum_{\ell=1}^K (c_{14} + c_{15}) + 4 \cdot 2K^2 L \mu + 4 \cdot 2 \frac{1}{|\mathcal{H}|^2} K \frac{\varphi^2 G^2 d}{\nu} \\
 &\leq 4KL^2 \sum_{\ell=1}^K \left(5K \eta^2 \frac{\varphi^2 G^2 d}{|\mathcal{H}| \nu} + 5\eta^2 16K^2 L \mu \right) + 4K \frac{(1+\epsilon)}{(1-\epsilon)} \kappa \sum_{\ell=1}^K \left(2 \frac{\varphi^2 G^2 d}{\nu} + 6L \right) \\
 &\quad + 4 \cdot 2K^2 L \mu + 4 \cdot 2 \frac{1}{|\mathcal{H}|^2} K \frac{\varphi^2 G^2 d}{\nu} \\
 &\leq 4K^2 L^2 \left(5K \eta^2 \frac{\varphi^2 G^2 d}{|\mathcal{H}| \nu} + 5\eta^2 16K^2 L \mu \right) + 4K^2 \frac{(1+\epsilon)}{(1-\epsilon)} \kappa \left(2 \frac{\varphi^2 G^2 d}{\nu} + 6L \right) \\
 &\quad + 4 \cdot 2K^2 L \mu + 4 \cdot 2 \frac{1}{|\mathcal{H}|^2} K \frac{\varphi^2 G^2 d}{\nu} \\
 &\leq c_5 \triangleq 4K \frac{\varphi^2 G^2 d}{\nu} \left(5K^2 L^2 \eta^2 \frac{1}{|\mathcal{H}|} + 2K \frac{(1+\epsilon)}{(1-\epsilon)} \kappa + \frac{8}{|\mathcal{H}|^2} \right) + 4K^2 L \left(5\eta^2 16K^2 L^2 \mu + 6\kappa \frac{(1+\epsilon)}{(1-\epsilon)} + 2\mu \right)
 \end{aligned}$$

By taking the expectation over (6) and replacing $\mathbb{E} \left[\left\| K \nabla F_{\mathcal{H}}(\mathbf{w}_t) - \sum_{\ell=1}^K \mathbf{Z}_{t,\ell} R_{t,\ell} \right\|^2 \right]$ by (11), we can write

$$\begin{aligned}
 &\mathbb{E} [F_{\mathcal{H}}(\mathbf{w}_{t+1})] - \mathbb{E} [F_{\mathcal{H}}(\mathbf{w}_t)] \\
 &\leq -\eta/(2)K \mathbb{E} \left[\|\nabla F_{\mathcal{H}}(\mathbf{w}_t)\|^2 \right] + \left(\frac{\eta^2 L}{2} - \frac{\eta}{2K} \right) \mathbb{E} \left[\left\| \sum_{\ell=1}^K R_{t,\ell} \mathbf{Z}_{t,\ell} \right\|^2 \right] + \eta/(2K) \mathbb{E} \left[\left\| K \nabla F_{\mathcal{H}}(\mathbf{w}_t) - \sum_{\ell=1}^K R_{t,\ell} \mathbf{Z}_{t,\ell} \right\|^2 \right] \\
 &\stackrel{(a)}{\leq} -\eta/(2)K \mathbb{E} \left[\|\nabla F_{\mathcal{H}}(\mathbf{w}_t)\|^2 \right] + \eta/(2K) \left(c_3 \mathbb{E} \left[\|\nabla F_{\mathcal{H}}(\mathbf{w}_t)\|^2 \right] + c_4 c_2 + c_5 \right) \\
 &\stackrel{(b)}{\leq} -\frac{\eta K}{4} \mathbb{E} \left[\|\nabla F_{\mathcal{H}}(\mathbf{w}_t)\|^2 \right] + \eta/(2K) (c_4 c_2 + c_5),
 \end{aligned}$$

where (a) holds when $\eta \leq \frac{1}{KL}$ and (b) assumes that $\eta/(2K)c_3 = \eta/(2K)4K^2 L^2 5 \cdot 16\eta^2 K^2 \leq \frac{\eta K}{4}$. The learning rate must hence satisfy $\eta^2 \leq \frac{1}{8 \cdot K^2 L^2 5 \cdot 16}$, and consequently $\eta \leq \frac{1}{26KL}$.

Reordering and telescoping over t , we obtain

$$\frac{1}{T} \sum_{t=1}^T \mathbb{E} \left[\|\nabla F_{\mathcal{H}}(\mathbf{w}_t)\|^2 \right] \leq \frac{4(\mathbb{E} [F_{\mathcal{H}}(\mathbf{w}_1)] - \mathbb{E} [F_{\mathcal{H}}(\mathbf{w}_{T+1})])}{T\eta K} + \eta/(2K) (c_4 c_2 + c_5)$$

with probability $1 - \delta KT$ by a union bound argument over all global iterations T . Noting that $F_{\mathcal{H}}(\mathbf{w}_{T+1}) \geq F_{\mathcal{H}}^*$ by definition concludes the proof.

Since the learning rates must satisfy $\eta \leq \frac{1}{6KL} \leq \sqrt{\frac{1}{32L^2 K^2}}$, $\eta \leq \frac{1}{4K\sqrt{D^2 + \zeta^2}} \leq \sqrt{\frac{1}{12K^2(D^2 + \zeta^2)}}$ and $\eta \leq \frac{1}{26KL}$ for all lemmas to hold, and hence $\eta \leq \min \left\{ \frac{1}{26KL}, \frac{1}{4K\sqrt{D^2 + \zeta^2}} \right\}$, we have

$$\begin{aligned}
 &\eta/(2K) (c_4 c_2 + c_5) \\
 &= \frac{\eta}{2K} \left(4\eta^2 K^3 \frac{\varphi^2 G^2 d}{\nu} + 12\eta^2 K^3 L \right) \left(20 \cdot 16K^4 L^2 \eta^2 D^2 + 4K \frac{(1+\epsilon)}{(1-\epsilon)} \kappa 6(D^2 + \zeta^2) + 4KD^2 \right) \\
 &\quad + 4K \frac{\varphi^2 G^2 d}{\nu} \frac{\eta}{2K} \left(5K^2 L^2 \eta^2 \frac{1}{|\mathcal{H}|} + 2K \frac{(1+\epsilon)}{(1-\epsilon)} \kappa + \frac{8}{|\mathcal{H}|^2} \right) + 4K^2 L \frac{\eta}{2K} \left(5\eta^2 16K^2 L^2 \mu + 6\kappa \frac{(1+\epsilon)}{(1-\epsilon)} + 2\mu \right)
 \end{aligned}$$

$$\begin{aligned}
 &= 2\eta^3 K^2 \left(\frac{\varphi^2 G^2 d}{\nu} + 3L \right) \left(20 \cdot 16K^4 L^2 \eta^2 D^2 + 4K \frac{(1+\epsilon)}{(1-\epsilon)} \kappa 6(D^2 + \zeta^2) + 4KD^2 \right) \\
 &+ 2 \frac{\varphi^2 G^2 d}{\nu} \eta \left(5K^2 L^2 \eta^2 \frac{1}{|\mathcal{H}|} + 2K \frac{(1+\epsilon)}{(1-\epsilon)} \kappa + \frac{8}{|\mathcal{H}|^2} \right) + 4K^2 L \frac{\eta}{2K} \left(5\eta^2 16K^2 L^2 \mu + 6\kappa \frac{(1+\epsilon)}{(1-\epsilon)} + 2\mu \right) \\
 &= 2\eta K \left(\frac{\varphi^2 G^2 d}{L^2 \nu} + 3 \frac{1}{L} \right) \left(13KD^2 + 4 \frac{(1+\epsilon)}{(1-\epsilon)} \kappa 6(D^2 + \zeta^2) + 4D^2 \right) \\
 &+ 2\eta \frac{\varphi^2 G^2 d}{\nu} \left(\frac{1}{5|\mathcal{H}|} + 2K \frac{(1+\epsilon)}{(1-\epsilon)} \kappa + \frac{8}{|\mathcal{H}|^2} \right) + 2KL\eta \left(6\kappa \frac{(1+\epsilon)}{(1-\epsilon)} + 6\mu \right).
 \end{aligned}$$

We let $\Delta \triangleq \delta KT$, and obtain $\epsilon \geq \sqrt{\frac{64}{\nu} \log(\frac{2(|\mathcal{H}|-1)}{\delta})} = \sqrt{\frac{64}{\nu} \log(\frac{2(|\mathcal{H}|-1)TK}{\Delta})}$. Since it is required to satisfy $\epsilon < 1$, the proof holds for $\nu \geq 64 \log(\frac{2(|\mathcal{H}|-1)TK}{\Delta})$. This concludes the proof. \square

Proof of Lemma B.10. For the proof of the zero-order approximated gradient variance, we rely on the following intermediate lemma.

Lemma B.13 (Lemma 5.3, (Tang et al., 2020)). *Let F be G -Lipschitz. Then for any $\mathbf{w} \in \mathbb{R}^d$, \mathbf{z} and $\mu > 0$, we have*

$$\mathbb{E} \left[\|\mathbf{z}^T g(\mathbf{w}, \mathbf{z}, \mu, \mathcal{D})\|^2 \right] \leq \varphi^2 G^2 d$$

We bound the zero-order approximated gradient variance as follows: Since $\mathbb{E} \left[\|Z - \mathbb{E}[Z]\|^2 \right] \leq \mathbb{E} \left[\|Z\|^2 \right]$, and $\mathbb{E} \left[\mathbf{z}_{t,\ell}^r g_i(\mathbf{w}_{t,\ell}^i, \mathbf{z}_{t,\ell}^r) \right] = \nabla F_i^\mu(\mathbf{w}_{t,\ell}^i)$, we have

$$\begin{aligned}
 &\mathbb{E} \left[\|\mathbf{Z}_{t,\ell} \mathbf{g}_i(\mathbf{w}_{t,\ell}^i, \mathbf{Z}_{t,\ell}) - \nabla F_i^\mu(\mathbf{w}_{t,\ell}^i)\|^2 \right] = \mathbb{E} \left[\left\| \frac{1}{\nu} \sum_{r=1}^{\nu} \mathbf{z}_{t,\ell}^r g_i(\mathbf{w}_{t,\ell}^i, \mathbf{z}_{t,\ell}^r) - \nabla F_i^\mu(\mathbf{w}_{t,\ell}^i) \right\|^2 \right] \\
 &\stackrel{(a)}{=} \frac{1}{\nu^2} \sum_{r=1}^{\nu} \mathbb{E} \left[\|\mathbf{z}_{t,\ell}^r g_i(\mathbf{w}_{t,\ell}^i, \mathbf{z}_{t,\ell}^r) - \nabla F_i^\mu(\mathbf{w}_{t,\ell}^i)\|^2 \right] \\
 &\leq \frac{1}{\nu^2} \sum_{r=1}^{\nu} \mathbb{E} \left[\|\mathbf{z}_{t,\ell}^r g_i(\mathbf{w}_{t,\ell}^i, \mathbf{z}_{t,\ell}^r)\|^2 \right] \stackrel{(b)}{\leq} \frac{\varphi^2 G^2 d}{\nu}
 \end{aligned}$$

where (a) is due to the independence of $\mathbf{z}_{t,\ell}^r g_i(\mathbf{w}_{t,\ell}^i, \mathbf{z}_{t,\ell}^r)$ and $\mathbf{z}_{t,\ell}^{r'} g_i(\mathbf{w}_{t,\ell}^i, \mathbf{z}_{t,\ell}^{r'})$ for $r \neq r'$. (b) is by Lemma B.13. \square

Proof of Lemma B.9. By definition, $\mathbb{E} \left[\|\hat{\mathbf{w}}_{t,1} - \mathbf{w}_t\|^2 \right] = 0$. From (18), we have for $\ell \in \{2, \dots, K\}$,

$$\begin{aligned}
 &\mathbb{E} \left[\|\hat{\mathbf{w}}_{t,\ell} - \mathbf{w}_t\|^2 \right] \\
 &\leq (1 + \frac{1}{\tau}) \mathbb{E} \left[\|\hat{\mathbf{w}}_{t,\ell-1} - \mathbf{w}_t\|^2 \right] + 8(1 + \tau) \eta^2 \mathbb{E} \left[\left\| \frac{1}{|\mathcal{H}|} \sum_{i \in \mathcal{H}} \nabla F_i^\mu(\mathbf{w}_{t,\ell-1}^i) - \frac{1}{|\mathcal{H}|} \sum_{i \in \mathcal{H}} \nabla F_i(\mathbf{w}_{t,\ell-1}^i) \right\|^2 \right] \\
 &+ 8(1 + \tau) \eta^2 \mathbb{E} \left[\|\nabla F_{\mathcal{H}}(\mathbf{w}_t)\|^2 \right] \\
 &+ 8(1 + \tau) \eta^2 \mathbb{E} \left[\left\| \frac{1}{|\mathcal{H}|} \sum_{i \in \mathcal{H}} \nabla F_i(\mathbf{w}_{t,\ell-1}^i) - \nabla F_{\mathcal{H}}(\hat{\mathbf{w}}_{t,\ell-1}) \right\|^2 \right] + 8(1 + \tau) \eta^2 \mathbb{E} \left[\|\nabla F_{\mathcal{H}}(\hat{\mathbf{w}}_{t,\ell-1}) - \nabla F_{\mathcal{H}}(\mathbf{w}_t)\|^2 \right] \\
 &+ 2\eta^2 \frac{1}{|\mathcal{H}|^2} \sum_{i \in \mathcal{H}} \mathbb{E} \left[\|\mathbf{Z}_{t,\ell-1} \mathbf{g}_i(\mathbf{w}_{t,\ell-1}^i, \mathbf{Z}_{t,\ell-1}) - \nabla F_i^\mu(\mathbf{w}_{t,\ell-1}^i)\|^2 \right]
 \end{aligned}$$

$$\begin{aligned}
 &\stackrel{(a)}{\leq} \left(1 + \frac{1}{\tau}\right) \mathbb{E} \left[\|\hat{\mathbf{w}}_{t,\ell-1} - \mathbf{w}_t\|^2 \right] + 8(1+\tau)\eta^2 L\mu + 8(1+\tau)\eta^2 \mathbb{E} \left[\|\nabla F_{\mathcal{H}}(\mathbf{w}_t)\|^2 \right] \\
 &+ 8(1+\tau)\eta^2 \frac{D^2}{|\mathcal{H}|} \sum_{i \in \mathcal{H}} \mathbb{E} \left[\|\mathbf{w}_{t,\ell-1}^i - \hat{\mathbf{w}}_{t,\ell-1}\|^2 \right] + 8(1+\tau)\eta^2 L^2 \mathbb{E} \left[\|\hat{\mathbf{w}}_{t,\ell-1} - \mathbf{w}_t\|^2 \right] \\
 &+ 2\eta^2 \frac{1}{|\mathcal{H}|^2} \sum_{i \in \mathcal{H}} \frac{\varphi^2 G^2 d}{\nu} \\
 &= \left(\left(1 + \frac{1}{\tau}\right) + 8(1+\tau)\eta^2 L^2 \right) \mathbb{E} \left[\|\hat{\mathbf{w}}_{t,\ell-1} - \mathbf{w}_t\|^2 \right] + 8(1+\tau)\eta^2 L\mu \\
 &+ (8(1+\tau)\eta^2) \mathbb{E} \left[\|\nabla F_{\mathcal{H}}(\mathbf{w}_t)\|^2 \right] \\
 &+ \left(8(1+\tau)\eta^2 \frac{D^2}{|\mathcal{H}|} \right) \sum_{i \in \mathcal{H}} \mathbb{E} \left[\|\mathbf{w}_{t,\ell-1}^i - \hat{\mathbf{w}}_{t,\ell-1}\|^2 \right] + 2\eta^2 \frac{1}{|\mathcal{H}|} \frac{\varphi^2 G^2 d}{\nu},
 \end{aligned}$$

where (a) follows from Assumption 5.1, Assumption 5.4 and an intermediate step in the proof of Lemma B.2.

To ensure the bound holds uniformly for all $\ell \in [K]$, we now choose $\tau = 2K - 1$ and the learning rate small enough so that $\left(\left(1 + \frac{1}{\tau}\right) + 8(1+\tau)\eta^2 L^2 \right) \leq 1 + \frac{1}{K-1}$, i.e., that $8(1+\tau)\eta^2 L^2 \leq \frac{1}{2K}$. Hence, the learning rate is required to satisfy $\eta \leq \sqrt{\frac{1}{32L^2K^2}}$. With this choice of the learning rate, we have

$$\begin{aligned}
 &\mathbb{E} \left[\|\hat{\mathbf{w}}_{t,\ell} - \mathbf{w}_t\|^2 \right] \\
 &\leq \left(1 + \frac{1}{K-1}\right) \mathbb{E} \left[\|\hat{\mathbf{w}}_{t,\ell-1} - \mathbf{w}_t\|^2 \right] + 8(1+\tau)\eta^2 L\mu + (8(1+\tau)\eta^2) \mathbb{E} \left[\|\nabla F_{\mathcal{H}}(\mathbf{w}_t)\|^2 \right] \\
 &+ \left(8(1+\tau)\eta^2 \frac{D^2}{|\mathcal{H}|} \right) \sum_{i \in \mathcal{H}} \mathbb{E} \left[\|\mathbf{w}_{t,\ell-1}^i - \hat{\mathbf{w}}_{t,\ell-1}\|^2 \right] + 2\eta^2 \frac{1}{|\mathcal{H}|} \frac{\varphi^2 G^2 d}{\nu} \\
 &\stackrel{(d)}{\leq} c'_6(\ell) \mathbb{E} \left[\|\nabla F_{\mathcal{H}}(\mathbf{w}_t)\|^2 \right] + c'_7(\ell) + c'_8 \sum_{\ell'=1}^{\ell-1} \sum_{i \in \mathcal{H}} \mathbb{E} \left[\|\mathbf{w}_{t,\ell'}^i - \hat{\mathbf{w}}_{t,\ell'}\|^2 \right],
 \end{aligned}$$

where (e) is by the recursive application of (d) and the fact that $\left(1 + \frac{1}{K}\right)^\ell \leq \left(1 + \frac{1}{\ell}\right)^\ell \leq e \leq 5$ for all $\ell \in [K]$. This concludes the proof. The constants are given as

$$\begin{aligned}
 c'_6(\ell) &\triangleq 5(\ell-1) (8(1+\tau)\eta^2) \leq c_6 \triangleq 5 \cdot 16\eta^2 K^2 \\
 c'_7(\ell) &\triangleq 5(\ell-1) \left(2\eta^2 \frac{1}{|\mathcal{H}|} \frac{\varphi^2 G^2 d}{\nu} + 8(1+\tau)\eta^2 L\mu \right) \\
 &\leq c_7 \triangleq 5K\eta^2 \frac{\varphi^2 G^2 d}{|\mathcal{H}|\nu} + 5\eta^2 16K^2 L\mu \\
 c'_8 &\triangleq 5 (8(1+\tau)\eta^2 D^2) \leq c_8 \triangleq 5 \cdot 16\eta^2 (KD^2)
 \end{aligned}$$

□

Proof of Lemma B.11. Using (20), we obtain

$$\begin{aligned}
 &\sum_{m=1}^{\ell} \frac{1}{|\mathcal{H}|} \sum_{i \in \mathcal{H}} \mathbb{E} \left[\left\| \mathbf{Z}_{t,m} \mathbf{g}_i(\mathbf{w}_{t,\ell}^i, \mathbf{Z}_{t,\ell}) - \frac{1}{|\mathcal{H}|} \sum_{j \in \mathcal{H}} \mathbf{Z}_{t,m} \mathbf{g}_j(\mathbf{w}_{t,m}^j, \mathbf{Z}_{t,m}) \right\|^2 \right] \\
 &\stackrel{(a)}{\leq} 2 \sum_{m=1}^{\ell} \mathbb{E} \left[\left(3 \frac{D^2}{|\mathcal{H}|} + 3 \frac{\zeta^2}{|\mathcal{H}|} \right) \sum_{i \in \mathcal{H}} \|\hat{\mathbf{w}}_{t,m} - \mathbf{w}_{t,m}^i\|^2 + 3L \right] \\
 &+ 2 \sum_{m=1}^{\ell} \frac{1}{|\mathcal{H}|} \sum_{i \in \mathcal{H}} \left(\frac{\varphi^2 G^2 d}{\nu} \right)
 \end{aligned}$$

$$\leq \sum_{m=1}^{\ell} \frac{1}{|\mathcal{H}|} \sum_{i \in \mathcal{H}} c_{13} \mathbb{E} \left[\|\hat{\mathbf{w}}_{t,m} - \mathbf{w}_{t,m}^i\|^2 \right] + \sum_{m=1}^{\ell} (c_{14} + c_{15})$$

where (a) is due to Lemma B.10. Thereby,

$$c_{13} \triangleq 6D^2 + 6\zeta^2$$

$$c_{14} \triangleq 2 \frac{\varphi^2 G^2 d}{\nu}$$

$$c_{15} \triangleq 6L$$

□

Proof of Lemma B.12. From Lemma B.11, we have

$$\begin{aligned} & \sum_{\ell=1}^K \frac{1}{|\mathcal{H}|} \sum_{i \in \mathcal{H}} \mathbb{E} \left[\|\mathbf{w}_{t,\ell}^i - \hat{\mathbf{w}}_{t,\ell}\|^2 \right] = \sum_{\ell=1}^K \frac{1}{|\mathcal{H}|} \sum_{i \in \mathcal{H}} \mathbb{E} \left[\left\| \eta \sum_{m=1}^{\ell} \left(\mathbf{z}_{t,m} \mathbf{g}_i(\mathbf{w}_{t,\ell}^i, \mathbf{Z}_{t,\ell}) - \frac{1}{|\mathcal{H}|} \sum_{j \in \mathcal{H}} \mathbf{z}_{t,m} \mathbf{g}_j(\mathbf{w}_{t,m}^j, \mathbf{Z}_{t,m}) \right) \right\|^2 \right] \\ & \leq \eta^2 \sum_{\ell=1}^K \ell \sum_{m=1}^{\ell} \frac{1}{|\mathcal{H}|} \sum_{i \in \mathcal{H}} \mathbb{E} \left[\left\| \mathbf{z}_{t,m} \mathbf{g}_i(\mathbf{w}_{t,\ell}^i, \mathbf{Z}_{t,\ell}) - \frac{1}{|\mathcal{H}|} \sum_{j \in \mathcal{H}} \mathbf{z}_{t,m} \mathbf{g}_j(\mathbf{w}_{t,m}^j, \mathbf{Z}_{t,m}) \right\|^2 \right] \\ & = \eta^2 \sum_{\ell=1}^K \ell \sum_{m=1}^{\ell} \sum_{i \in \mathcal{H}} \frac{1}{|\mathcal{H}|} c_{13} \mathbb{E} \left[\|\hat{\mathbf{w}}_{t,m} - \mathbf{w}_{t,m}^i\|^2 \right] + \eta^2 \sum_{\ell=1}^K \ell \sum_{m=1}^{\ell} c_{14} + \eta^2 \sum_{\ell=1}^K \ell \sum_{m=1}^{\ell} c_{15} \\ & \leq \eta^2 \sum_{\ell=1}^K \frac{1}{|\mathcal{H}|} \sum_{i \in \mathcal{H}} K^2 c_{13} \mathbb{E} \left[\|\hat{\mathbf{w}}_{t,\ell} - \mathbf{w}_{t,\ell}^i\|^2 \right] + \eta^2 p u t \sum_{\ell=1}^K \ell \sum_{m=1}^{\ell} c_{14} + \eta^2 \sum_{\ell=1}^K \ell \sum_{m=1}^{\ell} c_{15} \end{aligned}$$

We rewrite the expression as

$$(1 - \eta^2 K^2 c_{13}) \sum_{\ell=1}^K \frac{1}{|\mathcal{H}|} \sum_{i \in \mathcal{H}} \mathbb{E} \left[\|\mathbf{w}_{t,\ell}^i - \hat{\mathbf{w}}_{t,\ell}\|^2 \right] \leq \eta^2 \sum_{\ell=1}^K \ell \sum_{m=1}^{\ell} c_{14} + \eta^2 \sum_{\ell=1}^K \ell \sum_{m=1}^{\ell} c_{15}$$

and choose the learning rate small enough so that $(1 - \eta^2 K^2 c_{13}) = (1 - 6\eta^2 K^2 (D^2 + \zeta^2)) \geq \frac{1}{2}$. Hence, we obtain

$$\sum_{\ell=1}^K \frac{1}{|\mathcal{H}|} \sum_{i \in \mathcal{H}} \mathbb{E} \left[\|\mathbf{w}_{t,\ell}^i - \hat{\mathbf{w}}_{t,\ell}\|^2 \right] \leq c'_2,$$

where

$$c'_2 \triangleq 2\eta^2 \sum_{\ell=1}^K \ell \sum_{m=1}^{\ell} c_{14} + 2\eta^2 \sum_{\ell=1}^K \ell \sum_{m=1}^{\ell} c_{15} \leq c_2 \triangleq 4\eta^2 K^3 \frac{\varphi^2 G^2 d}{\nu} + 12\eta^2 K^3 L.$$

The learning rate must satisfy $\eta \leq \sqrt{\frac{1}{12K^2(D^2 + \zeta^2)}}$. This concludes the proof. □